VERIFIED SYNTHESES OF ZEOLITIC MATERIALS

Third Revised Edition
S. Mintova, Editor
N. Barrier, XRD Patterns

Second Edition
H. Robson, Editor
K.P. Lillerud, XRD Patterns

Published on behalf of the Synthesis Commission of the International Zeolite Association

ISBN: 978-0-692-68539-6
:

Published on behalf of the Synthesis Commission of the International Zeolite Association

2016

ISBN: 978-0-692-68539-6

Cover page designed by Mohamad El Roz

Verified Syntheses of Zeolitic Materials

Table of contents

I. Preface to the third edition 2
II. Synthesis commission 4
III. Introduction and explanatory notes 5
IV. Conditions for recording of XRD patterns 10
V. Contributors 11
VI. Introductory Articles 24
1.Initial materials for synthesis of zeolites 24
2. Synthesis of new molecular sieves using novel structure-directing agents 29
3. Synthesis design of new molecular sieves 36
4. Zeolite nanocrystals 42
5. Synthesis of single-unit-cell zeolites 48
6. Synthesis of aluminophosphate analogues of zeolites 53
7. Disassembly as a route to new materials 61
8. Synthesis of zeolites: seeding approach 66
9. Post synthesis modification of zeolites 72
10. Diffraction methods for zeolite structural characterization 78
11. Advanced methods applied on zeolites 84
12. Modeling of zeolites: from the unit cell to the crystal 89
14. New zeolite-based catalytic processes 100
VI. Synthesis recipes 106
ABW.....Li-A (BW) 107
AEI.....$AlPO_4$-18 111
AEI.....Nanosized AlPO4-18 114
AEI.....SAPO-18 (DPEA method) 116
AEI.....SAPO-18 (TEA method) 119
AEL.....$AlPO_4$-11 122
AET.....$AlPO_4$-8 125
AFI.....$AlPO_4$-5 127
AFI.....SAPO-5 130
AFI.....CoAPO-5 133
AFI.....SSZ-24 136
AFO.....Nanosized AlPO-41 139
AFO.....SAPO-41 141

AFS.....MAPO-46 144
ANA.....Analcime 147
AST.....$AlPO_4$-16 150
ATN.....MAPO-39 153
BEA.....Beta 156
BEA.....Sn-Beta 159
BEA.....[Ti,Al] Beta 163
BEC.....ITQ-17 166
CAN.....Cancrinite 169
CDO.....CDS-1 172
CHA.....Chabazite 175
CHA.....SSZ-13 178
CHA.....SAPO-34 181
CHA.....SAPO-44 184
CLO.....Cloverite (GaPO4) 186
CON.....CIT-1 189
DON.....UTD-1F 192
EAB.....TMA-E 194
EDI.....Barrer K-F 197
EDI.....Linde Type F 199
EDI.....Nanosized Linde F 202
EMT.....EMC-2 204
EMT.....Nanosized Na-EMC-2 207
ERI.....Erionite 210
EUO.....[Ga] EU-1 212
FAU.....Linde Type X 215
FAU.....Silica Type X (LSX) 218
FAU.....Linde Type Y 221
FAU.....Nanosized Linde Type Na-X 224
FAU.....Nanosized Linde Type TMA-Y 226
FAU.....High-Si Faujasite EMC-1[a] 228
FAU.....[Ga] Type Y 231
FAU.....SAPO-37 234
FER.....ZSM-35 237
GIS.....Zeolite P 240
IMF.....IM-5 242

ITT.....ITQ-33.....245
KFI.....ZK-5.....247
KFI.....High-Silica KFI.....250
LEV.....[B]-Levyne.....252
LTA.....Linde Type A.....255
LTA.....Nanosized Linde Type TMA-A.....258
LTA.....ZK-4.....260
LTA.....Zeolite Alpha.....263
LTA.....$GaPO_4$.....266
LTF.....LZ-135.....268
LTL.....Linde Type L.....271
LTL.....Nanosized Linde Type L.....274
MAZ.....Mazzite.....276
MEL.....Nanosized TBA-Silicalite-2.....279
MER.....Linde W.....281
MFI.....High-Al ZSM-5.....284
MFI.....Nanosized TPA-silicalite-1.....287
MFI.....Template-free ZSM-5.....289
MFI.....Silicalite-1.....292
MFI.....[B] ZSM-5.....294
MFI.....[Fe]-ZSM-5.....296
MFI.....[Ti] ZSM-5.....298
MFI.....[Ti,Al] ZSM-5.....301
MFS.....ZSM-57.....304
MOR.....Mordenite.....307
.....309
MOZ.....ZSM-10.....310
MSE.....MCM-68.....313
MTN.....ZSM-39.....315
MTT.....SSZ-32.....318
MTT.....ZSM-23.....321
MTW.....ZSM-12.....324
MTW.....[Ga] ZSM-12.....327
MWW.....MCM-22.....330
NAT.....[Ga] Natrolite.....333
OFF.....Linde Type T.....336

OFF.....Offretite.....339
OFF.....[Ga] Offretite.....342
PAU.....ECR-18.....345
PAU.....Paulingite (Seeded).....347
PHI.....Phillipsite.....350
PHI.....High-alumina Philipsite.....352
RHO.....High Silica Rho.....355
RSN.....RUB-17.....358
SEW.....SSZ-82.....360
SOD.....NaBr-Sodalite.....363
STI.....TNU-10.....367
STT.....SSZ-23.....369
TON.....ZSM-22.....372
TUN.....TNU-9.....374
UOS.....IM-16.....377
UOV.....IM-17.....380
UOZ.....IM-10.....383
UTL.....Al-IM-12.....386
UTL.....B-IM-12.....389
UTL.....IM-12.....392
VFI.....VPI-5 (DPA method).....395
VFI.....VPI-5 (TBA method).....398
VSV.....VPI-7.....401
SUZ-4.....403

I. Preface to the third edition

The first edition of Verified Syntheses of Zeolitic Materials was published in Microporous and Mesoporous Materials (1998) Volume 22, 4-6. Distribution was limited to subscribers to the Journal.

The second edition was published on behalf of the Synthesis Commission of the International Zeolite Association in 2001, Elsevier, ISBN: 0-444-50703-5. The 2nd edition of the book reprinted all the recipes from the first edition plus 24 new recipes. The introductory section includes the articles from the first edition (some with substantial revisions) and five new articles.

The current 3rd edition (ISBN-10: 0-692-68539-1) has reprinted all the recipes (72) from the second edition plus 36 new recipes (total 108 recipes). The introductory section contains 14 new articles reporting on the very recent developments in the area of zeolite synthesis. The introductory articles present the state of the art topics related with zeolites including: synthesis of new molecular sieves using novel structure-directing agents, design of new molecular sieves via new synthesis approaches, synthesis of zeolites with nanosized dimensions, synthesis of single-unit-cell hierarchical zeolites, synthesis of aluminophosphate analogues of zeolites, and post synthesis modifications of zeolites. Additionally, the main approaches used for characterization of zeolites including: diffraction methods, advanced spectroscopic methods, and adsorptive separation techniques are revealed. Important contributions on modeling of zeolites from the unit cell to the crystals and development of new zeolite-based catalytic processes are added. The intended audience of this book is researchers, specialists from academia and industry in the area of zeolites, zeo-type porous materials. Additionally, students at undergraduate, PhD and Post Doctoral levels involved in the syntheses of zeolites and related materials will use it as a reference book. This book will be of interest for specialized master courses in Materials Science and Practice.

The XRD patterns presented in the third edition have been recorded using different instrument from those in the first and second editions.

Zeolite synthesis is an active field of research. The 2nd edition of this book was published in 2001 when the zeolite structures known during that time were about 130. Due to the great interest in the zeolite synthesis, which is driven by the need for existing and new applications, the number of zeolite structures increased substantially, and in 2016 more than 231 different zeolites are available. With the development of new synthesis approaches and modeling of the syntheses processes, many new zeolites types were synthesized. Besides, known zeolites with unique properties were prepared by applying new synthesis methods combined with novel techniques for characterizations.

These zeolitic materials find great applications in catalysis, sorption and ion exchange processes. Additionally, zeolites become attractive materials for nanotechnology applications, medicine, cosmetics, pharmaceutical, and food industries. The IZA Synthesis Commission (http://www.iza-online.org/synthesis/default.htm) prepared the 3rd edition of the book in order to enlarge the existing collection and to include new materials of interest to the zeolite research community. Besides the introductory articles revealed the most important developments from the last decade associated with synthesis, characterization and application of zeolites.

The IZA Synthesis Commission will continue to enlarge this collection and will include all phases of interest to the zeolite research community.

Svetlana Mintova
Normandie Université, ENSICAEN, UNICAEN,
CNRS, Laboratoire Catalyse et Spectrochimie,
6 boulevard Maréchal Juin, 14050 Caen, France

II. Synthesis commission
of the INTERNATIONAL ZEOLITE ASSOCIATION

Chairperson:
Svetlana Mintova

Co-chairperson:
Gregory Lewis

Members:
Kenneth Balkus
Jiri Cejka
Suk Bong Hong
Qisheng Huo
Yoshihiro Kubota
Roberto Millini
Jean-Louis Paillaud
Fernando Rey
Wieslaw Roth
Wilhelm Schwieger
Steve Wilson
Jihong Yu
Stacey Zones

III. Introduction and explanatory notes

The Synthesis Commission consists of experts in the synthesis area of zeolite and zeo-type materials. The format for the recipes in the 3rd edition of the book follows the style of the previous two books. The table format is intended to assist the reader by placing the information in the same relative positions for all recipes.
The table form describing the synthesis experiments follows the typical sequence: batch preparation, crystallization, product recovery, and characterization.

1. Framework Type Codes

The three-letter codes (top line - far left) are arranged in alphabetical order as in the Atlas of Zeolite Structure Types (http://www.iza-structure.org/databases/). They define the topography, but not the composition of the crystalline materials. The third edition of the book contain multiple entries for a single code with differing Si/Al ratio products, products with differing T-atoms, products of essentially the same composition produced by different synthesis procedures, and materials with different particle sizes.

2. Product Name

The product name (top line - center) is the name by which the product is usually referred to in the literature. There may be several products of similar composition but different names. The choice among competing names has been left to the contributing author in most cases. The number of framework type codes is large but limited; the number of products or recipes is unlimited.

3. T-atom Composition

T-atom composition (top line - far right) refers to the elements, which occupy tetrahedral positions in the framework and their relative numerical abundance (basis: 100 T-atoms). The values are based on the elemental analysis of the product of the recipe as given in Product Characterization. In most cases, values are rounded to integer values except where a minor T component has particular significance.

4. Contributed by

The name(s) indicate the person or persons who actually prepared the entry and is intended to identify the one most likely to respond to communications regarding the recipe. The entries are not intended for full scientific recognition for the research, which produced the recipes; in most cases, recognition has already occurred elsewhere in the literature. Authors are identified by name only; academic titles and institutional affiliation are given in the contributor's section.

5. Verified by

Verifiers are those Independent investigators who have reproduced the synthesis experiment and obtained a satisfactory product by their own evaluation. Again, only names are given here; for institutional affiliation, see the contributors list. Negative responders, those who replicated the experiment but obtained a product other than the

desired phase, are acknowledged in the contributors' section. In many cases, the responses of verifiers have prompted changes in the recipes.

6. Type Material

Type material refers to contents of the unit cell as indicated by the elemental analysis. In most cases, the product has been washed and dried but not calcined. Thus the template is often a component of the product composition. Water contents of the products are not consistent; only in some cases has the synthesis product been equilibrated under controlled humidity.

7. Method

Method Cites the literature report on which the recipe is based, usually the authors report but sometimes an earlier, more general reference. Patent references have been avoided unless they are specific. It is the intention of this volume that the reader be directed to the single recipe that gives the best chance of immediate success in the synthesis.

8. Batch Composition

Batch composition refers to the product of batch preparation stated in ratios of oxides, template molecules and neutralization products. The basis is usually a single formula weight of Al_2O_3 or another trivalent oxide; occasionally the base is SiO_2 or P_2O_5

9. Source Materials

Source materials are those actual materials used to prepare the batch along with their purity and supplier. Generally, the source materials are stated in the order in which they are used in preparing the batch. The authors have been encouraged to be specific as to the suppliers because many failures to replicate have been traced to the change of supplier for a source material, particularly in the case of silica or alumina. In most cases, the balance of the composition of the component is assumed to be H_2O and should be included in calculating batch composition.

10. Batch Preparation

Batch preparation refers to actual quantities of materials plus the preparation steps used to prepare material for the crystallization step. The estimate of product yield is intended for the readers' convenience. For each step, the materials added and the orders of addition are indicated within the brackets. Order of addition has been found to be critical in some cases. Instructions for completing the step follow the brackets. Combination at room temperature is contemplated unless otherwise stated. Completion of the batch preparation in a matter of minutes or of hours is expected unless delay is specifically required.

11. Crystallization

Crystallization refers to the experimental conditions and temperature profile, which converts the finished batch to product slurry of zeolite crystals in a "mother liquor." The containing vessel is assumed to be inert except in special cases. Accidental seeding by residues of earlier experiments has been shown to be a problem. If autoclaves or their liners are reused, they should be carefully cleaned. Rapid heat-up to the crystallization

temperature is contemplated; rarely is the heat-up time a significant portion of the total treatment. Temperature fluctuations during treatment are to be expected.

Aging or incubation of the finished batch at ambient or some intermediate temperature is part of some treatments. Time / temperature tradeoffs are described in the literature; the intention here is to give the authors best guess as to the optimum treatment. Monitoring the progress of crystallization can be instructive, but it is difficult in closed autoclaves at temperatures above 100ºC. Rather than sample at temperature or cool, sample, and reheat, the usual approach is to divide the batch into several vessels and treat the aliquots for progressively longer times.

Static treatments or only modest or intermittent agitation is the usual case. Continuous agitation may be required for specific preparations. Any particular conditions of hydrothermal treatment of zeolites if apply are added in the section “Notes”.

12. Product Recovery

Product recovery refers to the procedure for separating the desired product from the byproducts of the crystallization process. Most zeolite products are micron-sized crystals, which are easily filtered while the "mother liquor is a solution of excess alkali silicate, excess template, etc. Very fine product crystals may require centrifugation for good product recovery. For alkaline synthesis, the pH drops as the washing proceeds; pH = 7-10 for the final wash is usually sufficient. For fluoride synthesis or $AlPO_4$-type materials, other criteria for adequate washing are required.

Although most zeolite products are water stable, prolonged washing can produce subtle changes in their composition. Hydrolysis may replace cations with H_30^+ salt or template inclusions may be reduced or eliminated. Some investigators prefer to wash with dilute NaOH rather than pure water. In general, washing conditions must be considered part of the synthesis. Additional information on the purification of nanosized zeolite crystals via high-speed centrifugation is added to the specific recipes.
Drying usually is accomplished in a laboratory oven at ~100C. It is good technique to equilibrate the dried sample at a constant 50% humidity to make it stable to handling in laboratory air. Freeze-drying technique is applied for drying of nanosized zeolites in order to avoid post synthesis agglomeration of nanocrystals.

Yield here is expressed as percent of theoretical yield based on the limiting component (usually Al_2O_3 or SiO_2). In the literature, yield is sometimes expressed as percent by weight based on the finished crystallization batch.

12.1 Flocculation

Sometimes flocculation, a method of agglomerating fine particles to filterable size, is advantageous. An example of an organic flocculant is a detergent-type molecule, which adsorbs with the hydrophilic end on the hydrophilic zeolite particle surface, with the hydrophobic end extending into the aqueous medium. The thus generated hydrophobic particles coagulate to form flocs or flocks, which can be filtered and washed on the filter with water.

Before applying such an organic flocculant, the alkalinity of the crystallized reaction mixture needs to be reduced. The application of an electrolyte, such as NaCl, as a flocculant, however, has the disadvantage that colloidal silica present in the mother liquor

is coagulated as well, so that the crystallinity of, for example, zeolite alpha will be <90%. If this is acceptable, NaCl is added with mild stirring (magnet bar) until, after turning off the stirrer, flocs become visible, first where the meniscus meets the glass. The flocculated product will settle, and the supernatant liquid can be decanted. The sediment may be filtered, but washing with water causes the flocs to disintegrate, and the crystallites will pass the filter again. Washing, however is not necessary. Instead, the filter cake is reslurried, and now an organic flocculant, such as Betz No. 1192, which is added in small portions of a 0.2% solution, until complete flocculation is observed, can be applied. The thus flocculated product can be filtered and washed with water.

If coagulation of the colloidal silica is to be avoided, the strongly diluted crystallized reaction mixture can be left undisturbed for settling, if necessary, for as long as a few days, or centrifuged. The supernatant solution is cautiously decanted from the sediment. If complete settling is not achieved, the small amount of solids left in suspension may be sacrificed. The sediment is then reslurried and flocculated with an organic flocculant, such as Betz No. 1192, filtered and washed, as described above

13. Product characterization

Product characterization identifies the crystalline product and compares its properties to those of known standards. For this volume, basic characterizations are the X-ray diffraction pattern, elemental analysis and crystal size and habit from SEM. For particular applications, several other characterizations might be desired, such as sorptive capacity, ion exchange properties, thermal analysis, nuclear magnetic resonance, particle size, etc. Not many authors report their products in such detail, and in some cases it is difficult to obtain data reproducible in another laboratory. Secondary characterization, when provided, is reported in the Notes section.

14. XRD

XRD refers to the principal phase as identified by comparison of its x-ray diffraction pattern with those in the literature. Unit cell parameters are usually given. When competing crystalline phases have been identified from extraneous lines, they are indicated plus an estimate of amorphous material from the background intensity. A reference pattern for the product in the "as synthesized" is attached. In some cases, a second pattern of the calcined product is provided. Some of the calcined materials, particularly $AlPO_4$ and $GaPO_4$, are moisture-sensitive. For other cases the calcined material is virtually identical in the XRD pattern to the as-synthesized sample. In such cases no XRD trace of the calcined product is given. A separate article describes the instrument conditions for recording the XRD patterns.

15. Elemental Analysis

Elemental analysis gives ratios of metal cations present usually expressed as the ratios of their oxides. The editor prefers the direct analytical result (weight percent of the element or its oxide based on the dry sample). Most authors give ratios of the oxides based on one formula weight of Al_2O_3 or SiO_2. In most cases, these were determined by inductively coupled plasma emission spectroscopy. In some cases, the content of water or template molecules in the product as indicated by thermal analysis is also included.

16. Crystal Size and Habit

Crystal size is an estimate of the crystallite size and/or the aggregate particle size. Habit is a qualitative description of the sample as observed in the SEM.

17. References

References indicate the primary literature report on which the recipe is based plus selected general references recommended by the author. This list is intentionally limited and is intended to start the users search of the literature, not complete it.

18. Notes

The notes give additional instructions or information which the author believes helpful to the reader but which do not fit into the recipe format. The additional instructions are intended to substitute for a private conversation with the author before the reader/user begins the synthesis experiment. It is potentially the most valuable part of the contribution.

IV. Conditions for recording of XRD patterns

Nicolas Barrier
Normandie Université, ENSICAEN, UNICAEN, CNRS, CRISMAT, 6 boulevard Maréchal Juin, 14050 Caen, France
36 new samples included in the 3rd edition

The powder X-ray diffraction (PXRD) patterns were recorded with a BRUKER D8 advance diffractometer in Bragg-Brentano geometry. The diffractometer was equipped with a Ge-focusing primary monochromator giving Cu-Kα radiation (λ = 1.5406 Å), a Lynxeye detector operated with 3.5° opening. A fix divergence slit of 0.6 mm was used as well as primary and secondary Soller slits of 2.5°. A beam knife and an 8 mm anti scattering slit placed in front of the Lynxeye detector were also used. All diffraction patterns were recorded within the 2θ range 2 - 50° with a step size of ~0.014° and a time per step of 4 s. Since no diffraction peaks are observed below 4°(2θ) all patterns were rescaled on the 2θ range: 4 - 50°. The diffraction patterns are presented in the as measured condition without any background subtraction or smoothing.
All samples have been intimately crushed in an agate mortar and then placed on back loading sample holders to limit preferential orientation. For samples in too small amounts the powder was deposited on a flat silicon zero-background sample holder.

Karl Petter Lillerud
Department of Chemistry University of Oslo P.R.1033 Blindem, N-0315 Norway
72 samples reproduced from the 2nd edition

The X-ray diffraction (XRD) patterns were recorded with a SIEMENS D5000 diffractometer. The diffractometer was equipped with a Ge-focusing primary monochromator giving Cu-Kα radiation (λ = 1.5406 Å), a BROWN 70 mm linear position sensitive detector (PSD) and a 40 position sample changer. The PSD is operated with 8° opening. A variable entrance slit giving a constant 6 x 12 mm exposed area is used. The reported intensity distribution is for fixed slit geometry. The diffraction patterns are recorded with variable slit, but presented with at the intensity distribution recalculated to simulate fixed slit mode. The intensity scale (ordinant) for all patterns is K-Counts/second. For comparison with measured diffraction patterns is it important to note that routine measurements are often pefformed with a slit that will expose more than the sample area at low angle. The observed intensities at low angle will therefore be too small compared with these reference patterns and calculated patterns. In this version of the collection all patterns are scaled to the same absolute intensity. The diffraction patterns are presented in the as measured condition without any background subtraction or smoothing. Some samples contain elements that give raised fluorescence, like Fe and Co. No filter or secondary monochromator has been used to remove this radiation.

V. Contributors

The authors of recipes with mailing addresses and institutional affiliation in this volume are identified by name only in the recipe. A truthful effort has been made to update or verify addresses from the second edition recipes, which are included in the third. Changes of affiliation are to be expected.

Dr. Shakeel Ahmed
Center for refining and Petrochemicals, KFUPM Dhahran 31261, Saudi Arabia

Dr. Wha-Seung Ahn
Inha University, Department of Chemical Engineering
Inchon 402-751, Korea

Prof. Rosario Aiello
University of Calabria
Department of Chemistry and Materials Engineering, 87030 Rende (CS), Italy

Dr. Deepak B. Akolekar
R&D Center, Dow Chemical International Private Limited, Pune, Maharashtra 411 006, India

Dr. Duncan E. Akporiaye
SINTEF, Postboks 124 Blindem
N-0314 Oslo, Norway

Prof. Alberto Alberti
Department of Earth Sciences, University of Ferrara, Via Saragat, 1, I-44100 Ferrara, Italy

Dr. Michael W. Anderson
School of Chemistry, University of Manchester, Manchester M13 9PL, United Kingdom

Dr. Sunil Ashtekar
Shell Technology India, Pvt. Ltd. India

Dr. Hussein Awala
Laboratoire Catalyse et Spectrochimie, Normandie Université, ENSICAEN, CNRS, 6 Maréchal Juin, 14050 Caen, France

Dr. Kenneth J. Balkus
Department of Chemistry, Univ. of Texas at Dallas, Richardson, TX 75083-0688, USA

Dr. Rajib Bandyopadhyay
Department of Instrumentation and Electronics Engineering, Jadavpur University, Kolkata 700 098, India

Dr. Theo P. M. Beelen
Eindhoven University of Technology, Laboratory Inorganic Chemistry and Catalysis
P. O. Box 513, 5600 MB Eindhoven, The Netherlands

Dr. Elena I. Basaldella
CINDECA, (CONICET-CIC-UNLP) 47 No 257, B1900 AJK La Plata, Argentina

Prof. Peter Behrens
Laboratorium für Nano- und Quantenengineering (LNQE), Leibniz Universität Hannover, Hannover, Germany

Prof. Alexis T. Bell
Dept. of Chemical and Biomolecular Engineering, Univ. of Calif., Berkeley, CA 94720-1462, USA

Brice Bellet
Institut de Science des Matériaux de Mulhouse (IS2M) UMR 7361 CNRS – UHA, 3bis rue Alfred Werner, 68093 Mulhouse Cedex, France

Dr. Giuseppe Bellussi
SVP Downstream R&D Development, Operations & Technology, Via Maritano, 26 - 20097 San Donato Milanese, Italy

Nuria Benavent

Instituto de Tecnología Química (UPV-CSIC) 46022-Valencia, Spain

Dr. Teresa Blasco
Instituto Tecnologia Quimica UPV-CSIC, Universidad, Politecnica Valencia, 46022 Valencia, Spain

Dr. Ramesh B, Borade
Lawrence Berkeley National Laboratory, Life Sciences Division, One Cyclotron Road, MS 55-121, Berkeley, CA 94720, USA

Marcela Bottale
Ingeniero Hugo A Destefanis
Universidad Nacional de Salta Consejo Nacional de Investigaciones Cientificas y Tecnicas, Buenos Aires 177, 4400 Salta-R, Argentina

Prof. Susan M. Bradley
Department of Chemistry, University of Calgary, Vancouver, B. C. V6T IZl, Canada

Prof. Jocelyne Brendle
Institut de Science des Matériaux de Mulhouse (IS2M) UMR 7361 CNRS – UHA, 3bis rue Alfred Werner, 68093 Mulhouse Cedex, France

Mr. Henk van Breukelen
NOB Scenic Services, Postvak D-11, P.O. Box 10,1200 JB, HILVERSUM, The Netherlands

Dr. Josip Bronic
Division of Materials Chemistry, Ruder Boskovic Institute, Bijenicka 54 10000 Zagreb, Croatia

Dr. Angelika Bruckner
Leibniz-Institut für Katalyse an der Universität Rostock, Albert-Einstein-Strasse 29a, 18059 Rostock, Germany

Prof. J.-Ch. Buhl
Institut fur Mineralogie, Universitat Hannover, D-30167 Hannover, Germany

Dr. Miguel A. Camblor
Instituto de Ciencia de Materiales de Madrid (ICMM), Consejo Superior de Investigaciones Científicas (CSIC), Sor Juana Inés de la Cruz 3, 28039 Madrid, Spain

Prof. J. M. Campelo
Department of Organic Chemistry, Cordoba University, Campus de Rabanales, Edificio C-3, Carretera Nacional IV-A, km 396, 14014-Cordoba, Spain

Dr. Angela Carati
EniTechnologie Gruppo Eni
20097 San Donato Milanese, Italia

Mr. Dilson Cardoso
Federal Univ. Sao Carlos, Chemical Engineering Dept. P. O. Box 676, 13565-905 Sao Carlos, SP, Brazil

Dr. Juergen Caro
Institut für Physikalische Chemie und Elektrochemie, Leibniz Universität Hannover, Callinstr. 22, D-30167 Hannover, Germany

Dr. Vinton Carter
School of Chemistry, University of St Andrews, North Haugh, St. Andrews KY16 9ST, UK

Dr. Mario J. Castagnola
School of Chemistry, The QjLieen's University of Belfast, Belfast BT9-5AG, UK

Prof. Philippe Caullet
Institut de Science des Matériaux de Mulhouse (IS2M) UMR 7361 CNRS – UHA, 3bis rue Alfred Werner 68093 Mulhouse Cedex, France

Dr. Jiri Cejka
J. Heyrovský Institute of Physical Chemistry, Academy of Sciences of the Czech Republic, Prague, Czech Republic

Prof. D. K. Chakrabarty

Department of Chemistry, Indian Institute of Technology, Bombay 400 076, India

Seung Hyeok Cha
School of Environmental Science and Engineering/Department of Chemical Engineering, POSTECH, Pohang 790-784, Korea

Prof. Kuei-Jung Chao
National Tsing Hua University, Dept. of Chemistry, Hsinchu, Taiwan 30043, ROC

Dr. Thierry Chatelain
Institut Textile de France
BP 60, 69132 Ecully Cedex, France

Dr. Anthony K. Cheetham
Department of Materials Science and Metallurgy, University of Cambridge, Cambridge, UK

Dr. Jie-Sheng Chen
School of Chemistry and Chemical Engineering, Shanghai Jiao Tong University, Shanghai, China

Dr. Watcharop Chaikittisilp
School of Engineering, Department of Chemical System Engineering, University of Tokyo, Japan

Mrs. Marie-Agnes Chevallier
Aarhus University, Langelandsgade 140, 8000 Aarhus, Denmark

Prof. Shu-Hua Chien
Institute of Chemistry, Academia Sinica, Taipei 11529, Taiwan, ROC

Dr. S. V. V. Chilukuri
Catalysis & Inorganic Chemistry Division, CSIR-National Chemical Laboratory, Dr Homi Bhabha Road, Pune-411 008, India

Dr. Osamu Chiyoda
California Institute of Technology
Pasadena, CA 91125, USA

Dr. Thierry Cholley
Elf, Centre de Recherche ELF Solaize, BP 22, F-69360 Solaize, France

Dr. Andrzej Cichocki
Faculty of Chemistry, Dept. of Chemical Technology, Jagiellonian University, 30-060 Krakow, Poland

Dr. Ankica Cizmek
Ruder Boskovic' Institute, P. O. Box 1016, HR-10001 Zagreb, Croatia

Prof. Carmine Colella
Dipartimento di Ingegneria dei Materiali e della Produzione, Universita Federico II P. Le V. Tecchio 80, 80125 Napoli, Italy

Prof. Avelino Corma
Institute de Tecnologia Quimica (ITQ), UPV-CSIC, Universidad Politecnica de 46022 Valencia, Spain

Miss Sarah L Cresswell
School of Natural Sciences, Griffith University, Australia

Dr. Eddy Creyghton, CTCAT/3
Shell Research and Technology Center, Amsterdam Badhuisweg 3, 1031 CM, Amsterdam, The Netherlands

Dr. Tracy M. Davis
Chevron Energy Technology Company
100 Chevron Way, 10-1506, Richmond, CA 94802, USA

Dr. Mark E. Davis
Chemical Engineering Dept. California Inst of Technol. Pasadena, CA 91125, USA

Dr. In Rob de Ruiter
Hoechst Holland N.V., Vestiging Vlissingen, Postbus 654380 AB VLISSINGEN, The Netherlands

Dr. Jean Daou
Institut de Science des Matériaux de Mulhouse (IS2M) UMR 7361 CNRS –

UHA, 3bis rue Alfred Werner, 68093 Mulhouse Cedex, France

Dr. Uwe Deforth
Johannes Gutenberg - Universitat Mainz Institut fur Anorganische Chemie und Analytische Chemie W-55099 Mainz, Germany

Dr. Miroslaw Derewinski
Intitute of Catalysis, Polish Academy of Sciences, Poland
Pacific Northwest National Laboratory, United States

Dr. Maria-Jose Diaz-Cabanas
Depto. de Ingeniería, Área Farmacia y Tecnología Farmacéutica, Universidad Miguel Hernández, Carretera Alicante-Valencia km. 87, 03550 San Juan, Alicante, Spain

Dr. Jinxiang Dong, Chem MRSC
Research Institute of Special Chemicals, Taiyuan University of Technology, Taiyuan 030024 Shanxi, PRC

Prof. Emil Dumitriu
Technical University “Gh. Asachi”, Faculty of Chemical Engineering and Environmental Protection, Lasi, Romania

Prof. John Dwyer
Centre for Microporous Materials, UMIST, P. O. Box 88, Manchester, M60 IQD, UK

Prof. Alan Dyer
Department of Chemistry and Applied Chemistry
University of Salford, Salford, M5 4WT, UK

Prof. Stefan Ernst
Department of Chemistry, Chemical Technology, University of Kaiserslautern, P. O. Box 3049, D-67653 Kaiserslautern, Germany

Dr. Mohamad El-Roz
Laboratoire Catalyse et Spectrochimie, Normandie Université, ENSICAEN, CNRS, 6 Maréchal Juin, 14050 Caen, France

Dr. N. P. Evmiridis
Department of Chemistry, University of loannina 45110 loannina, Greece

Prof. Eduardo Falabella Sousa-Aguiar
Department of Organic Chemistry, School of Chemistry, Federal University of Rio de Janeiro, Brazil

Prof. Wei Fan
Goessmann Laboratory Chemical Engineering Department University of Massachusetts Amherst 686 N. Pleasant Street Amherst, MA 01003-9303, USA

Prof. Faezeh Farzaneh
Department of Chemistry, University of Azzahra,
Teheran, Iran

Ms. Anne Catherine Faust
Institut de Science des Matériaux de Mulhouse (IS2M), UMR 7361 CNRS – UHA, 3bis rue Alfred Werner, 68093 Mulhouse Cedex, France

Prof. Pal Fejes
Department of Applied & Environmental Chemistry
University of Szeged, H-6720 Szeged, Rerrich B. ter 1, Hungary

Ms. Pingyun Feng
Chemistry Department, University of California, Santa Barbara, CA 93106, USA

Prof. Pingyun Feng
Dept. of Chemistry, Univ. of California at Riverside, Riverside, CA 92521, USA

Prof. Gerard Ferey
Institut Lavoisier, UMR CNRS 8180, Université de Versailles–Saint-Quentin,

45, avenue des États-Unis, 78035 Versailles, France

Dr. Arthur Ferreira
Dept. of Chemistry, University of Aveiro, 3810 Aveiro, Portugal

Dra. Maria Jose Franco
Centro de Investigacion, CEPSA, Picos de Europa 7 San Fernando de Henares, 28850 Madrid, Spain

Dr. Keith C. Franklin
Research & Technology, BNFL Springfields Works, Salwick Preston, Lancashire PR4 OXJ, UK

Dr. Rolf Fricke
Institute of Applied Chemistry Richard-Willstaetter-Str. 12 12489 Berlin-Adlershof, Germany

Dr. Zelimir Gabelica
Institut de Science des Matériaux de Mulhouse (IS2M) UMR 7361 CNRS – UHA, 3bis rue Alfred Werner, 68093 Mulhouse Cedex, France

Dr. Thomas Gaffney
Air Products & Chemicals, Inc., 7201 Hamilton Blvd. Allentown, PA 18195-1501, USA

Dr. Zhixian Gao
Tianjin Key Laboratory of Risk Assessment and Control Technology for Environment and Food Safety, Tianjin Institute of Health and Environmental Medicine, Tianjin 300050, China

Dr. Juan Garces
Dow Chemical, CR-1776 Bldg. Midland, MI 48674, USA

Mr. Bryan W. Gamey
Building A19.1, Atomic Weapons Establishment, Aldermaston, Reading, England RG7 4PR, UK

Dr. Feifei Gao
Department of Materials and Environmental Chemistry, Stockholm University Svante Arrhenius V. 16C SE-106 91 Stockholm, Sweden

Dr. Vesela Georgieva
Laboratoire Catalyse et Spectrochimie, Normandie Université, ENSICAEN, CNRS, 6 Maréchal Juin, 14050 Caen, France

Mr. Godefroy Gbery
Department of Chemistry, University of Texas at Dallas Richardson, TX 75083-0688, USA

Mr. Arjan Giaya
Triton Systems, Inc., Chelmsford, Massachusetts, USA

Dr. Thurman E. Gier
Dept. of Chemistry, Univ. of California at Santa Barbara, CA 93106-9510, USA

Prof. Girolamo Giordano
University of Calabria, Department of Chemistry and Materials Engineering, 87036 Rende (CS), Italy

Mr. Craig Gittleman
General Motors Research and Development Center, Warren, MI 48093, USA

Dr. Julien Grand
Laboratoire Catalyse et Spectrochimie, Normandie Université, ENSICAEN, CNRS, 6 Maréchal Juin, 14050 Caen, France

Dr. R. Van Grieken
Superior School of Experimental Sciences and Technology (ESCET), Rey Juan Carlos University, 28933 Mostoles, Madrid, Spain

Dr. Xinwen Guo
State Key Laboratory of Fine Chemicals, PSU-DUT Joint Center for Energy Research, School of Chemical

Engineering, Dalian University of Technology, Dalian 116024, PR China

Prof. Martin Hartmann
Friedrich-Alexander-Universität Erlangen-Nürnberg, Erlangen Catalysis Resource Center, Egerlandstrasse 3, 91058, Erlangen, Germany

Prof. Kenji Hashimoto
Department of Chemical, Engineering, Kyoto University
Kyoto 606-01, Japan

Dr. David Hayhurst
University of South Alabama, College of Engineering Mobile, AL 36688-0002 USA

Mr. Chang-Qing He
College of Chemistry and Chemical Engineering, Hunan Institute of Science and Technology, Yueyang, Hunan, China

Dr. Heyong He
Department of Chemistry and Shanghai Key Laboratory of Molecular Catalysis and Innovative Materials, Fudan University, Shanghai 200433, China

Prof. Suk Bong Hong
National Creative Research Initiative Center for Ordered Nanoporous Materials Synthesis, Department of Chemical Engineering, POSTECH, Pohang 790-784, Korea

Prof. Qisheng Huo
State Key Laboratory of Inorganic Synthesis & Preparative Chemistry
Jilin University, 2699 Qianjin Street
Changchun 130012, China

Prof. Jan H. C. van Hooff
Department of Inorganic Chemistry and Catalysis, Eindhoven University of Technology,13 5600 MB Eindhoven, The Netherlands

Dr. P. D. Hopkins
Sud-Chemie Inc., 1600 W. Hill St. Louisville, KY 40120, USA

Dr. Satoshi Inagaki
Division of Materials Science and Chemical Engineering, Yokohama National University, Tokiwadai 79-5, Hodogaya-ku, Yokohama 240-8501, Japan

Dr. Shinji Iwamoto
Graduate School of Science and Technology, Gunma University, Japan

Dr. Akira Iwasaki
Electro technical Laboratory, 1-1-4 Umezono, Tsukuba Ibaraki 305-8568, Japan

Dr. Mi Young Jeon
Department of Chemical Engineering & Material Sciences, University of Minnesota 421 Washington Ave. SE, Minneapolis, USA

Dr. Changbum Jo
Korea Advanced Institute of Science and Technology, 305-701 Daejeon, Korea

Dr. Wha Jung Kim
Department of Materials Chemistry and Engineering, Konkuk University, 1-Hwa Yang Dong, Kwang Jin Gu, Seoul 143-701, Republic of Korea

Anastasia Kharchenko
Laboratoire Catalyse et Spectrochimie, Normandie Université, ENSICAEN, CNRS, 6 Maréchal Juin, 14050 Caen, France

Prof. Christine Kirschhock
Centre for Surface Chemistry and Catalysis, KU Leuven, Celestijnenlaan 200f - box 2461, 3001 Leuven, Belgium

Dr. Sarah Komaty
Laboratoire Catalyse et Spectrochimie, Normandie Université, ENSICAEN, CNRS, 6 Maréchal Juin, 14050 Caen, France

K. Komura
Division of Materials Science and Chemical Engineering, Graduate School of Engineering, Yokohama National University, Tokiwadai 79-5, Hodogaya-ku, Yokohama 240-8501, Japan

Dr. Ilina Kondofersky
Department of Chemistry
Ludwig-Maximilians-Universität München (LMU)
Butenandtstr. 5-13 (E)
81377 München, Germany

Prof. Yoshihiro Kubota
Division of Materials Science and Chemical Engineering, Yokohama National University, Tokiwadai 79-5, Hodogaya-ku, Yokohama 240-8501, Japan

Dr. Louwanda Lakiss
Laboratoire Catalyse et Spectrochimie, Normandie Université, ENSICAEN, CNRS, 6 Maréchal Juin, 14050 Caen, France

Dr. Christopher M. Lew
Chevron Energy Technology Company, 100 Chevron Way, 10-1506 Richmond, CA 94802, USA

Prof. Xinjin Liu
Department of Chemistry, Xiamen University Xiamen, Fujian, 361005, PRC

Prof. Zhongmin Liu
State Key Laboratory of Catalysis, Dalian Institute of Chemical Physics, Chinese Academy of Sciences, Dalian 116023, China

Dr. Huann-Jih Lo
Dept. of Geo Sciences, National Taiwan University, Taipei, Taiwan, ROC

Prof. Raul F. Lobo
Catalysis Center for Energy Innovation, Department of Chemical and Biomolecular Engineering, University of Delaware, Newark, DE, 19716, USA

Dr. Thierry Loiseau
Unité de Catalyse et Chimie du Solide (UCCS)-UMR CNRS 8181, Université de Lille Nord de France, 59652 Villeneuve d'Ascq, France

Prof. Yingcai Long
Fudan University, Department of Chemistry, Shanghai 200433 PRC

Dr. Carmen M. Lopez
Universidad Central de Venezuela, Facultad de Ciencias, Escuela de Quimica, Apartado 47102 Caracas 1020-A, Venezuela

Dr. J. M. Lopez Nieto
Instituto Tecnologia Quimica UPV-CSIC, Universidad Politecnica Valencia, 46022 Valencia, Spain

Prof. Joao Lourengo
Universidade do Algarve, Unidade de Ciencias Exactese Humanas, 8000 Faro, Portugal

Dr. Maria M. Ludvig
AKZO Nobel Catalysts, UC, 13000 Bay Park Rd. Pasadena, TX 77507, USA

Dr. Jim MacDougall
Air Products & Chemicals, Inc., 7201 Hamilton Blvd. Allentown, PA 18195-1501, USA

Dr. Francisco J. Machado
Centro de Catalisis Petroleo y Petroquimica, Universidad Central de Venezuela Caracas 1020-A, Venezuela

Dr. Alain Matijasic
Institut de Science des Matériaux de Mulhouse (IS2M) UMR 7361 CNRS – UHA, 3bis rue Alfred Werner, 68093 Mulhouse Cedex, France

Dr. Gerardo Majano
ExxonMobil, New Jersey, USA

Dr. Lynne B. McCusker
Department of Materials, ETH Zurich, CH-8093 Zurich, Switzerland

Dr. J. A. Melero
Department of Chemical and Energy Tech., Mechanical Tech. and Analytical Chemistry, ESCET, Rey Juan Carlos University, 28933 Móstoles, Madrid, Spain

Dr. Xianping Meng
Department of Chemistry, Peking University
Beijing 100871, PRC

Dr. Paul Meriaudeau
Institut de Recherches sur la Catalyse, 69626 Villeurbanne, France

Dr. Abdallah Merrouche
Laboratoire des Matériaux inorganiques, Université Mohamed Boudiaf, M'Sila 28000, Algeria

Dr. Machteld M. Mertens
ExxonMobil Chemical, Hermeslaan, 2 1831 Machelen, Belgium

Dr. Dean M. Millar
The Dow Chemical Company, Corporate R and D, Chemical Sciences, 1776 Bldg., USA

Dr. Stephen Miller
The George and Josephine Butler Laboratory for Polymer Research, University of Florida, Gainesville, Florida 32611, USA

Dr. Roberto Millini
Renewable Energy&Environmental Laboratories, Eni S.p.A., Via Fauser 4, I-28100 Novara, Italy

Dr. Svetlana Mintova
Laboratoire Catalyse et Spectrochimie, Normandie Université, ENSICAEN, CNRS, 6 Maréchal Juin, 14050 Caen, France

Dr. Manuel Moliner
Instituto de Tecnología Química (UPV-CSIC) 46022, Valencia, Spain

Maja Mrak
National Institute of Chemistry, Hajdrihova 19 Sl-1001 Ljubljana, Slovenia

Dr. Oki Muraza
Department of Chemical Engineering, King Fahd University of Petroleum & Minerals (KFUPM)
Bld 15-3114 PO Box 5040 Dhahran 31261 KSA

Prof. Alexandra Navrotsky
Peter A. Rock Thermochemistry Laboratory, Department of Chemistry, University of California Davis, 1 Shields Avenue, Davis, CA 95616, USA

Dr. Nguyen Huu Phu
National Center for Science and Technology of Vietnam, Vien Hoa hoc, NCST Duong Hoang Quoc Viet, Nghia do Cau Giay, Hanoi-Vietnam

Prof. Eng-Poh Ng
School of Chemical Sciences Universiti, Sains Malaysia 11800 USM, Pulau Pinang, Malaysia

Dr. Poul Norby
Department of Energy Conversion and Storage, Technical University of Denmark, Risø Campus, 4000 Roskilde, Denmark

Dr. Mario Occelli
MLO Consultants, 6105 Blackwater Trail, Atlanta, GA 30328, USA

Prof. Tatsuya Okubo
Department of Chemical System Engineering, The University of Tokyo, 7-3-1 Hongo, Bunkyo-ku, Tokyo 113-8656, Japan

Yasunori Oumi
Division of Instrument Analysis, Life Science Research Center, Gifu

University, 1-1 Yanagido, Gifu 501-1193, Japan

Dr. G. Ovejero
Chemical Engineering Dept, Faculty of Chemistry, Universidad Complutense, 28040 Madrid, Spain

Dr. Anders E. C. Palmqvist
Department of Chemical and Biological Engineering, Chalmers University of Technology, SE 412 96 Göteborg, Sweden

Dr. John Parise
Geosciences, State Univ. of New York at Stony Brook, Stony Brook NY 11794-2100, USA

Pr. Sohyun Park
Department of Earth and Environmental Sciences, Ludwig-Maximilians-Universität München, Theresienstr. 41, 80333 Munich, Germany

Dr. Ana Palčić
Division of Materials Chemistry, Ruder Boskovic Institute, Bijenicka 54 10000 Zagreb, Croatia

Dr. Jean-Louis Paillaud
Institut de Science des Matériaux de Mulhouse (IS2M), UMR 7361 CNRS – UHA, 3bis rue Alfred Werner, 68093 Mulhouse Cedex, France

Dr. Joel Patarin
Institut de Science des Matériaux de Mulhouse (IS2M), UMR 7361 CNRS – UHA, 3bis rue Alfred Werner 68093 Mulhouse Cedex, France

Dr. M. L Pavlov
Zelinsky Institute of Organic Chemistry, Leninsky Pr. 47, 117334 Moscow, Russia

Dr. Joaquin Perez-Pariente
Instituto de Catálisis y Petroleoquímica, ICP-CSIC, C/Marie Curie 2, 28049 Madrid, Spain

Dr. Patrick M. Piccione
Chemical Engineering Department
California Institute of Technology
Pasadena, CA 91125, USA

Dr. A. M. Prakash
Department of Chemistry, University of Houston, Houston, TX 77204-5641, USA

Pr. Geoffrey Price
Department of Chemical Engineering, University of Tulsa, 600 South College Ave.Tulsa, OK 74104-3189, USA

Dr. Andreas Puškarić
Division of Materials Chemistry, Ruder Boskovic Institute, Bijenicka 54 10000 Zagreb, Croatia

Dr. Mojca Rangus
National Institute of Chemistry
Hajdrihova 19 SI-1001 Ljubljana, Slovenia

Prof. Jeffrey D. Rimer
University of Houston, Department of Chemical and Biomolecular Engineering 4800 Calhoun Road, S222 Engineering Building 1 Houston, TX 77204-4004, USA

Dr. Raman Ravishankar
Centrum voor Oppervlaktechemie en Katalyse Kardinaal Mercierlaan 92, B-3001 Heverlee, Belgium

Dr. K. M. Reddy
Department of Materials Science and Engineering, The Ohio State University, Columbus, OH 43210, USA

Dr. K. S. N. Reddy
National Chemical Laboratory, Pune - 411 008, India

Prof. L. V. C. Rees
Department of Chemistry, University of Edinburgh
Edinburgh EH9 3JJ, UK

Prof. Hyun-Ku Rhee

School of Chemical Engineering and Institute of Chemical Processes, Seoul National University Kwanak-ku, Seoul 151-742, Korea

Dr. Fernando Rey
Instituto de Tecnología Química (UPV-CSIC) 46022-Valencia, Spain

Dr. F. Ramoa Ribeiro
Institute for Biotechnology and Bioengineering, Centre for Biological and Chemical Engineering, Instituto Superior Técnico, Universidade Técnica de Lisboa Lisboa, Portugal

Dr. Alenka Ristic
National Institute of Chemistry
Hajdrihova 19, SI-1001 Ljubljana
Slovenia

Dr. Harry Robson
Dept of Chemical Engineering, Louisiana State Univ., Baton Rouge, LA 70803-7303, USA

Prof. Joao Rocha
Department of Chemistry, CICECO, University of Aveiro, 3810-193 Aveiro, Portugal

Dr. Javier Agundez Rodriguez
Instituto de Catalisis y Petroleoquimica. CSIC, Campus U.A.M. Cantoblanco, 28049 Madrid, Spain

Dr. Radu Russu
Research Institute for Petroleum Processing and Petrochemistry (ICERP) Bd. Republicii nr. 29 lA, Ploiesti 2000, Romania

Prof. Douglas M. Ruthven
Department of Chemical and Biological Engineering, Univ. of Maine, Orono, ME 04469, USA

Prof. Ryong Ryoo
Dept. of Chemistry, Korea Advanced Institute of Science and Technology, 305-701 Daejeon, Korea

T. Sano
Division of Materials Science and Chemical Engineering, Yokohama National University, Tokiwadai 79-5, Hodogaya-ku, Yokohama 240-8501, Japan

Prof. Mitsuo Sato
Department of Chemistry, Gunma University
Kiryu, Gunma 376, Japan

Dr. Oliver Schaf
Laboratoire MADIREL - UMR7246
Aix-Marseille Université, Campus Scientifique de St. Jérôme
F-13397 Marseille Cedex 20, France

Dr. Franziska Scheffler
Institut für Chemie (ICH)
Universitätsplatz 2, 39106, Magdeburg, G16-102, Germany

Dr. Dusan Stosic
Laboratoire Catalyse et Spectrochimie, Normandie Université, ENSICAEN, CNRS, 6 Maréchal Juin, 14050 Caen, France;
Vinca Institute of Nuclear Sciences, PO Box 522, RS-11001 Belgrade, University of Belgrade, Serbia

Jiho Shin
School of Environmental Science and Engineering/Department of Chemical Engineering, POSTECH, Pohang 790-784, Korea

Dr. Wolfgang Schmidt
Max-Planck-Institut für Kohlenforschung, Kaiser-Wilhelm-Platz 1, 45470 Mülheim an der Ruhr, Germany

Dr. Brian Schoeman
Dow Chemical Company, Catalysis R and DCR- 1776 Building, Midland, MI 48674, USA

Dr. Celine Schott-Darie

Laboratoire de Cristallographie, CNRS
Bat. F., BP 166, 38042 Grenoble, France

Dr. Laurence Schreyeck
Laboratoire de Chimie Moleculaire et Environnement, Universite de Savoie – ESIGEC, 73376 Le Bourget de Lac Cedex, France

Prof. Gunter Schulz-Ekloff
Institut fur Angewandte und Physikalische Chemie, University Bremen, 28334 Bremen, Germany

Dr. Stephan Andreas Schunk
AG - the high throughput experimentation company, Kurpfalzring 104, 69123 Heidelberg, Germany

Prof. Ferdi Schiith
Max-Planck-Institut fuer Kohlenforschung, Kaiser-Wilhelm-Platz 1, 45470 Muelheim, Germany

Dr. Stephan Schwarz
Dupont Central Research and Development, Wilmington DE 19880-0262, USA

Dr. Albert E. Schweizer
Dow Chemical Company, Catalysis R and D, 1776 Building, Midland, MI 48674

Dr. D. P. Serrano
Instituto IMDEA Energía
Avda. Ramón de la Sagra, 3
Parque Tecnológico de Móstoles
E-28935 Móstoles, Madrid, Spain

Dr. Daniel F. Shantz
Department of Chemical and Biomolecular Engineering 323 Boggs Laboratory, Tulane University, New Orleans, LA 70118-5674, USA

Prof. Baojian Shen
College of Chemical Engineering
China University of Petroleum
18 Fuxue Road, Changping, Beijing, 102249, China

Dr. Jimin Shi
Dept. of Chemistry, University of Texas at Dallas, Richardson, TX 75083, USA

Dr. Li Shi
City University of Hong Kong
Department of Biology and Chemistry, Hong Kong

Jiho Shin
National Creative Research Initiative Center for Ordered Nanoporous Materials Synthesis, Department of Chemical Engineering, POSTECH, Pohang 790-784, Korea

Dr. M. A. Shubaeva
Russian Academy of Sciences, Moscow, Russia

Dr. P. Sidheswaran
Hindustan Lever Research Center
Bombay, 400 099, India

Dr. A. K. Sinha
National Chemical Laboratory, Pune - 411 008, India

Dr. S. Sivasanker
Catalysis Division, National Chemical Laboratory
Pune-411 008, India

Dr. Antonio Souza de Araujo
Federal University of Rio Grande do Norte Department of Chemistry, CP 1662 59078-970 Natal RN, Brazil

Prof. Andreas Stein
Department of Chemistry, University of Minnesota, 207 Pleasant St. SE, Minneapolis, MN 55455-0431, USA
Dr. Michael Stocker
SINTEF Oslo, Postboks 124 Blindem, N-0314, Oslo, Norway

Dr. Karl G. Strohmaier
ExxonMobil Research & Engineering Co., Corp. Strategic Research, Adv. Materials, Rt. 22 East Annandale, NJ 08801, USA

Dr. Boris Subotic
Lab. for the synthesis of new materials
Institute Rudjer Boskovic, Bijenicka 54,
10000 Zagreb, Croatia

Dr. Yan Sun
Department of Chemistry, Jilin
University, Changchun 130023, China

Dr. Flaviano Testa
Dipartimento di Ingegneria Chimica e
dei Materiali Universita degla Studi
della Calabria, Via Pietro Bucci, 87030
Arcavacata di Rende (CS), Italy

Prof. John Meurig Thomas
The Master's Lodge, Peterhouse
Cambridge CB2 IaV, UK

Dr. R. W. Thompson
Department of Chemical Engineering,
Worcester Polytechnic Institute,
Worcester, MA 01609-2280, USA

Dr. Huiping Tian
Division 14, Research Institute of
Petroleum Processing, 18 Xueyuan
Rd., Beijing 100083, China

Dr. Lubomira Tosheva
Division of Chemistry & Environmental
Science, Manchester Metropolitan
University
Chester Street, Manchester M1 5GD,
UK

Prof. Michael Tsapatsis
Department of Chemical Engineering &
Material Sciences, University of
Minnesota 421 Washington Ave. SE,
Minneapolis, USA

Dr. Natasa Novak Tusar
National Institute of Chemistry,
Hajdrihova 19,1000 Ljubljana, Slovenia

Dr. Maria A. Uguina
Faculty of Chemistry, Dept. of Chemical
Engineering, University Complutense,
28040 Madrid, Spain

Dr. Myriam Uytterhoeven
SIS-Consult, Rotspoelstraat 361
B 3001, Heverlee, Belgium

Dr. Valentin Valtchev
Laboratoire Catalyse et Spectrochimie,
Normandie Université, ENSICAEN,
CNRS, 6 Maréchal Juin, 14050 Caen,
France

Dr. D. E. W. Vaughan
Pennsylvania State University
276 Materials Research Laboratory,
Hastings Road
University Park, PA 16802-4800

Ms. An Verberckmoes
Centrum voor Oppervlaktechemie en
Katalyse, Katholieke Universiteit
Leuven, B-3001 Heverlee, Belgium

Dr. Dominic Wales
Department of Chemical Engineering,
University of Bath, Somerset, BA2 7AY,
UK

Dr. Ka Lun Wong
Nanyang Technological University
1 Nanyang Walk 637616, Singapore

Changjiu Xia
Department of Materials and
Environmental Chemistry, Stockholm
University Svante Arrhenius V. 16C SE-
106 91 Stockholm, Sweden

Prof. Jihong Yu
State Key Lab of Inorganic Synthesis
and Preparative Chemistry, Jilin
University, 2699 Qianjin Street,
Changchun, China

Dr. Moussa Zaarour
Laboratoire Catalyse et Spectrochimie,
Normandie Université, ENSICAEN,
CNRS, 6 Maréchal Juin, 14050 Caen,
France

Dr. Stacey Zones
Chevron Energy Technology Company,
100 Chevron Way, 10-1506 Richmond,
CA 94802, USA

Prof. Xiaoqin Zou
State Key Lab of Inorganic Synthesis and Preparative Chemistry, Jilin University
2699 Qianjin Street, Changchun, China

Prof. Xiadong Zou
Department of Materials and Environmental Chemistry, Stockholm University Svante Arrhenius V. 16C SE-106 91 Stockholm, Sweden

Prof. Hannelore Vinek
Technical University of Vienna, Institut for Physical Chemistry, A-1210 Vienna, Austria

Dr. Dong Fan
Laboratoire Catalyse et Spectrochimie, Normandie Université, ENSICAEN, CNRS, 6 boulevard Maréchal Juin, 14050 Caen, France

Dr. Zhengxing Qin
Laboratoire Catalyse et Spectrochimie, Normandie Université, ENSICAEN, CNRS, 6 boulevard Maréchal Juin, 14050 Caen, France

Dr. Kristin Vinje
SINTEF Materials Technology, Polymer Chemistry Dept., Postboks 124 Blindern, N-0314 Oslo, Norway

Dr. Juliusz Warzywoda
CAMMP, Northeastern University
342 Snell Engineering Center, Boston, MA 02115, USA

VI. Introductory Articles

1. Initial materials for synthesis of zeolites

Jean-Louis Paillaud and Joël Patarin

Institut de Science des Matériaux de Mulhouse (IS2M), Groupe Matériaux à Porosité Contrôlée, UMR 7361 CNRS - Université de Haute-Alsace, 3 bis, rue Alfred Werner, 68093 Mulhouse Cedex, France

Introduction

The origin of zeolites comes from microporous aluminosilicates. Today, the word 'zeolite' is no longer restricted to this type of materials. It refers to any silica-based crystalline microporous solid in which some of the silicon is replaced by other elements T such as the trivalent elements T = Al, Fe, B, Ga, etc., or tetravalent elements T = Ti, Ge, etc. Depending on the Si/T molar ratio, the materials are classified into two groups; zeolites when the Si/T < 500 and zeosils with the Si/T > 500.

Zeosils and clathrasils form the two classes of silicic materials in the porosil family. Phosphate-type crystalline microporous solids are commonly called related microporous solids. Generally, the microporous solids are characterized by a 3D framework resulting from the stringing together of tetrahedral units TO_4 with shared oxygen vertices (T = Si, Al, P, Ge, Ga, etc.); channels and/or cavities with molecular-sized cross-sections, connected with the surrounding medium. The formed channel systems are 1-, 2- or 3-dimensional. Microporous materials with cage structures are 0-dimensional.

Real structures may deviate from this ideal definition by the presence of units with non-tetrahedral coordination, e.g., TX_5, or TX_6 polyhedra, where X = O, F, or non-bridging neighboring units, e.g., T–OH, T–F or $T–O^-$ end groups as in interrupted frameworks. The structural code comprises three capital letters, which are attributed by the structure commission of the International Zeolite Association (IZA) to each structure obtained in this way. If the framework is interrupted, the 3-letters are preceded by a hyphen. In the case of zeolites crystallizing as disordered structures, a star precedes the 3-letters codes. Only few structures have both [1].

Synthesis of zeolites and related materials

Zeolite and related materials are usually obtained by hydrothermal crystallization of a gel comprising a liquid and a solid phase. The reaction medium contains:
-a sources of framework elements T = Si, Al, P, etc.,
-a sources of mineralizing agents OH^-, F^-,
-an inorganic cations and/or organic species (neutral molecules or cations),
-a solvent (usually water).

Zeolites are generally synthesized in a basic medium at temperatures below 200°C and low pressures (autogenous pressure < 20 bar). In the case of related microporous materials (aluminophosphates, etc.), the pH of the reaction medium is general in the range 3–10. The anions OH^- [2] or F^- [3-5] solubilize the reactive species in the gel (formation of silicates and fluorosilicates) and enable their transfer to the growing crystals. The time required for this kind of synthesis is extremely variable, but generally somewhere between a few hours and several days.

The nature of the reactants and their purity can have a huge impact on the synthesis of these solids [6]. The presence of impurities can cause undesired species to nucleate. It can be the case for the synthesis of zeosils (pure-silica zeolites) where a pure-silica source has to be used as reactant. Indeed, the silica source can be contaminated by traces of aluminum used for shaping for instance. Therefore, zeolites with high silicon to aluminum ratio are obtained instead of pure zeosils. In some cases, less pure reactants can be used to prepare zeolites but their composition can be varied from one batch to the other and from one supplier to the other. Therefore, the source materials for zeolite synthesis and technical grade materials need to be assayed and analyzed for impurities. A description of the most popular reactants is given below.

Sources of silica

Several kinds of silica sources can be found, fumed silica, precipitated silica or colloidal silica. As mentioned above, depending on the type of microporous solids to be synthesized, the choice of the silica source can be crucial.

Zeosils can be prepared using fumed silica. These silica sources correspond to pure SiO_2. Such sources are on the market. The water content is very low (about 3 wt. %) Such silica sources allow to get zeosils with Si/Al molar ratios above 10,000.

Other pure silica sources are the tretraalkylorthosilicates. The most common source is the tetraethylorthosilicate (TEOS). Its hydrolysis leads to the formation of SiO_2 and four molecules of ethanol. Be careful, the presence of alcohol can change the synthesis medium; the main solvent being not water but a mixture of water/ethanol. Although the effect is slight, this can lead to synthesis of non-desired compounds. However, ethanol can be removed before synthesis (evaporation by heating). With such silica sources, pure zeosils can be synthesized.

When Si/Al ratios above 6,000 are acceptable, colloidal silica solution can be used. These sources are available with different SiO_2 concentrations; the water coming from the silica source has to be taken into account for the molar composition of the reactant mixture.

Precipitated silica allows to obtain zeolites with Si/Al molar ratios above 200. A widely used silica source is aqueous sodium silicate also known as water glass or liquid glass. According to the manufacturer, it contains different amount of water. It is slightly cloudy; a small contamination with aluminum prevents zeolites with Si/Al ratios above 300 to be crystallized.

Sources of aluminum

Sodium aluminate may be used in zeolite synthesis in particular for zeolites with a low Si:Al molar ratio. This is because CO_2 gas present in air reacts with sodium aluminate just upon storage, forming Na_2CO_3 and aluminum hydrate and therefore lowering the pH of solutions. Therefore, it is recommended to use fresh prepared sodium aluminate solutions. An interesting aluminum source is pseudoboehmite of formula AlOOH. Among the aluminum salts, hydrated aluminum sulfates $Al_2(SO_4)_3$ is often used in zeolites synthesis. Alkoxides are also sources of aluminum; the most used is aluminum isopropoxide. For high Si/Al molar ratios, the presence of isopropanol after hydrolysis in the reacting mixture has a less influence on the synthesis but this is not true in the case of the synthesis aluminophosphate for which the Al:P molar ratio is often 1. Metallic aluminum dissolves in alkaline solution may represent an alternative when other salts do not enable the formation of zeolites. Finally, a zeolite itself like Y zeolite may be used as a source of aluminum; in this case a dissolution-recrystallization process during the hydrothermal treatment is involved.

Sources of hetero T elements

The most widely synthesized metallosilicates are borosilicates, gallosilicates, zincosilicates, titanosilicates and ferrisilicates [7]. Another main family is germanium-containing zeolite (germanosilicates and silicogermanates) [8-9]. It is important to note that the presence of hetero-elements (other than silicon or aluminum) can direct the synthesis and promotes the formation of structures unobtainable in their absence. The nature of the heteroatom associated to silicon can have a real structure-directing role. This is the case of zinc or beryllium, which allow the crystallization of different topologies in (Si,Al) medium, forming 3-membered ring cycles (3-MRs) occupying preferably [10] like for the zincosilicate VPI-7 [11] and beryllosilicate OSB-1 [12] . Other heteroelements such as boron or gallium allowed to obtain original microporous solids such as the borosilicate RUB-13 [13] or gallosilicate TNU-1 [14].

The main sources of boron are boric acid and sodium borate [15]. Also, calcined boron-□ zeolite has been be advantageously used as reactant [16]. Gallium halide salts and gallium oxide or oxy hydroxide obtained by slow calcination at 300°C under air of gallium nitrate are usually the gallium sources. Germanium halide salts, amorphous GeO_2, which dissolves easily in basic solutions, are mainly used as the germanium sources but fine powder of crystallized Ge-quartz is also possible.

The isomorphic substitution of Si by Ti atoms into a zeolite framework is achievable but in a less extent in comparison with aluminum. The first titanosilicate molecular sieve described was Ti-silicalite-1 (TS-1) [17]. The titanium sources are tetraethylorthotitanate, titanium tetrabutoxide or halides $TiCl_4$ and TiF_4. Iron halides, nitrate and sulfate more or less hydrated are used to synthesis iron containing zeolites [18].

Sources of mineralizing agent

In alkali media, the mineralizing agent is OH^- [2], alkali hydroxide (NaOH, KOH), sodium aluminate and hydroxide salts of organic structure directing agents are the main sources. Fluoride anions are generally introduced as HF, NaF, NH_4HF_2 or NH_4F salts in the synthesis mixture. In the case of porosils, the fluoride route has the important advantage to lead to materials with a much lower density of defects due to the charge balance role of the fluoride anions against the positive charge of the organic cations [19-20]. Apart from their mineralizing role, the fluoride anions can play a co-structuring role by stabilizing certain units in the building of the inorganic structure, in particular for the double-four membered rings units (*d4r*) [5,19-20].

Structure-directing agents

The structure-directing agent (SDA) can have multiple roles. It may compensate the charge of the inorganic structure (in the case of a cation). The properties of the synthesis mixture may be modified, e.g. it contributes to an increase of the pH of the reaction gel in the case of cations having OH^- as counter ion. Finally, these species have a structuring effect, i.e. the ability to direct the synthesis to a specific zeolite. There are two types of structure-directing agents in zeolite synthesis, inorganic (ISDA) and organic (OSDA). Alkaline and alkaline earth metals are the main ISDA that play a crucial structure-directing role in zeolites synthesis [21] in particular for zeolites with a low Si/Al molar ratio prepared in highly basic media. Since their first use [22], OSDAs allowed the increase of the number of zeolitic frameworks with different chemical compositions. Many of these topologies have not a natural counter-part. Typically, they are primary, secondary, tertiary, and quaternary amines. Other molecules like alcohols [23] and crown ethers [24] are used. They increase crystallinity and influence the Si/Me molar ratio of the framework. Generally, cationic OSDAs possess a single positive charge but dicationic OSDAs leading to several new topologies, there are diquaternary ammonium

salts [9]. More recently, phosphonium and diphosphonium salts have been successfully used in the synthesis of new zeolites [25-26].

Several behaviors of the OSDA molecules have been identified and classified into three categories [27]. First, the true "OSDA", they correspond to organic species that lead to a zeolite framework to adopt specific geometric and electronic configurations of the OSDA. This is a very rare case illustrated by the example of zeolite ZSM-18 [28]. The second category concerns “structuring agents”, i.e. OSDAs that lead to a zeolite type, and are therefore specific to that topology. Finally, the third category of OSDAs is represented by species that act as “pore-filling” and are therefore not specific to a topology: a given molecule will yield several different materials depending on the synthesis conditions and compositions of the reaction mixtures.
Simple OSDAs are commercially available but most of those used by zeolite chemists are home made in laboratories.

Water content

Dilution of synthetic gels is an important parameter. Indeed, gels differing only by the water content can lead to the crystallization of different structures. Thus, in the pure silica system, high concentrated synthesis media (very low amount of water, H_2O/Si molar ratio below 10) led to pure-silica *BEA-type zeolite [29]. This is also particularly true in the (Si,Ge) and (Si,Ge,Al) system and well illustrated by the ITQ-33 example [30]. It is recommended that the water contained in reactants always must be considered in the preparation of the synthesis mixture [6].

Summary

Hydrothermal synthesis of zeolites and related inorganic microporous materials requires mainly inorganic reactants but the presence of organic species as structure-directing agents may be necessary. These reagents are mixed together to form a gel whose composition must be controlled. For that, it is imperative for the zeolite chemists to check carefully the chemical composition of the reactants before undertaking a synthesis. In this introductory section, we list different sources of reactants that are used for the hydrothermal synthesis of zeolites or related molecular sieves.

References

[1]C. Baerlocher, L.B. McCusker, Database of Zeolite Structures, http://www.iza-structure.org/databases/.
[2]R.M. Barrer, Hydrothermal chemistry of zeolites, Academic Press, London; New York, 1982.
[3]E.M. Flanigen, R.L. Patton, US Patent No. 4073865, (1978)
[4]J.L. Guth, H. Kessler, R. Wey, in: Y. Murakami, A. Iijima, J.W. Ward (Eds.) Stud. Surf. Sci. Catal., Elsevier, 1986, pp. 121-128.
[5]J. Patarin, J.-L. Paillaud, H. Kessler, in: F. Schüth, K.S.W. Sing, J. Weitkamp (Eds.) Handbook of Porous Solids, Wiley-VCH Verlag GmbH, 2002, pp. 815-876.
[6]G. Kühl, in: H. Robson, K.P. Lillerud (Eds.) Verified Syntheses of Zeolitic Materials, Elsevier Science, Amsterdam, 2001, pp. 19-20.
[7]R. Fricke, H. Kosslick, G. Lischke, M. Richter, Chem. Rev., 100 (2000) 2303-2406.
[8]A.K. Inge, X. Zou, in: Q. Xu (Ed.) Nanoporous Materials, CRC Press, 2013, pp. 319-350.
[9]M. Moliner, C. Martínez, A. Corma, Angew. Chem. Int. Ed. Engl., 54 (2015) 3560-3579.
[10]M.A. Camblor, M.E. Davis, J. Phys. Chem., 98 (1994) 13151-13156.

[11]M.J. Annen, M.E. Davis, J.B. Higgins, J.L. Schlenker, Chem. Commun., (1991) 1175-1176.
[12]A.K. Cheetham, H. Fjellvg, T.E. Gier, K.O. Kongshaug, K.P. Lillerud, G.D. Stucky, in: A. Galarneau, F. Fajula, F.D. Renzo, J. Vedrine (Eds.) Stud. Surf. Sci. Catal., Elsevier, 2001, pp. 158.
[13]S. Vortmann, B. Marler, H. Gies, P. Daniels, Microporous Mater., 4 (1995) 111-121.
[14]S. Bong Hong, S. Hern Kim, Y. Gon Kim, Y. Chai Kim, P. A. Barrett, M. A. Camblor, J. Mater. Chem., 9 (1999) 2287-2289.
[15]S.I. Zones, S.-J. Hwang, Microporous Mesoporous Mater., 146 (2011) 48-56.
[16]S.I. Zones, Y. Nakagawa, Microporous Mater., 2 (1994) 557-562.
[17]G. Peregot, G. Bellussi, C. Corno, M. Taramasso, F. Buonomot, A. Esposito, in: A.I. Y. Murakami, J.W. Ward (Eds.) Stud. Surf. Sci. Catal., Elsevier, 1986, pp. 129-136.
[18]G. Giordano, A. Katovic, S. Perathoner, F. Pino, G. Centi, J.B. Nagy, K. Lazar, P. Fejes, in: G.G. R. Aiello, F. Testa (Eds.) Stud. Surf. Sci. Catal., Elsevier, 2002, pp. 477-484.
[19]P. Caullet, J.-L. Paillaud, A. Simon-Masseron, M. Soulard, J. Patarin, C. R. Chim., 8 (2005) 245-266.
[20]J.-L. Paillaud, P. Caullet, J. Brendlé, A. Simon-Masseron, J. Patarin, in: A. Tressaud (Ed.) Functionalized Inorganic Fluorides, John Wiley & Sons, Ltd, 2010, pp. 489-518.
[21]E.M. Flanigen, in: R.F. Gould (Ed.) Molecular Sieves, Advances in Chemistry, American Chemical Society, 1973, pp. 119-139.
[22]R.M. Barrer, P.J. Denny, E.M. Flanigen, US Patent No. 3306922, (1967)
[23]D.M. Bibby, M.P. Dale, Nature, 317 (1985) 157-158.
[24]F. Delprato, L. Delmotte, J.L. Guth, L. Huve, Zeolites, 10 (1990) 546-552.
[25]A. Corma, M.J. Diaz-Cabanas, J.L. Jorda, F. Rey, G. Sastre, K.G. Strohmaier, J. Am. Chem. Soc., 130 (2008) 16482-16483.
[26]R. Simancas, D. Dari, N. Velamazán, M.T. Navarro, A. Cantín, J.L. Jordá, G. Sastre, A. Corma, F. Rey, Science, 330 (2010) 1219-1222.
[27]R. Lobo, S. Zones, M. Davis, J. Inclusion Phenom. Mol. Recognit. Chem., 21 (1995) 47-78.
[28]S.L. Lawton, W.J. Rohrbaugh, Science, 247 (1990) 1319-1322.
[29]M.A. Camblor, A. Corma, S. Valencia, Chem. Commun., (1996) 2365-2366.
[30]A. Corma, M.J. Diaz-Cabanas, J.L. Jorda, C. Martinez, M. Moliner, Nature, 443 (2006) 842-845.

2. Synthesis of new molecular sieves using novel structure-directing agents

Christopher M. Lew, Tracy M. Davis, and Saleh Elomari

Chevron Energy Technology Company, Richmond, California, USA

Introduction

Tremendous progress has been made in zeolite synthesis over the past half century through the pioneering innovations of the zeolite community. At the center of these advancements is the use of organic structure-directing agents (SDAs). Since the early work of Barrer and many others, [1, 2, 3, 4] SDAs have been used to create over 230 unique structural frameworks and any number of different chemical compositions. Initially, small simple molecules, such as tetraalkylammonium cations, were utilized as SDAs, but today, diquaternary and triquaternary ammonium cations, along with phosphonium- and sulfonium-based SDAs are frequently considered in the synthesis of novel zeolites. Figure 1 highlights the key innovations that have driven the field forward and that will be discussed in this article. Using different amine reactions, researchers have created libraries of ammonium SDAs using commercially available reagents. [5, 6, 7, 8] The diversity of SDA sizes, shapes, and charge densities has allowed for the discovery of many new zeolites under a variety of inorganic conditions.

While the mechanism of zeolite nucleation is often related to zeolite-SDA interaction energies, it is well-known that zeolite crystallization is a kinetically controlled process. In addition to SDA choice, several synthesis factors can influence phase selectivity, such as the silica and alumina sources, alkali/alkaline earth cations, hydroxide/fluoride mineralizing agents, gel concentration, and hydrothermal processing conditions. Still, some general rules about SDA size and shape have been observed. For example, large SDAs generally produce large cage-based structures, whereas clathrates and small cage zeolites are templated by smaller SDAs. The synthesis of one-dimensional zeolites is often directed by linear SDAs, while branched SDAs tend to create multi-dimensional frameworks. [9] These trends have been discussed further by others. [10, 11]

The utility of an organic compound as a zeolite SDA is additionally dependent on its stability at the high temperature and pH typical of hydrothermal syntheses. For example, quaternary ammonium SDAs can undergo the Hofmann elimination reaction to an amine and an alkene in the presence of a base and heat. Additionally, organic compounds selected for use as SDAs need to be adequately soluble in water. Zones and co-workers demonstrated that SDAs with an intermediate C/N^+ ratio (between 11 and 16) have the highest tendency to crystallize high-silica zeolites, as they are soluble in water but sufficiently hydrophobic such that there is preferred interaction with the silicate species. [12]

In this article, we highlight a few novel and inventive uses of SDAs that have recently been developed to create new frameworks, compositions, and morphologies. Many reviews have been written on SDAs and their role in zeolite synthesis, [13, 14, 5] and we refer the reader to these papers for further information.

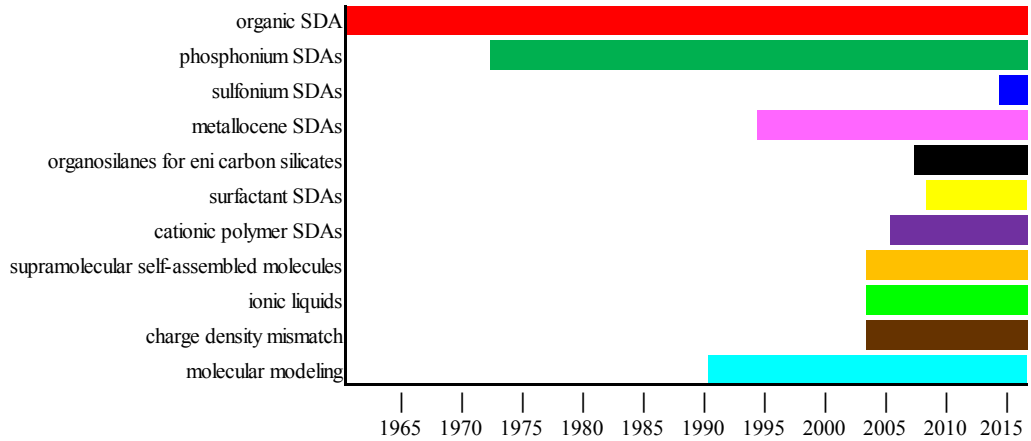

Figure 1. Timeline of key SDA innovations.

Novel SDAs

Non-Ammonium SDAs

In an effort to discover new zeolite materials, many research groups have begun to explore novel types of SDA chemistries. For example, phosphonium-based SDAs, which have been in use since the early days of synthetic zeolites, [15] have recently enabled the discovery of new zeolite structures. Importantly, unlike ammonium SDAs, phosphonium analogues do not degrade via the Hofmann elimination reaction and can therefore be used at higher pH and temperature. Corma and co-workers have recently found several new structures using novel phosphonium-based SDAs, including ITQ-26, ITQ-27, ITQ-34, ITQ-40, ITQ-47, ITQ-49, ITQ-52, and ITQ-53. [16] In related work, Sano and co-workers have studied the interzeolite conversion of FAU to 8-ring zeolites using phosphonium SDAs and have shown that the phosphorus in the SDA can be used as a modification agent to the zeolite. [17]

Application of phosphazene chemistries that enable the synthesis of SDAs from smaller phosphonium and amine building blocks have also caught the attention of the zeolite community. Due to the large number of commercially available amines with various alkyl groups, this SDA synthesis route is ripe with possibility. Moreover, because these compounds are highly basic, the silica is easily mobilized in these types of zeolite synthesis gels. Corma and co-workers have applied this idea to create the first synthetic example of boggsite, which is a 10- x 12-membered-ring (MR) zeolite with catalytic potential. [18]

As another example of novel non-ammonium SDAs, Ryoo and co-workers recently used sulfonium-based SDAs in their discovery of an aluminosilicate MEL and three germanosilicates. [19] Two of the germanosilicates, ISV and ITT, were previously synthesized using mono and diquaternary ammonium SDAs, respectively, and the third germanosilicate is a new 15- x 12- x 12-MR open framework structure. Whereas ammonium-based SDAs are typically limited to C/N^+ ratios between 11 and 16, those made from sulfonium can have higher C/S^+ ratios due to the higher solubility of the sulfonium compounds in water. In turn, this opens up the opportunity to create new structures with extra-large pores from larger and bulkier SDAs.

Two more innovations serve as final examples of the use of non-ammonium SDAs. Balkus and co-workers discovered the first 14-MR zeolite using a cobaltocene complex as the SDA. [20] Importantly, this was the first extra-large pore silicate-based material; previously, extra-large pore materials were phosphate-based. In the work of Bellussi and co-workers, the organic was incorporated into the silica source, resulting in the discovery of a new class of materials called eni carbon silicates (ECSs). By using a

series of organosilanes, Bellussi's team synthesized a number of new organic-inorganic hybrid ECSs with highly porous and complex structures. [21]

Surfactant and Polymer SDAs for Hierarchical Zeolites

In order to accommodate larger reactant molecules and increase mass transfer, the zeolite community has long desired a material with both micropores (< 2 nm) and mesopores (2-50 nm). Early attempts to synthesize these hierarchical materials employed a co-templating strategy where both traditional SDAs and surfactants were added to the synthesis gel. In theory, the desired zeolite framework is dictated by the SDA, and the surfactant templates ordered mesopores from micelle-like structures. However, in practice, a physical mixture of separate microporous and mesoporous materials usually results. More recent co-templating strategies have resulted in true hierarchical zeolites by controlling either the synthesis parameters or the surfactant. [22, 23]

The landmark work of Ryoo and co-workers demonstrated that lamellar zeolite nanosheets could be grown using a single SDA in a one-pot synthesis. The first organic molecule used in this synthesis approach combined a long alkyl chain (to prevent crystal growth in the z-direction) with a diquaternary ammonium head group known to direct the synthesis of MFI. [24] By changing the ammonium head group, lamellar BEA, MRE, MTW, AEL, AFI, and ATO frameworks were also synthesized. [25, 26]

Xiao and co-workers have used cationic polymers to create hierarchical materials. Here, the cations are similar to traditional ammonium SDAs, which direct for specific zeolite frameworks. However, the longer length scale of the polymerized cations causes the molecule to act as a porogen, resulting in the formation of disordered mesopores. Using this strategy, Xiao's team has developed hierarchical BEA, MFI, and FAU. [27, 28, 29]

Supramolecular Self-Assembled Molecules as SDAs

In order to create extra-large pore zeolites (> 12 MR), many groups have endeavored to synthesize bulkier SDA molecules. However, as previously discussed, solubility of the organic in water requires that the C/N^+ ratio be kept below ~16. As a way to circumvent this issue, Corma and co-workers used organic compounds with aromatic rings that can self-assemble through pi-pi interactions into larger dimers and trimers. [30] Moliner recently wrote a good review on this subject from which a few important examples have been selected for discussion here. [31]

..... The original demonstration of supramolecular self-assembled molecules as SDAs by Corma's group provided a route for the synthesis of pure-silica LTA. Subsequently, Yan and co-workers found that the same SDA enables crystallization of either LTA or AST, depending on the SDA concentration. [32] Both Yan and Gómez-Hortigüela's groups studied this SDA system in solution and in the framework and found that the molecular aggregation behavior depends on the SDA concentration. Consequently, there is some degree of control over the void space in the resulting nanoporous network. [32, 33]

As an extension of this work, Gómez-Hortigüela and co-workers have performed studies using several supramolecular molecules to prepare different types of both AlPO and SAPO structures. Specifically, ICP-1, a new 1D aluminophosphate structure, and three new layered aluminophosphate structures have been discovered. [34, 35] In the latter example, the organics self-assemble between the layers in a manner similar to nanosheets developed by Che and co-workers. [36] Like the surfactant chain on Ryoo's SDA, the pi-pi interactions between the aromatic rings prevent crystal growth between lamellar layers. In related work, Corma and co-workers synthesized ITQ-51 (a silicoaluminophosphate form of IFO) [37] by using 1,8-bis(dimethylamino)naphthalene

as the SDA. This molecule is highly basic and acts as a proton sponge, which allows it to be protonated in the high pH solutions typical of zeolite syntheses. In turn, this favors the organic-inorganic interactions that are necessary for the nucleation and crystallization of zeolites.

Alternative Synthetic Approaches

Ionic Liquids

..... Ionic liquids have been used in zeolite syntheses to simultaneously serve as a solvent and an SDA. [38] These compounds are attractive solvents because they are environmentally benign and non-flammable. Furthermore, ionic liquids have tunable physicochemical properties due to the large range of commercially available cations and anions, which makes them excellent at solvating a wide variety of organic and inorganic compounds. Finally, the high autogenous pressures typically produced during the hydrothermal synthesis of zeolites may be avoided when ionic liquids are employed because these unique solvents have negligible vapor pressure, low melting temperatures, and are thermally stable.

..... Use of ionic liquids in zeolite synthesis was first demonstrated by Morris and co-workers and led to their discovery of several AlPO-type materials. [39] Tian and co-workers subsequently produced AlPO forms of AFI and ATV, [40] and both groups continue to have success creating MAPO materials. [41, 42] However, the synthesis of siliceous zeolites from ionic liquids is more difficult and requires careful attention to the poor solubility of silica in this medium. Morris and co-workers recently showed that by partially exchanging the bromide anion for hydroxide on imidazolium-type ionic liquids, dissolution of silica can be sufficiently improved so as to enable the synthesis of pure-silica MFI and TON. [43

Charge Density Mismatch

..... The Charge Density Mismatch (CDM) approach was developed by Lewis and co-workers at UOP. [44] In this zeolite synthesis technique, a relatively large organocation is first added to a synthesis mixture containing an excess of negative charges due to a low Si/Al ratio. Then, a stoichiometric amount of a smaller cation with a high charge density (e.g., a small organocation or halide salt of an alkali/alkaline earth cation) is added to compensate the charge; crystallization occurs through cooperative templating between the larger and smaller cations. Importantly, this method provides a route for the synthesis of new materials and does not require the use of novel or exotic SDAs. Furthermore, identification of unique cation combinations allows for some amount of rational design of new structures and new compositions. Using this technique, the UOP group has discovered a new phase UZM-5 (UFI) (Lewis, Miller, Moscoso, Wilson, Knight, & Wilson, 2004), as well as several new compositions of existing structures. Hong and co-workers have expanded on the CDM method by finding many new combinations of SDAs, high-charge density cations, and temperatures resulting in novel compositions and structures. [45] In addition, they have further studied the mechanism of this synthesis technique. [46]

Rational Design of SDAs and the Role of Molecular Modeling

Molecular modeling and simulation have found several uses in the zeolite field. [47] While the ultimate goal is *a priori* design of an SDA that promotes nucleation of a targeted hypothetical zeolite framework, there are several more modest and yet notable ways modeling aids in the rational synthesis of zeolites. For example, guest-host energy values determined by molecular dynamics provide a measure of the relative “goodness” of the SDA, and in some studies have enabled the discovery of new SDAs for existing

zeolite structures. In addition, computational techniques have led to the development of theoretical zeolite databases and provide a means for simulating zeolite nucleation.

Many groups use modeling to find the optimum SDA configuration in zeolite frameworks. Although inorganic synthesis conditions also play a role in phase selectivity, SDA-zeolite interaction energies allow researchers to rationalize zeolite phase selectivity. As an example, Burton, Zones, and co-workers calculated the stabilization energies of several cyclic and polycyclic SDAs in cage-based 8-MR zeolites and found that the energies were strong predictors of the phase selectivity for a given set of inorganic conditions. [48] In addition, Harris and Zones identified a strong correlation between template fit and crystallization rate. [49]

Several groups have also used modeling techniques to identify alternative SDAs for known zeolite frameworks. Through computations, Schmitt and Kennedy discovered two new SDAs for ZSM-18, [50] and Corma and co-workers used molecular modeling to find an SDA that selects for ISV over BEC. [51] Deem and co-workers devised a computational method where they can “sprout and grow” an SDA within a zeolite framework from a library of commercial chemical precursors that react through known chemical reactions (e.g., Menshutkin reaction). [52] Using this technique, Deem, Davis, and co-workers synthesized STW, AEI, and SEW using computationally predicted SDAs. [53, 54, 55] This method follows on the pioneering work of Lewis and co-workers where new SDAs for LEV and MFI were identified. [56]

Conclusions

..... Step-out thinking has led to the development of a variety of new zeolite templating approaches and ultimately to the discovery of many new microporous materials. Innovations in SDA use, along with new inorganic synthesis methods, will continue to move the area of zeolite synthesis forward. While new zeolite discoveries are often initially a result of using novel and expensive SDAs, research aimed at finding cheaper SDAs for potentially useful zeolites will also prove important. [57]

References

[1] R. M. Barrer and P. J. Denny, J. Chem. Soc., pp. 983-1000, 1961.
[2] G. T. Kerr, J. Phys. Chem., vol. 70, no. 4, pp. 1047-1050, 1966.
[3] R. L. Wadlinger, G. T. Kerr and E. J. Rosinski.US Patent 3,308,069, 1967.
[4] R. M. Barrer, Hydrothermal Chemistry of Zeolites, London: Academic Press, 1982.
[5] A. W. Burton and S. I. Zones, Stud. Surf. Sci. Catal., vol. 168, pp. 137-179, 2007.
[6] Y. Nakagawa.US Patent 5,281,407, 1994.
[7] S. Elomari.US Patent 6,616,911, 2003.
[8] S. Elomari.US Patent 6,632,417, 2003.
[9] H. Gies and B. Marler, Zeolites, vol. 12, no. 1, pp. 42-49, 1992.
[10] F. Liebau, in Structural Chemistry of Silicates, Berlin, Springer-Verlag, 1985, p. 242.
[11] M. E. Davis and S. I. Zones, "A Perspective on Zeolite Synthesis: How Do You Know What You'll Get?," in Synthesis of Porous Materials: Zeolites, Clays, and Nanostructures, Occelli, M.L. and Kessler, H., eds., New York, Marcel Dekker, 1997, pp. 1-34.
[12] Y. Kubota, M. M. Helmkamp, S. I. Zones and M. E. Davis, Micro. Mater., vol. 6, pp. 213-229, 1996.
[13] M. E. Davis and R. F. Lobo, Chem. Mater. A, vol. 4, pp. 756-768, 1992.
[14] M. Moliner, F. Rey and A. Corma, Angew. Chem. Int. Ed., vol. 52, no. 52, pp. 13880-13889, 2013.

[15] P. Chu.US Patent 3,709,979, 1973.
[16] E. T. C. Vogt, G. T. Whiting, A. D. Chowdhury and B. M. Weckhuysen, Advances Catal., vol. 58, pp. 143-314, 2015.
[17] Y. Yamasaki, N. Tsunoji, Y. Takamitsu, M. Sadakane and T. Sano, Micro. Meso. Mater., vol. 223, pp. 129-139, 2016.
[18] R. Simancas, D. Dari, N. Velamazan, M. T. Navarro, A. Cantin, J. L. Jorda, G. Sastre, A. Corma and F. Rey, Science, vol. 330, pp. 1219-1222, 2010.
[19] C. Jo, S. Lee, S. J. Cho and R. Ryoo, Angew. Chem. Int. Ed., vol. 54, no. 43, pp. 12805-12808, 2015.
[20] K. J. Balkus and A. G. Gabrielov.US Patent 5,489,424, 1996.
[21] G. Bellussi, A. Carati, E. Di Paola, R. Millini, W. O. Parker Jr., C. Rizzo and S. Zanardi, Micro. Meso. Mater., vol. 113, pp. 252-260, 2008.
[22] Y. Zhu, Z. Hua, J. Zhou, L. Wang, J. Zhao, Y. Gong, W. Wu, M. Ruan and J. Shi, Chem. A Eur. J., vol. 17, no. 51, pp. 14618-14627, 2011.
[23] L. Wu, V. Degirmenci, P. C. M. M. Magusin, B. M. Szyja and E. J. M. Hensen, Chem. Commun., pp. 9492-9494, 2012.
[24] M. Choi, K. Na, J. Kim, Y. Sakamoto, O. Terasaki and R. Ryoo, Nature, vol. 461, pp. 246-249, 2009.
[25] W. Kim, J. C. Kim, J. Kim, Y. Seo and R. Ryoo, ACS Catal., vol. 3, pp. 192-195, 2013.
[26] Y. Seo, S. Lee, C. Jo and R. Ryoo, J. Amer. Chem. Soc., vol. 135, pp. 8806-8809, 2013.
[27] F. S. Xiao, L. Wang, C. Yin, K. Lin, Y. Di, J. Li, R. Xu, D. S. Su, R. Schlogl, T. Yokoi and T. Tatsumi, Angew. Chem. Int. Ed., vol. 45, pp. 3090-3093, 2006.
[28] S. Liu, X. Cao, L. Li, C. Li, Y. Ji and F. S. Xiao, Col. Surf. A, vol. 318, no. 1-3, pp. 269-274, 2008.
[29] L. Wang, Z. Zhang, C. Yin, Z. Shan and F. S. Xiao, Micro. Meso. Mater., vol. 131, pp. 58-67, 2010.
[30] A. Corma, F. Rey, J. Rius, M. J. Sabater and S. Valencia, Nature, vol. 431, pp. 287-290, 2004.
[31] M. Moliner, Top. Catal., vol. 58, pp. 502-512, 2015.
[32] M. Sun, H. K. Hunt, C. M. Lew, R. Cai, Y. Liu and Y. Yan, Chin. J. Catal., vol. 33, pp. 85-91, 2012.
[33] L. Gomez-Hortiguela, S. Hamad, F. Lopez-Arbeloa, A. B. Pinar, J. Perez-Pariente and F. Cora, J. Amer. Chem. Soc., vol. 131, no. 45, pp. 16509-16524, 2009.
[34] T. Alvaro-Munoz, A. B. Pinar, D. Sisak, J. Perez-Pariente and L. Gomez-Hortiguela, J. Phys. Chem. C, vol. 118, pp. 4835-4845, 2014.
[35] L. Gomez-Hortiguela, A. Sanz, T. Alvaro-Munoz, F. Lopez-Arbeloa and J. Perez-Pariente, Micro. Meso. Mater., vol. 183, pp. 99-107, 2014.
[36] D. Xu, Y. Ma, Z. Jing, L. Han, B. Singh, J. Feng, X. Shen, F. Cao, P. Oleynikov, H. Sun, O. Terasaki and S. Che, Nat. Commun., vol. 5, pp. 1-9, 2014.
[37] R. Martinez-Franco, A. Cantin, A. Vidal-Moya, M. Moliner and A. Corma, Chem. Mater., vol. 27, no. 8, pp. 2981-2989, 2015.
[38] E. R. Parnham and R. E. Morris, Acc. Chem. Res., vol. 40, no. 10, pp. 1005-1013, 2007.
[39] E. R. Cooper, C. D. Andrews, P. S. Wheatley, P. B. Webb, P. Wormald and R. E. Morris, Nature, vol. 430, pp. 1012-1016, 2004.
[40] L. Wang, Y. Xu, Y. Wei, J. Duan, A. Chen, B. Wang, H. Ma, Z. Tian and L. Lin, J. Amer. Chem. Soc., vol. 128, pp. 7432-7433, 2006.
[41] E. R. Parnham and R. E. Morris, J. Amer. Chem. Soc., vol. 128, no. 7, pp. 2204-2205, 2006.

[42] L. Wang, Y. P. Xu, B. C. Wang, S. J. Wang, J. Y. Yu, Z. J. Tian and L. W. Lin, Chem. A Eur. J., vol. 14, no. 34, pp. 10551-10555, 2008.
[43] P. S. Wheatley, P. K. Allan, S. J. Teat, S. E. Ashbrook and R. E. Morris, Chem. Sci., vol. 1, pp. 483-487, 2010.
[44] G. J. Lewis, M. A. Miller, J. G. Moscoso, B. A. Wilson, L. M. Knight and S. T. Wilson, Stud. Surf. Sci. Catal., vol. 154, pp. 364-372, 2004.
[45] M. B. Park, S. J. Cho and S. B. Hong, J. Amer. Chem. Soc., vol. 133, no. 6, pp. 1917-1934, 2011.
[46] M. B. Park, Y. Lee, A. Zheng, F. S. Xiao, C. P. Nicholas, G. J. Lewis and S. B. Hong, J. Amer. Chem. Soc., vol. 135, no. 6, pp. 2248-2255, 2013.
[47] C. S. Cundy and P. A. Cox, Chem. Rev., vol. 103, pp. 663-701, 2003.
[48] A. W. Burton, G. S. Lee and S. I. Zones, Micro. Meso. Mater., vol. 90, pp. 129-144, 2006.
[49] T. V. Harris and S. I. Zones, Stud. Surf. Sci. Catal., vol. 84, pp. 29-36, 1994.
[50] K. D. Schmitt and G. J. Kennedy, Zeolites, vol. 14, no. 8, pp. 635-642, 1994.
[51] G. Sastre, A. Cantin, M. J. Diaz-Cabanas and A. Corma, Chem. Mater., vol. 17, no. 3, pp. 545-552, 2005.
[52] R. Pophale, F. Daeyaert and M. W. Deem, J. Mater. Chem. A, vol. 1, pp. 6750-6760, 2013.
[53] J. E. Schmidt, M. W. Deem and M. E. Davis, Angew. Chem. Int. Ed., vol. 126, pp. 8512-8514, 2014.
[54] J. E. Schmidt, M. W. Deem, C. Lew and T. M. Davis, Top. Catal., vol. 58, pp. 410-415, 2015.
[55] T. M. Davis, A. T. Liu, C. M. Lew, D. Xie, A. Benin, S. Elomari, S. I. Zones and M. W. Deem, Chem. Mater., in press, 2016.
[56] D. W. Lewis, D. J. Willock, C. R. A. Catlow, J. M. Thomas and G. J. Hutchings, Nature, vol. 382, pp. 604-606, 1996.
[57] S. I. Zones, Micro. Meso. Mater., vol. 144, pp. 1-8, 2011.

Acknowledgments

We thank Dr. Stacey I. Zones for helpful discussions on the manuscript, and Dr. C.Y. Chen and Dr. Robert J. Saxton for their support of research and development work at Chevron.

3. Synthesis design of new molecular sieves

Manuel Moliner, Fernando Rey, Avelino Corma*

Instituto de Tecnología Química (UPV-CSIC), Universidad Politécnica de Valencia, Consejo Superior de Investigaciones Científicas, Valencia, 46022, Spain

Introduction

Despite the fact that there are today 229 different zeolitic structures recognized by the International Zeolite Association (IZA), [1] the discovery of new crystalline molecular sieves with novel and targeted physico-chemical properties is a matter of much interest for their use in traditional and emerging applications. [2] To achieve this, the design of zeolites with predefined pore structures, and well-controlled active sites, would be highly desirable.

Unfortunately, the complete understanding of the mechanisms involving the nucleation and crystallization processes of zeolites is far from being achieved, and this lack of fundamental knowledge is the main limitation to rationalize the design and synthesis of new molecular sieves.[3] Nevertheless, the accumulated experience in zeolite synthesis during the last 50 years has allowed remarkable insight into the influence of different chemical variables in the synthesis of new molecular sieves.[4] In this sense, some of the most relevant organic and inorganic directing effects described recently in the literature allowing the crystallization of new zeolites will be highlighted below.

Organic structure directing agents (OSDAs)

The incorporation of organic moieties, such as tetraalkylammonium cations, into the synthesis media was a key breakthrough to synthesize new zeolites.[5] In general, the properties of these organic molecules, including size, shape, flexibility, and hydrophobicity, clearly influence the chemical and structural properties of the crystallized molecular sieves.[4,6] Systematic studies of different families of tetraalkylammonium cations acting as OSDAs, have not only allowed the discovery of several new zeolitic structures but have also introduced fundamental directing roles of the OSDAs depending on their size and shape.[6] For instance, increasing the size and rigidity of the organic molecules results in the crystallization of new zeolites with larger pores and/or cavities within their structures (see Figure 1), while using branched organic molecules allows synthesizing multidimensional zeolites.[6]

In the last years, the synthesis of zeolites presenting interconnected pores of different dimensions (multipore zeolites),[7] and small pore zeolites presenting large cavities within their structure have received significant attention.[8] On one hand, the presence of interconnected pores of different dimensions, may allow preferential adsorption and diffusion pathways for reagents and products, inducing unique catalytic activities and selectivities.[7] On the other hand, the recent application of small pore zeolites with large cavities in different industrially-relevant chemical processes, such as methanol-to-olefins,[9] or selective catalytic reduction of NOx,[10] has aroused the attention on this type of framework topologies. The preferred OSDAs for the synthesis of high silica small pore zeolites with large cavities in their structure are cyclic or polycyclic ammonium cations that are able to fit and stabilize the presence of the large cavities (see Figure 2). [8]

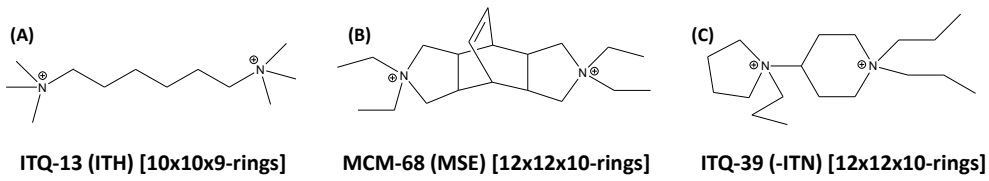

Figure 1. OSDA molecules used for the synthesis of zeolites with different size and flexibility.

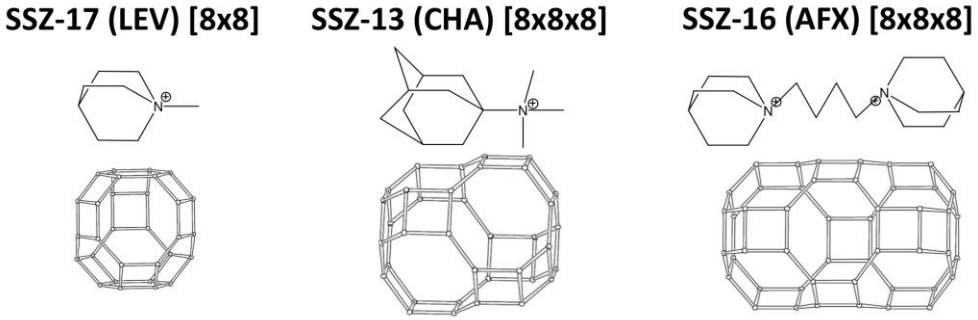

Figure 2. Polycyclic ammonium cations for the synthesis of small pore zeolites with large cavities.

In addition to the classical ammonium-based OSDAs for the synthesis of zeolites, the use of phosphorous-based organic molecules as OSDAs (P-OSDAs), such as phosphonium and phosphazenes, has allowed the preparation of different new zeolitic structures with different pore architectures depending on the size and shape of the P-OSDAs (see Figure 3).[11] P-based OSDAs are more stable and show different properties compared to classical ammonium-based OSDAs, influencing the nucleation and crystallization processes and permitting the growth of new molecular sieves.

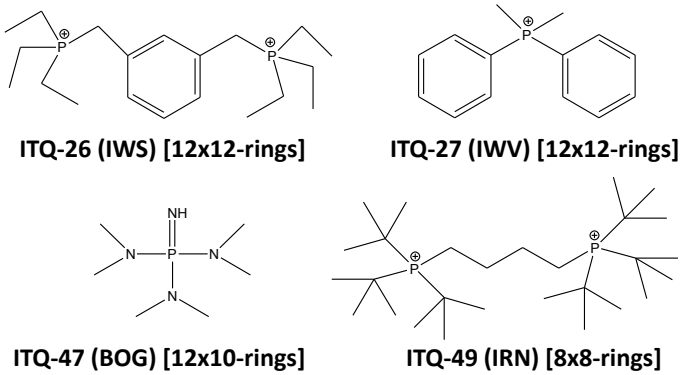

Figure 3. P-Based OSDAs used for the synthesis of zeolites.

In order to reduce the diffusion pathways through the pores of the zeolites when bulky reactants or products are involved, the synthesis of new layered or 2-D zeolite structures is highly desired, and different top-down (A) and bottom-up (B) preparation methods have been designed using different organic molecules.[12] In that way, delaminated zeolites, such as ITQ-2 (see Figure 4A) and ITQ-6, have been synthesized by exfoliating layered zeolite precursors using surfactants and controlled pHs,[12a] while the use of bifunctional di-quaternary ammonium-type surfactants has allowed the direct synthesis of zeolite nanosheets (see Figure 4B). [12b]

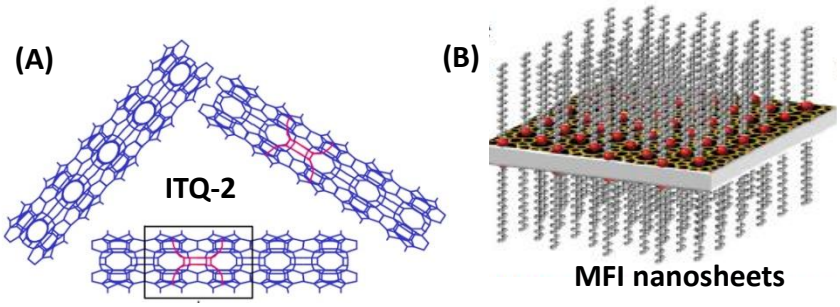

Figure 4. (A) Structure of the ITQ-2 zeolite and, (B) MFI nanosheets. Reproduced from references [12a] and [12b].

Directing effects of inorganic zeolite components

Besides the structure directing effects of the above described organic molecules, there are remarkable inorganic structure directing effects that permit the crystallization of new zeolitic structures.

In this sense, it is well-known that the introduction of some heteroatoms in the synthesis gel favors the formation of some particular secondary building units (SBUs), permitting the crystallization of zeolite structures that would be less stable without these specific heteroatoms.[4] Probably, the most outstanding inorganic directing effect has been achieved by the introduction of germanium atoms in the synthesis media, allowing the crystallization of several new zeolitic structures with very low framework densities (FD), large micropore volumes and, particularly, containing extra-large pores (see Figure 5).[13] The reason for that is because germanium atoms are able to stabilize double-4-rings (D4R) and double-3-rings (D3R) secondary building units (SBUs), and the presence of these small cages favors the crystallization of zeolites with lower FD and larger pore dimensions, even with smaller organic structure directing agents.[14] The fact that the introduction of Ge would favor the formation of these SBUs has been theoretically and experimentally shown.[15] Most interesting is that some of the silicogermanates have also been later synthesized without Ge, such as zeolites ITQ-17 and ITQ-24.

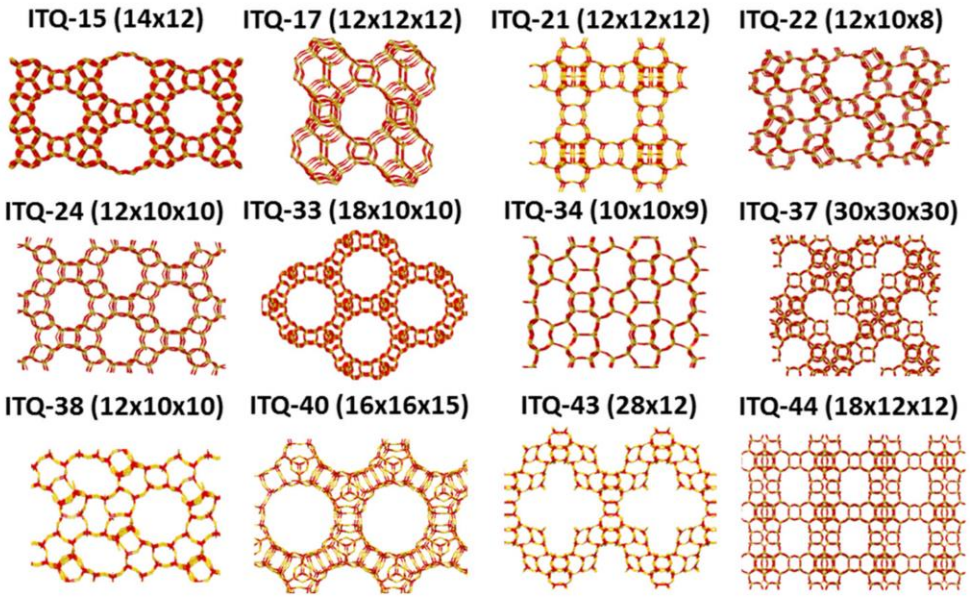

Figure 5. New zeolitic structures with different pore architectures synthesized by introducing germanium atoms in the synthesis gel. Reproduced from [4b].

Synthesis of zeolites by postsynthesis treatment of existing ones

A different methodology to prepare new zeolitic structures is based on secondary post- synthesis treatments, transforming pre-crystallized layered precursors into new crystalline structures by pillaring the interlayer region with other atoms. New zeolites have been recently synthesized following this pillaring method, such as APZ-4 (12x10-rings), [16] and COE-4 (10x10-rings), [17] which have been achieved by pillaring with silicon atoms the PRE-FER and PRE-CDO layered precursors, respectively.
Finally, different new zeolite structures have been synthesized through the so-called Inverse Sigma Expansion, [18] or Assembly-Disassembly-Reassembly (ADOR) methodology (see Figure 6). [19] These procedures are based on the selective removal of a layer of Ge framework atoms, in germanosilicates previously synthesized, followed by a structure reassembly that enables the synthesis of new materials with different pore architectures. This method has allowed the transformation of the germanosilicate UTL (ITQ-15, 14x12-rings), [13a] in different multipore high-silica zeolitic structures, such as IPC-2 or COK-14 (12x10-rings), [18,19] IPC-4 (10x8-rings), IPC-6 (12x10x8-rings), and IPC-7 (14x12x10-rings). [20]

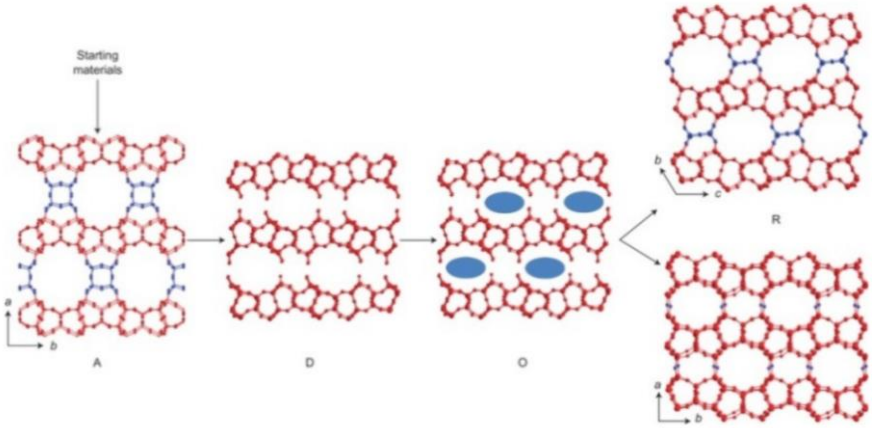

Figure 6. New zeolitic structures synthesized following the ADOR methodology. Reproduced from reference [19a].

Conclusions

As it has been shown, the rational use of different organic and inorganic structure directing agents in the synthesis of zeolites has allowed the crystallization of many new zeolitic structures. It is expected that original and innovative advances in designing new OSDAs, by combining theoretical calculation and innovative synthesis methodologies, allow the crystallization of new molecular sieves with controlled chemical compositions and pore topologies. We are contemplating a strong revival in the field of zeolites that involve the synthesis of new and older modified materials, electron diffraction techniques for solving crystalline structures, and applications in the fields of gas molecular separation, catalysis, molecular control releases, sensors, among others.

References

[1] www.iza-structure.org/databases, (November, 2015)
[2] (a) M. E. Davis, Nature 417 (2002) 813; (b) S. Mintova, M. Jaber, V. Valtchev, Chem. Soc. Rev. 44 (2015) 7207
[3] C. S. Cundy, P. A. Cox, Micropor. Mesopor. Mater. 82 (2005) 1
[4] (a) A. Corma, M. E. Davis, ChemPhysChem. 5 (2004) 304; (b) M. Moliner, F. Rey, A. Corma, Angew. Chem., Int. Ed. 52 (2013) 13880
[5] R. M. Barrer, P. J. Denny, J. Chem. Soc. (1961) 971
[6] R. F. Lobo, S. I. Zones, M. E. Davis, J. Inclusion Phenom. Mol. Recognit. Chem. 21 (1995) 47
[7] (a) R. F. Lobo, M. Pan, I. Chan, H. X. Li, R. C. Medrud, S. I. Zones, P. A. Crozier, M. E. Davis, Science 262 (1993) 1543; D. L. Dorset, S. C. Weston, S. S. Dhingra, J. Phys. Chem. B 110 (2006) 2045; (c) M. Moliner, C. Martínez, A. Corma, Angew. Chem., Int. Ed. 127 (2015) 3630
[8] (a) S. I. Zones, US Patent 4,544,538 (1985); (b) P. Wagner, Y. Nakagawa, G. S. Lee, M. E. Davis, S. Elomari, R. C. Medrud, S. I. Zones, J. Am. Chem. Soc. 122 (2000) 263; (c) C. Kim, S. J. Hwang, A. W. Burton, S. I. Zones, Micropor. Mesopor. Mater. 116 (2008) 227
[9] B. V. Vora, T. L. Marker, P. T. Barger, H. R. Nielsen, S. Kvisle, T. Fuglerud, Stud. Surf. Sci. Catal. 107 (1997) 87
[10] I. Bull, R. S. Boorse, W. M. Jaglowski, G. S. Koermer, A. Moini, J. A. Patchett, W. M. Xue, P. Burk, J. C. Dettling, M. T. Caudle, U.S. Patent 0,226,545 (2008)
[11] (a) D. L. Dorset, G. J. Kennedy, K. G. Strohmaier, M. J. Díaz-Cabañas, F. Rey, A. Corma, J. Am. Chem. Soc. 128 (2006) 8862; (b) R. Simancas, D. Dari, N. Velamazan,

M. T. Navarro, A. Cantín, J. L. Jordá, G. Sastre, A. Corma, F. Rey, Science 330 (2010) 1219
[12] (a) A. Corma, V. Fornes, S. B. Pergher, T. L. M. Maesen, J. G. Buglass, Nature 396 (1998) 353; (b) M. Choi, K. Na, J. Kim, Y. Sakamoto, O. Terasaki, R. Ryoo, Nature 461 (2009) 246
[13] (a) A. Corma, M. J. Díaz-Cabañas, F. Rey, S. Nicolopoulus, K. Boulahya, Chem. Commun. (2004) 1356; (b) A. Corma, M. J. Diaz-Cabañas, J. L. Jordá, C. Martínez, M. Moliner, Nature 443 (2006) 842; (c) J. Sun, C. Bonneau, A. Cantin, A. Corma, M. J. Díaz-Cabañas, M. Moliner, D. Zhang, M. Li, X. Zou, Nature 458 (2009) 1154
[14] G. O. Brunner, W. M. Meier, Nature 337 (1989) 146
[15] (a) T. Blasco, A. Corma, M. J. Díaz-Cabañas, F. Rey, J. A. Vidal-Moya, C. M. Zicovich-Wilson, J. Phys. Chem. B 106 (2002) 2637; (b) G. Sastre, J. A. Vidal-Moya, T. Blasco, J. Rius, J. L. Jordá, M. T. Navarro, F. Rey, A. Corma, Angew. Chem., Int. Ed. 41 (2002) 4722
[16] T. Ikeda, S. Kayamori, Y. Oumi, F. Mizukami, J. Phys. Chem. C 114 (2010) 3466
[17] T. Baerdemaeker, M. Feyen, T. Vanbergen, U. Muller, B. Yilmaz, F. S. Xiao, W. Zhang, T. Yokoi, X. Bao, D. E. De Vos, H. Gies, Chem. Mater. 27 (2015) 316
[18] E. Verheyen, et al., Nat. Mater. 11 (2012) 1059
[19] (a) W. J. Roth, P. Nachtigall, R. E. Morris, P. S. Wheatley, V. R. Seymour, S. E. Ashbrook, P. Chlubná, L. Grajciar, M. Položij, A. Zukal, O. Shvets, J. Čejka, Nat. Chem. 5 (2013) 628; (b) R. E. Morris, J. Cejka, Nat. Chem. 7 (2015) 381
[20] P. S. Wheatley, P. Chlubna-Eliasova, H. Greer, W. Zhou, V. R. Seymour, D. M. Dawson, S. E. Ashbrook, A. B. Pinar, L. B. McCusker, M. Opanasenko, J. Cejka, R. E. Morris, Angew. Chem., Int. Ed. 53 (2014) 13210

4. Zeolite nanocrystals

Valentin Valtchev

Laboratoire Catalyse & Spectroscopy, CNRS – ENSICAEN - University of Normandy, 6 boulevard Marechal Juin, 14050 Caen, France

Introduction

Nanomaterials and nanotechnology are not words that are used solely in the scientific vocabulary. These terms are now adopted and largely employed in the daily language, which demonstrates the high interest of the society in the developments in this field. This interest is related to the expectations that nanomaterials and nanotechnology will make most products lighter, stronger, cleaner, less expensive, and more precise. These expectations are already reality for a number of materials and technologies, which motivates academic and apply scientists to perform more extensive research and developments.

In the material science *nano* is a synonym of extremely small (size, time interval, etc.). The goal is usually to accentuate the property of interest and thus to improve material's performance. The decrease of the size of particles changes the ratio between surface and bulk atoms. A major difference between dense and porous materials is in the accessible fraction of atoms. In the case of porous materials, the intra crystalline pores make a larger part of atoms accessible.

This short overview is devoted to nanosized crystalline zeolite-type materials. Zeolite crystals, known also as molecular sieves, are built of corner sharing SiO_4- and AlO_4- tetrahedral units that form channels and cages with sizes below 2 nm. The well-defined pore systems and flexible chemical compositions are the origin of the unique characteristics of zeolites, namely shape selectivity, high specific surface area, high thermal and chemical stability, and controllable hydrophilic/hydrophobic properties. Consequently, zeolites are the most widely used materials in the chemical process industry.

The uniform pore dimensions of a zeolite allow separation of molecules with size below 1 Å. This shape selectivity, however, is coupled with diffusion limitations that bring a number of undesirable side effects. For instance, the pore blocking and active sites deactivation is the most important drawback in the use of zeolite catalysts. The decrease of zeolite crystals size is a straightforward solution to this problem. Crystallites of nano dimensions offer also a number of other advantages such as improved reaction kinetics and large external surface areas. Zeolite nanocrystals in colloidal form can be used for the preparation of supported zeolite layers by employing rapid deposition techniques as spin- or deep-coating.

Besides the traditional catalytic and separation applications, nanozeolites and particularly these with narrow particles size distributions and colloidal properties have shown potential for application in areas such as optics, electronics and medicine. These considerations motivated the research on nanozeolites during last two decades

Synthesis of nanozeolites

In general, the synthesis of zeolites takes place in a close system, where the gel molar composition, the type of the reactants and the physical conditions of the synthesis determine the physicochemical characteristics of the final product. In a conventional

synthesis, the size of the crystallites is about 1 μm. Much smaller crystallites, usually below 100 nm, are considered as nanocrystals and much larger crystals, 10 to several tens of microns, are considered as large or even giant crystals. The nucleation rate in the system determines to a great extent the final size of the crystallites, since the reaction stops with the exhaust of the nutrient pool. Hence, the synthesis of nanosized crystals requires abundant nucleation and simultaneous growth in the zeolite yielding system (Figure 1).

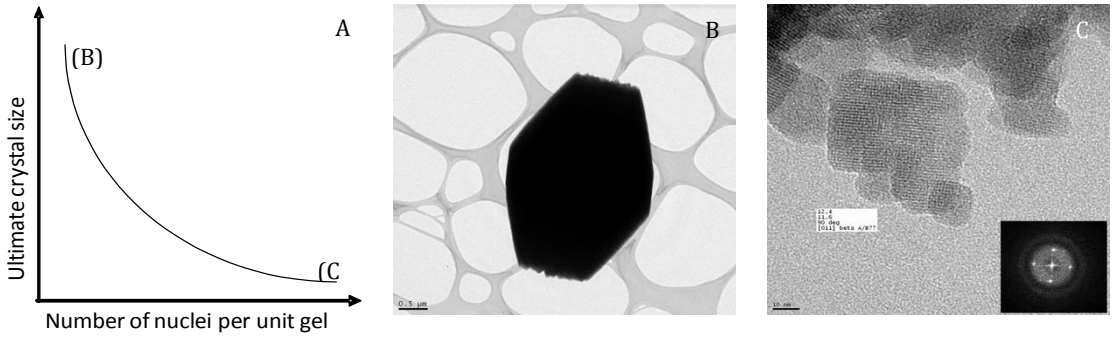

Figure 1. A) Number of nuclei - crystals size relationship in a zeolite yielding system; B) Large single zeolite Beta crystal synthesized in fluoride medium at 170 °C; C) Nanosized zeolite Beta crystals synthesized from a clear precursor suspension at 90 °C. Note: insets (B) and (C) in Figure A represents the products yield in low and high nucleation rate, respectively.

The first study devoted to the synthesis of nanozeolites was presented in 1992 during at 9th International Zeolite Conference. In this study, Meng et al. reported the synthesis of zeolite L with size of 30-70 nm. [1] Several years later the preparation of nanosized Al-LTL and Ga-LTL, including crystals in the form of colloidal suspensions, was patented by Verduijn et al. [2] First systematic studies on the synthesis of nanozeolites were performed in the early 1990s by Schoeman and colleagues. [3] They used clear precursor suspensions containing only discrete gel particles. The nucleation in such systems is abundant and simultaneity of crystallization events results in crystals with narrow particle size distributions in the form of stable colloidal suspensions. Important zeolite materials such as FAU- and LTA-type zeolites were synthesized using optically clear precursor suspensions. [3] This group has also reported the synthesis of MFI-type zeolite. [4] The system employed for the synthesis of Al-free MFI-type material (silicalite-1) was $9TPAOH:25SiO_2:480H_2O:100EtOH$, where TPAOH is tetrapropylammonium hydroxide and the ethanol (EtOH) is product from the hydrolysis of the silica source (tetraethylorthosilicate, TEOS). Subjected to hydrothermal treatment at 100°C for 24, the system yields single crystallites with a size of 95 nm. In contrast to the conventional systems where a vast diversity of (alumino)silicates species is present, the initial solution prepared by hydrolysis of TEOS with TPAOH contain a limited number of well defined discrete (3-4 nm) amorphous precursor particles. [5] This is particularly important for investigation of labile zeolite precursor particles. Briefly, the use of such a system facilitates the interpretation of the results and ambiguous conclusions are in general avoided. Consequently, the system with slight variations of H_2O/SiO_2 content was employed in many fundamental studies devoted to the zeolite nucleation. [6-9]

Zeolite Beta is another important zeolite that was synthesized in the form of a stable colloidal suspension. [10] Thus, in late 1990s all important from industrial point of view zeolites were available in nanosized form. In these syntheses, clear suspensions and relatively low crystallization temperatures were employed in order to favor the

nucleation over the growth and thus as small as possible particles to be obtained. It is worth mentioning that the stabilization of a clear precursor suspension requires very careful choice of initial reactants in order to control the polymerization reaction between initial species and avoid the formation of large, chemically inhomogeneous precursor particles. Usually the alkali metal content is kept very low in order to avoid the aggregation of gel particles. The low content of alkali metals is compensated by the abundant use of organic cations. The use of such initial systems and relatively mild synthesis conditions usually results in low crystalline yield. The conversion of (alumino)silicate precursor could vary between several wt. % to several tens wt. %, but in any case is substantially lower than the yield of a conventional hydrogel precursor. In summary, the first decade of intense research on nano-zeolites was marked by the efforts to obtain different zeolitic materials with nanosize dimensions without much attempt for optimization of the crystallization process. [11]

In the last decade this gap was fulfilled to some extent since much more research was targeted to the optimization of synthesis parameters and the increase of crystalline yield. [12] Microwave (MW) heating or sonication was used to promote uniform nucleation in zeolite yielding systems and thus nanocrystals to be obtained. Different non-conventional methods of zeolite synthesis were also developed in order to decrease the crystals size and increase the crystalline yield. Soft and hard templates were used to confine the growth of zeolite nanoparticles. Another approach was the use of silane coupling agents or multivalent surfactant for restricting the growth of zeolite particles. A substantial reduction of particle size was achieved, but the zeolite particles were heavily aggregated. Similar was the result of dry gel conversion, where substantial reduction of particle size and heavy agglomeration of the crystallites was observed. Although some interesting results were reported, the non-conventional methods remain marginal in the synthesis of nanozeolites.

A lot of work was devoted to the optimization of the nucleation and growth in conventional hydrogel systems free of organic template. The advances in the understanding of zeolite nucleation in such systems opened the door to more rational design of initial systems and control of the nucleation process. [13,14] It was found that the polymerization reaction between alumina and silica species can be controlled by the excess of NaOH in the system and the way of mixing. The use of very low temperature (4 °C) during mixing of the reactants also contributes to the controlled polymerization and the stabilization of discrete gel particles. Clear suspensions rich of alkali metal hydroxide were stabilized as the size of primary particles and their uniformity was similar to the ones obtained by the use of extensive amounts of organic structure directing agents (SDAs). Moderate temperatures, close to ambient, were preferred to convert the amorphous material into a zeolite and to suppress as much as possible the Ostwald ripening. Under such conditions, the transformation of the amorphous precursor particles into zeolite crystals, without substantial change of the particle size, was achieved (Figure 2).

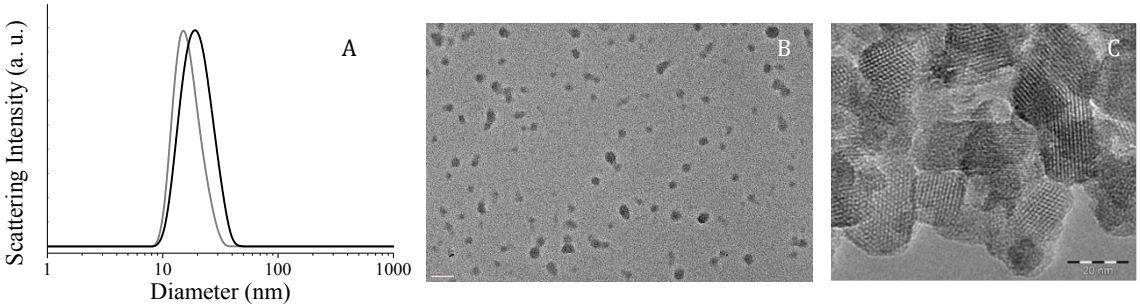

Figure 2. DLS curves of the zeolite precursor suspension (grey) and final crystalline product (black) in a FAU-type zeolite yielding system (A). TEM micrographs of the initial gel particles (B) and the ultimate zeolite nanocrystals (C).

This approach was used in the synthesis of EMT, which is the hexagonal counterpart of the largely used FAU-type zeolite. Until recently, this material with a high industrial potential was obtained only by the use of 18-crown-6 ether as SDA, which was the major obstacle to practical uses. By careful control of gel composition, the zeolite was obtained in a Na-rich system that does not contain any organic additives. First colloidal precursor particles with sizes of 10-20 nm were stabilized. Upon moderate heating (30 – 40 °C), the primary particles were transformed into pure EMT-type material with similar size. The use of a relatively low temperature allowed not only to synthesize nanocrystals with narrow particle size distribution, but also to avoid to formation of competing zeolite phases such as FAU-, LTA-, GIS- or SOD-type. Another advantage of the low temperature synthesis is that the kinetics of the growth can be controlled and the transformation to a denser phase to be avoided. The synthesized EMT-type material exhibited hexagonal shape, as the crystal dimensions were 13-15 to 3-4 nm in *a* and *c* direction, respectively. [15] The crystalline yield was more than 60 wt %, which was close to the value in a conventional zeolite synthesis.

Another important breakthrough was the synthesis of nanosized FAU-type (Y and X) zeolite in organic template free system. Zeolite Y is the primary active component in fluid cracking catalysts (FCC) and its impact on petroleum refining is enormous. The synthesis of nano zeolite Y, with high yield (> 60 %) using solely Na^+ as SDA is a big step to the application of nanocrystals. Again, the colloidal precursor particles were stabilized and upon moderate heating they were transformed into nanozeolite crystals with narrow particle size distributions (Figure 2A and B). [16] Well shaped octahedral crystallites with a size of 10-20 nm were synthesized (Figure 2C). The micropore volume of FAU-type crystals is equal to that of micron-sized ones confirming the high crystallinity of the zeolite. These high quality nanocrystals exhibit narrow particle size distributions and colloidal stability similar to their counterparts synthesized with organic structure directing agents.

Conclusion and prospects

There are 232 zeolite framework types at present. Less than 10 % of these crystalline molecular sieves are synthesized in the form of nanocrystals. Increase of the number of structure types synthesized, as nanocrystals is an important issue that zeolite scientific chemists will certainly address in the future. This short overview provides some general guidance of the synthesis of zeolite nanocrystals. However, there is not a general approach to nanocrystals that could be applied to any zeolitic material.

Therefore, new synthetic procedures will have to be developed and if possible generalized to a particular group of crystalline microporous materials.

Although the number of zeolites synthesized in the form of nanocrystals is not large, most of the industrially important zeolites are already available in the form of nanocrystals. Thus, FAU-, MFI and BEA/BAB-type nanocrystals with different framework compositions, controllable size and very high yield can be readily synthesized. The availability of high quality and cheap zeolite nanoparticles makes possible their use in large-scale processes, where nanozeolites are expected to overcome at least partially the negative impact of slow intra-pore diffusion. Improved adsorption/desorption kinetics is the straightforward effects of the replacement of conventional micron-sized zeolites with nanozeolite materials. In addition, the nanozeolites offer the advantage of large external surface areas that could be used for processing of bulky molecules that cannot reach the micropore space.

The synthesis of colloidal zeolite crystals from organic template free systems is important step ahead to new applications. Such products do not require a calcination step, which results in heavy and irreversible aggregation of zeolite particles. Consequently, discrete zeolite nanoparticles can be processed in the desired final form of the material. Further, the use of zeolites synthesized solely with alkali metal cations is favorable from economic and environmental points of view.

This overview of the nanozeolites is far from being comprehensive. More information can be found in recent review papers that address different aspect of the synthesis, properties and application of nanosized zeolites and related porous materials. [17,18]

References

[1] X. Meng, Y. Zhang, M. Meng, W. Pang, Proc. 9th IZC, July 5-10, 1992, Montreal, Canada, R. von Ballmoos, J. B. Higgins, M. M. J. Treacy (Eds.), Butterworth-Heinemann: London, 1993, p. 297.
[2] J. Verduijn, M. M. Mertens, M. H. Anthonis, PCT WO9703021, 1997.
[3] B. J. Schoeman, J. Sterte, J.-E. Otterstedt, Zeolites 14 (1994) 110.
[4] A. E. Persson, B. J. Schoeman, J. Sterte, J.-E. Otterstedt, Zeolites 15 (1995) 611.
[5] B. J. Schoeman, Microporous Mater. 9 (1997) 267.
[6] C. E. A. Kirschhock, V. Buschmann, S. Kremer, R. Ravishankar, C. J. Y. Houssin, B. L. Mojet, R. A. van Santen, P. J. Grobet, P. A. Jacobs, J. A. Martens, Angew. Chem., Int. Ed. 40 (2001) 2637.
[7] R. Harikrishnan, E. Kokkoli, M. Tsapatsis, Angew. Chem., Int. Ed. 43 (2004) 4558.
[8] C. T. G. Knight, S. D. Kinrade, J. Phys. Chem. B 106 (2002) 3329.
[9] D. D. Kragten, J. M. Fedeyko, K. R. Sawant, J. D. Rimer, D. G. Vlachos, R. F. Lobo, M. Tsapatsis, J. Phys. Chem. B 107 (2003) 10006.
[10] M. A. Camblor, A. Corma, S. Valencia, Microporous Mesoporous Mater. 25 (1998) 59.
[11] L. Tosheva, V. Valtchev, Chem. Mater. 17 (2005) 2494-2513.
[12] S. Mintova, M. Jaber, V. Valtchev, Chem. Soc. Rev. 44 (2015) 7207.
[13] L. Itani, K. N. Bozhilov, G. Clet, L. Delmotte, V. Valtchev, Chem. – A Eur. J. 17 (2011) 2199.
[14] L. Itani, Y. Liu, W. Zhang, K. Bozhilov, L. Delmotte, V. Valtchev, J. Am. Chem. Soc. 131 (2009) 10127.
[15] E.-P. Ng, D. Chataigner, T. Bein, V. Valtchev, S. Mintova, Science 335 (2012) 70.

[16] H. Awala, J.-P. Gilson, R. Retoux, P. Boullay, J.-M. Goupil, V. Valtchev, S. Mintova, Nature Mat. 14 (2015) 447.
[17] S. Mintova, J.-P. Gilson, V. Valtchev, Nanoscale 5 (2013) 6693.
[18] V. Valtchev, L. Tosheva, Chem. Rev. 113 (2013) 6734.

5. Synthesis of single-unit-cell zeolites

Qiang Guo, Limin Ren, Michael Tsapatsis

University of Minnesota, Department of Chemical Engineering & Materials Science, 421 Washington Ave SE, Minneapolis, MN 55455 USA

Introduction

Single-unit-cell zeolites have attracted attention due to potential applications in the areas of catalysis and separations. [1, 2] They are derived from layered precursors containing zeolite nanosheets arranged in parallel stacking though structure directing agents (SDA) placed in-between them. Single-unit-cell zeolites can be prepared by delaminating or pillaring of these layered zeolite precursors. [1,2] Recently, a direct synthesis method based on sequential rotational intergrowth has been developed. [3] Here, we provide a brief introduction of single-unit-cell zeolites. More extended reviews can be found in ref. (1, 2).

Top-down approach

MCM-22, the zeolite precursor of which (MCM-22(P)) consists of single-unit-cell thick layers, was reported in the early 1990's. [4] MCM-22(P) has an independent intralayer sinusoidal 10-MR channel and 12-MR cups on the surface of the layers. As a result of the condensation of hydroxyl groups between layers after thermal treatment of the layered precursors, a 10-MR interlayer pore opening connected to 12-MR supercages is created. If instead of calcination, the layered precursor is swollen with a cationic surfactant and pillared, a pillared zeolite with microporous layers is created. [5] If the swollen precursor is delaminated, then single unit cell zeolite layers can be obtained. [6] MCM-22 layers contain porosity within the layer but there are no pores perpendicular to the layer (the transport limited apertures are 6-MR). Other zeolite layered precursors exhibit similar lack of open porosity perpendicular to the layer. [7,8] In 2009, a layered MFI zeolite, named multilamellar MFI, was successfully created by using a bifunctional structure directing agent (SDA).[9] It is the first example of zeolite layers with 10-MR pores perpendicular to the zeolite layer. Conceptually, its synthesis is based on the idea that the di-quaternary head of the SDA directs the zeolite growth and the long tail serves as a space-filler between the zeolite layers (Figure 1).

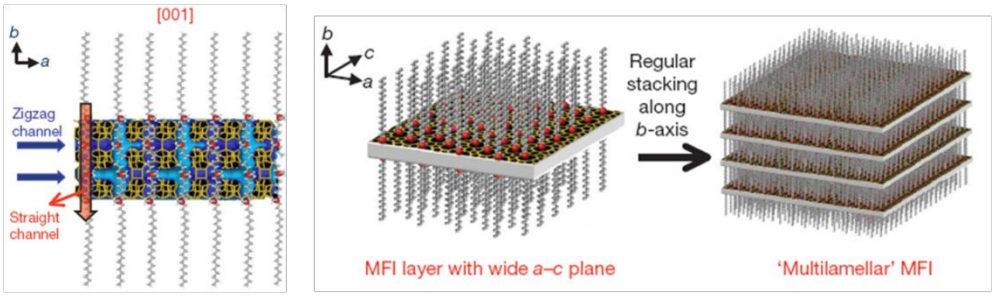

Figure 1. Structure model for the MFI nanosheets. From ref. [9]

Swelling of the layered zeolite precursor could be achieved by using long chain surfactants that interact with the silianols between the layers and expand the inter-layer spacing. Such swelling is not required for multilamellar MFI since the long chain of the

SDA serves this purpose in the as-made material. Oxide pillars can then be intercalated in the interlayer space [5, 10] or delamination can be realized by washing in acidic solution and sonication of the swollen material (Figure 2).[6] The delaminated zeolite is of interest for catalytic applications but also could be considered as a building block for ultrathin molecular sieve membranes.[11] For the later application, the preservation of the layer structure is critical and could be ensured by swelling, pillaring and delamination under mild conditions.[12, 13] Incorporation of heteroatoms into single-unit-cell hierarchical zeolites can be achieved by known synthesis and post-treatment methods as reported, for example, for delaminated Ti-MWW, pillared Ti-MWW and pillared Sn-MWW.[14-16] Generally, post-synthesis modification can be applied to all layered zeolite precursors to prepare single-unit-cell hierarchical zeolites. [17]

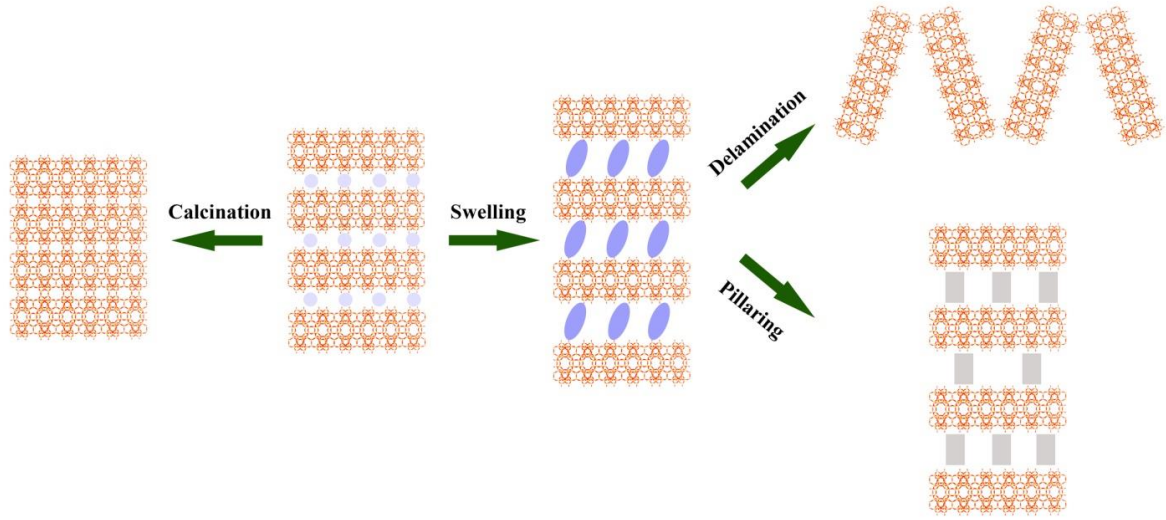

Figure 2. General process for single-unit-cell hierarchical zeolite preparation from layered zeolite precursors (shown here for ITQ-2 and MCM-22(P)).

For certain applications, it is required to remove the SDA from the single-unit-cell zeolite without using calcination. For example, for membrane applications it is important to avoid aggregation of nanosheets and this cannot be achieved when exfoliated powders are calcined. In this context, removal of SDA using solution-based approaches has been explored and it is now possible to prepare SDA-free non-aggregated suspensions of zeolite nanosheets (Figure 3). [18]

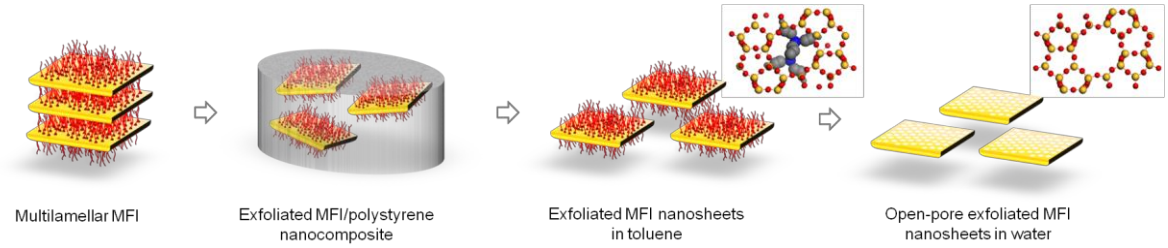

Figure 3. Schematic for the preparation of water suspension of open-pore MFI nanosheets from multilamellar MFI. [18]

Bottom-up approach

B*ottom-up* approach (direct synthesis) is attractive because the *top-down* approaches rely on multiple steps (hydrothermal synthesis of the layered zeolite precursor, followed by swelling of the precursor and then pillaring or delamination of the swollen materials) making them costlier to implement. In 2012, a one-step synthesis strategy of single-unit-cell zeolites was introduced. Conceptually, it is based on sequential rotational intergrowths of certain zeolite framework types, like MFI and MEL. [3]

When two crystal structures with different symmetry can intergrow at the single-unit-cell level, the higher symmetry one may act as a linker to connect single-unit-cell elements of the lower symmetry structure causing branching of the latter and a rotational intergrowth or twinning (Figure 4C, top). Self-pillared layered materials can be produced by the repetitive branching caused by such rotational intergrowths. For instance, self-pillared pentasil (SPP), a material formed by the intergrowth of MEL and MFI (Figure 4), can be synthesized using the readily available SDA tetrabutylphosphonium (TBPOH) or tetrabutylammonium hydroxide (TBAOH). [3, 19, 20] MFI and MEL frameworks can be described based on a common building unit (the pentasil chain) arranged with different symmetry operations. TBPOH and TBAOH are known to encourage the intergrowth of MFI and MEL. Under certain conditions, MEL domains can be inserted onto the predominantly MFI nanosheets during the synthesis of SPP using TBPOH or TPAOH as the SDA. The symmetry of MEL is higher than that of MFI. Thus, after MEL is formed, it can act as the linker and new MFI layers can emerge out of MEL. If MEL is inserted on the newly formed MFI layers, a new MFI branch can emerge, and the process can be repeated until the end of the crystal growth. As a result of this growth process, the zeolite lamellae are intergrown in a house-of-cards arrangement (Figure 4 C, bottom).

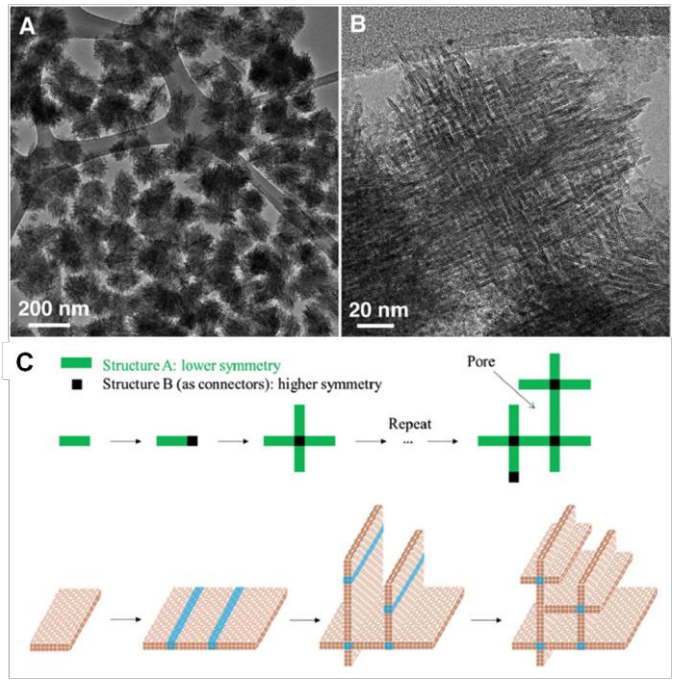

Figure 4. Low-magnification (A) and high-magnification (B) TEM images of the self-pillared pentasil (SPP) zeolite particles; Schematic growth of SPP (C) via intergrowth of MEL and MFI. [3, 19]

This approach does not rely on pillaring and/or use of long-chain surfactant SDA and, consequently, it is attractive for its simplicity and cost effectiveness. In addition to MFI, faujasite hierarchical materials have been prepared based on FAU/EMT intergrowths with a distinct branching mechanism caused by small amounts of EMT. However, in hierarchical faujasite, the layers are much thicker than single-unit-cell and are unlikely to be reduced further to single-unit-cell thickness. [21, 22]

In addition to the self-pillared materials discussed above, direct synthesis of non-intergrown single-unit-cell nanosheets has been reported. For example, the bifunctional template, which was used to prepare multilamellar MFI can also direct the synthesis of unilamellar MFI. [9] Recently, delaminated MWW zeolite nanosheets were synthesized directly using bifunctional templates (Figure 5) [23] as well as by use of a dual-template synthesis approach. [24] However, the direct synthesis of non-intergrown large-area zeolite nanosheets, which is desirable for thin film uses is yet to be achieved.

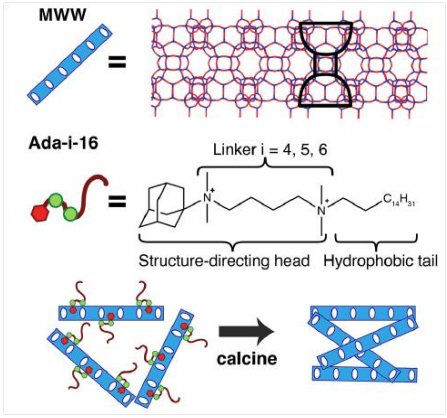

Figure 5. One-pot synthesis strategy to prepare delaminated MWW zeolite nanosheets. [23]

Conclusions

Single-unit-cell hierarchical zeolites have been successfully prepared first by pillaring or delamination (*top-down*) approaches and more recently by direct one-step (*bottom-up*) synthesis. Synthesis of non-intergrown zeolite nanosheets with large basal dimensions remains elusive.

References

[1] M. Tsapatsis, *AIChE J.*2014, *60*, 2374-2381.
[2] W. J. Roth, P. Nachtigall, R. E. Morris, J. Čejka, *Chem. Rev.,* 2014, *114*, 4807-4837.
[3] X. Zhang, D. Liu, D. Xu, S. Asahina, K. A. Cychosz, K. V. Agrawal, Y. Al Wahedi, A. Bhan, S. Al Hashimi, O. Terasaki, M. Thommes, M. Tsapatsis, *Science*, 2012, *336*, 1684-1687.
[4] M. E. Leonowicz, J. A. Lawton, S. L. Lawton, M. K. Rubin, *Science*, 1994, *264*, 1910-1913.
[5] W. J. Roth, C. T. Kresge, J. C. Vartuli, M. E. Leonowicz, A. S. Fung, S. B. McCullen, *Stud. Surf. Sci. Catal*., 1995, *94*, 301-308.
[6] A. Corma, V. Fornes, S. B. Pergher, Th. L. M. Maesen, J. G. Buglass, *Nature*, 1998, *396*, 353-356.
[7] Y. X. Wang, H. Gies, B. Marler, *Chem. Mater.,* 2005, *17,* 43-49.
[8] B. Marler, H. Gies, *Eur. J. Mineral.,* 2012, *24,* 405-428.

[9] M. Choi, K. Na, J. Kim, Y. Sakamoto, O. Terasaki, R. Ryoo, *Nature*, 2009, *461*, 246-249.
[10] K. Na, M. Choi, W. Park, Y. Sakamoto, O. Terasaki, R. Ryoo, *J. Am. Chem. Soc*., 2010, *132*, 4169-4177.
[11] K. Varoon, X. Zhang, B. Elyassi, D. D. Brewer, M. Gettel, S. Kumar, J. A. Lee, S. Maheshwari, A. Mittal, C. Sung, M. Cococcioni, L. F. Francis, A. V. McCormick, K. A. Mkhoyan, M. Tsapatsis, *Science*, 2011, *334*, 72-75.
[12] S. Maheshwari, E. Jordan, S. Kumar, F. S. Bates, R. L. Penn, D. F. Shantz, M. Tsapatsis, *J. Am. Chem. Soc*., 2008, *130*, 1507-1516.
[13] I. Ogino, M. M. Nigra, S. Hwang, J. Ha, T. Rea, S. I. Zones, A. Katz, *J. Am. Chem. Soc*., 2011, *133*, 3288-3291.
[14] P. Wu, D. Nuntasri, J. Ruan, Y. Liu, M. He, W. Fan, O. Terasaki, T. Tatsumi, *J. Phys. Chem. B*, 2004, *108*, 19126-19131.
[15] S. Kim, H. Ban, W. Ahn, *Catal. Lett*., 2007, *113*, 160-164.
[16] L. Ren, Q. Guo, M. Orazov, D. Xu, D. Politi, P. Kumar, S. M. Alhassan, K. A. Mkhoyan, D. Sidiras, M. E. Davis, M. Tsapatsis, *ChemCatChem*, 2016, 8, 1274-1278.
[17] U. Díaz, A. Corma, *Dalton Trans*., 2014, *43*, 10292-10316.
[18] H. Zhang, Q. Xiao, X. Guo, N. Li, P. Kumar, N. Rangnekar, M. Jeon, S. Al-Thabaiti, K. Narasimharao, S. N. Basahel, B. Topuz, F. J. Onorato, C. W. Macosko, K. A. Mkhoyan, M. Tsapatsis, *Angew. Chem. Int. Ed.,* 2016, Accepted.
[19] D. Xu, G. R. Swindlehurst, H. Wu, D. H. Olson, X. Zhang, M. Tsapatsis, *Adv. Funct. Mater*., 2014, *24*, 201-208.
[20] L. Ren, Q. Guo, P. Kumar, M. Orazov, D. Xu, S. M. Alhassan, K. A. Mkhoyan, M. E. Davis, M. Tsapatsis, *Angew. Chem. Int. Ed*., 2015, *54*, 10848-10851.
[21] A. Inayat, I. Knoke, E. Spiecker, W. Schwieger, *Angew. Chem. Int. Ed.,* 2012, *51,* 1962-1965.
[22] M. Khaleel, A. J. Wagner, K. A. Mkhoyan, M. Tsapatsis, *Angew. Chem. Int. Ed.,* 2014, *53,* 9456-9461.
[23] H. Y. Luo, V. K. Michaelis, S. Hodges, R. G. Griffin, Y. Roman-Leshkov, *Chem. Sci*., 2015, *6*, 6320-6324.
[24] V. J. Margarit, M. E. Martínez-Armero, M. T. Navarro, C. Martínez, A. Corma, *Angew. Chem. Int. Ed*., 2015, *54*, 13724-13728.

6. Synthesis of aluminophosphate analogues of zeolites

Alessandro Turrina and Paul A. Wright

EaStCHEM School of Chemistry, University of St Andrews, Purdie Building, North Haugh, St Andrews, KY169ST, United Kingdom

Introduction

Aluminophosphates (AlPOs) were reported for the first time in 1982 by Flanigen and co-workers at Union Carbide. [1] The AlPOs are zeolite-like materials (zeotypes) having neutral frameworks consisting of alternating corner-sharing aluminate and phosphate tetrahedra (Al/P = 1, known as Flanigen's rule). The difference in electronegativity between Al (1.61) and P (2.19) makes AlPOs moderately hydrophilic, compared to the hydrophobic behaviour shown by silicas (pure silica zeolites). At present, of the 229 framework type codes recognised by the SC-IZA, 53 are known to occur as AlPO-based framework (Table 1). [2] Some AlPOs possess structural types analogous to those of zeolites (*i.e.* AFX, AEI, CHA, SOD), [2] while others possess structure types not yet prepared in aluminosilicate form (*i.e.* AFT, AFV, AVL). [2] Due to the crystal-chemical requirement that AlO_4 and PO_4 must alternate, only frameworks containing even-numbered rings are formed. The only exception, so far, has been reported by Strohmaier et al., where SAPO ECR-40, analogous to that of ZSM-18 (MEI), contains three-member rings. [3] The presence of Si, ordered within the framework, is required. The limitation of forming odd-numbered rings tends to restrict the structural complexity of AlPOs, although Lee and co-workers recently reported the structure of a new medium-pore AlPO, denoted PST-6 (PSI), which has 36 crystallographically distinct tetrahedral sites within the asymmetric unit and a one-dimensional pore system consisting of parallel 10- and 8-ring channels. [4]

A large range of heteroatoms have been introduced into AlPOs by substitution at both Al and P sites. [5] By comparison with zeolites, the more ionic character of the AlPOs and the conditions of their synthesis (starting gel typically pH 6-8) allow more metal cations to be in solution during crystallisation and to be incorporated in the lattice. Aliovalent substitution of Al^{3+} by divalent metal cations such as Mg^{2+}, Mn^{2+}, Co^{2+} and Zn^{2+} results in the formation of MAPOs, [6] which have a negatively-charged framework. In the as-prepared material the negative charges are usually balanced by organic structure directing agents (SDAs);

$$M_x^{2+}Al_{1-x}PO_4 \cdot R_{x/m}^{m+}$$

whilst in the calcined material the protons on bridging hydroxyl groups or Lewis acid sites generated by incompletely tetrahedrally-coordinated heteroatoms, compensate the negative framework charge. Al can also be replaced by trivalent elements (isovalent substitution) such as B and Ga resulting in the formation of so-called BAPOs [7] and GaAPOs, [8] respectively.

The aliovalent replacement of phosphorus by silicon generates silicoaluminophosphates (SAPOs), a class of materials with important catalytic properties. [9] Furthermore, other elements such as vanadium and titanium can substitute P atoms within the framework (VAPO and TAPO, respectively). [10] The general composition for SAPOs can be described as:

$$Al_{1-y}P_{1-x}Si_{x+y}O_4$$

Three mechanisms were initially proposed for the incorporation of silicon atoms in crystalline aluminophosphate frameworks: [11] SM1 in which an aluminum atom is

replaced by a silicon atom, forming a positively charged crystalline framework; SM2 where a phosphorus atom is replaced by a silicon atom resulting in a negatively charged framework; SM3 in which two silicon atoms replace one aluminium and one phosphorus atom, resulting in an electrically neutral structure. The net frameworks charge resulting from the three different mechanisms of substitution would be +1, -1, and 0, respectively. Until now only negatively-charged frameworks have been synthesized; the SM1 mechanism seems not to occur. [12] The SM2 mechanism gives Si surrounded by four Al second nearest neighbors, giving a single ^{29}Si MAS NMR signal (at ca -90 ppm). By contrast, substitution of the silicon by a combination of SM2 and SM3 mechanisms results in the formation of aluminosilicate silicate islands within the AlPO framework which display a number of signals in the ^{29}Si MAS NMR, corresponding to a range of environmentsl. [13]

The charge-balancing H^+ ions in calcined SAPO materials can be replaced to some extent by transition metal cations, and the ion-exchanged products are denoted as Me, H-SAPO. The introduction of transition metal cations into framework sites of SAPOs is also of interest for the design of novel catalysts (MAPSOs). There are several ways to incorporate metals: impregnation, ion-exchange, vapour deposition and isomorphous substitution in which the transition metal ion salt is incorporated directly into the synthesis.[14] Recently, a new synthetic approach has been developed that utilises copper-polyamine or copper-aza-macrocycle complexes as templates, and enables the direct inclusion of complexed Cu^{2+} cations in the solids.[15-20] Calcination then releases the Cu^{2+} cations to extra-framework sites distributed throughout the crystals and removes the need for a cation-exchange step. This process was first demonstrated for SAPO STA-7, [15] and subsequently for SSZ-13, [16] SAPO-34, [17-19] and very recently for SAPO-18[20] giving active, selective and hydrothermally stable catalysts.

Synthesis of Aluminophosphate-based Zeotypes

Aluminophosphate-based zeotypes are usually prepared by hydrothermal synthesis. Typically, a gel is prepared by mixing together framework-building inorganic species such as aluminates (*i.e.* aluminium hydroxide, pseudoboehmite, aluminium isopropoxide), phosphates (*i.e.* orthophosphoric acid) and silicates (*i.e.* fumed silica, colloidal silica, CabOSil) with metal salts (*i.e.* acetates or sulphates) in water with the addition of organic structure directing agents, which also act to modify the pH (*i.e.* amines or hydroxides). Fluoride can also be employed as mineralising agent. F^- offers multiple benefits: (i) reduction of the crystallisation time; (ii) formation of larger and well defined crystals; (iii) crystallisation of a number of phases which usually do not form in a fluoride-free medium. [21]

The organic structure-directing agents (OSDAs) are added to the gel in order to favour the arrangement of tetrahedral anions and the crystallisation of desired structures. Quaternary ammonium cations, generally used in their hydroxide form (*i.e.* tetraethylammonium hydroxide) and secondary and particularly tertiary amines, protonated at the reaction pH (*i.e.* tri-*n*-propylamine and protonated diethylamine), are the most commonly used OSDAs for the synthesis of aluminophosphate zeotypes. Primary amines, tend rather to favour the formation of layered or chain aluminophospahtes structures, where the nitrogen atoms of the amines are hydrogen-bonded to phosphate oxygens that are not shared with framework cations. [22] In addition to promoting the crystallisation of specific structures, the addition of amines or alkylammonium hydroxides permits the pH of the starting gel to be controlled. The pH of

the overall gel must be close to neutral to favour the dissolution of the various components, thereby allowing the nucleation and growth of zeotype crystals. In fact, a pH lower than 3 causes the appearance of dense phases and one higher than 10 usually affects the final yield adversely. [23] The homogeneous gel made up of these components is then heated to a temperature between 100–200 °C in a Teflon-lined stainless steel autoclave (PTFE) for a period that can vary from few hours to several days.

Zeotypes have also been prepared employing the ionothermal synthesis methodology reported by Morris and co-workers. [24] In this method ionic liquid (*i.e.* alkylimidazolium-based or pyridinium-based ionic liquids) acts as both the solvent and the template provider. The absence of other solvents into the reaction mixture, apart from trace water, implies that there are no other molecules present to act as space fillers during zeotype synthesis. Therefore, the ionothermal synthesis ideally removes the competition between template–framework and solvent–framework interactions that are commonly present in hydrothermal preparations. Typically, under working conditions, a small fraction of the ionic liquid cations can decompose, resulting in smaller template cations which may preferentially act as the. Due to the very low vapour pressure of ionic liquids, syntheses may be carried out at ambient pressure, eliminating safety concerns associated with high hydrothermal pressures.

A similar synthetic strategy, named aminothermal synthesis, has been reported by Liu et al. for the preparation of SAPO-34, SAPO-18 and of a new silicoaluminophosphate denoted DNL-6 which possesses the RHO framework type. [25] Triethylamine or diethylamine were used as the solvent and template in the syntheses. However, in this case syntheses are carried out in PTFE-lined autoclaves at autogenous pressure. AlPOs and SAPOs can even be prepared solvothermally, where alcohols (*i.e.* di, tri, and tetraethylene glycol, butane-1,4-diol) are used as thesolvent. [26] It is worth noting that most solvothermal preparations of molecular sieves are not truly anhydrous, and the presence of small amount of water is essential to the crystallisation process.

Compared to the conventional hydrothermal crystallisation, microwave heating of zeotype synthesis mixtures offers the possibility to drastically reduce the crystallisation time and often to obtain small crystals less than a micron in size. For more details, the reader is referred to the review “Microwave Techniques in the Synthesis and Modification of Zeolite Catalysts” by Cundy. [27]

Table 1. List of AlPO-based framework types.

Framework type	Name	AlPO or M(S)APO	B	Co	Fe	Ga	Ge	Mg	Mn	Ni	Si	Ti	V	Zn
AEI	AlPO-18	✓	✓	✓	✓	✓	✓	✓	✓	✓	✓	✓	✓	✓
AEL	AlPO-11	✓	✓	✓	✓	✓	✓	✓	✓	✓	✓	✓	✓	✓
AEN	AlPO-53	✓	✘	✘	✘	✓	✘	✘	✘	✘	✓	✓	✘	✘
AET	AlPO-8, MCM-37	✓	✘	✘	✓	✘	✘	✘	✓	✘	✘	✓	✘	✘
AFI[a]	AlPO-5	✓	✓	✓	✓	✓	✓	✓	✓	✓	✓	✓	✓	✓
AFN	AlPO-14	✓	✓	✓	✘	✓	✓	✘	✓	✘	✘	✘	✘	✘
AFO[b]	AlPO-41	✓	✓	✓	✓	✓	✓	✓	✓	✘	✓	✓	✓	✘
AFR	AlPO-40	✓	✓	✓	✓	✓	✓	✘	✘	✘	✓	✓	✘	✓
AFS	AlPO-46	✓	✓	✓	✘	✓	✓	✓	✘	✘	✓	✘	✘	✘
AFT	AlPO-52	✓	✘	✘	✘	✘	✘	✘	✘	✘	✘	✓	✘	✘
AFV	AlPO-57	✓	✘	✘	✘	✘	✘	✓	✘	✘	✓	✘	✘	✓
AFX	AlPO-56	✓	✘	✘	✘	✘	✘	✓	✓	✘	✓	✓	✘	✘
AFY	AlPO-50	✓	✘	✓	✘	✘	✘	✓	✓	✘	✓	✘	✘	✓
AHT	AlPO-H2	✓	✘	✘	✘	✘	✘	✘	✘	✘	✘	✘	✘	✘
ANA	AlPO-24	✓	✘	✓	✘	✘	✘	✘	✘	✘	✓	✘	✘	✘
APC	AlPO-C, AlPO-H3	✓	✘	✓	✘	✘	✘	✘	✘	✘	✘	✘	✘	✘
APD	AlPO-D, APO-CJ3	✓	✘	✘	✘	✘	✘	✘	✘	✘	✘	✘	✘	✘
AST[c]	AlPO-16	✓	✓	✓	✓	✓	✓	✘	✓	✘	✓	✓	✓	✘
ATN	AlPO-39	✓	✓	✓	✓	✓	✓	✓	✘	✘	✓	✘	✘	✓
ATO[d]	AlPO-31	✓	✓	✓	✓	✓	✓	✓	✓	✓	✓	✓	✓	✓
ATS	AlPO-36	✓	✓	✓	✓	✓	✓	✓	✓	✘	✓	✓	✘	✓
ATT	AlPO-33, AlPO-12	✓	✘	✘	✘	✘	✘	✘	✘	✘	✘	✘	✘	✘
ATV	AlPO-25	✓	✘	✘	✘	✓	✘	✘	✘	✘	✘	✘	✘	✘

AVL	AlPO-59	✓	✘	✘	✘	✘	✘	✓	✘	✘	✓	✘	✘	✓
AWO	AlPO-21	✓	✘	✓	✘	✓	✘	✘	✘	✓	✘	✘	✘	✘
AWW	AlPO-22, AlPO-CJB1	✓	✘	✘	✘	✘	✘	✘	✘	✘	✓	✘	✘	✘
BPH	AlPO-65, STA-5	✓	✘	✘	✘	✘	✘	✓	✘	✘	✓	✘	✘	✓
CGF[e]		✘	✓	✘	✘	✓	✘	✘	✘	✘	✘	✘	✘	✓
CGS[f]		✘	✓	✘	✘	✓	✘	✘	✘	✘	✘	✘	✘	✓
CHA[g]	AlPO-34, AlPO-44, AlPO-47	✓	✓	✓	✓	✓	✓	✓	✓	✓	✓	✓	✓	✓
CLO[h]		✓	✘	✓	✘	✓	✘	✘	✓	✘	✘	✘	✘	✓
CZP[i]		✘	✓	✓	✘	✓	✘	✘	✓	✘	✘	✘	✘	✓
DFT[j]	DAF-2, UiO-20	✓	✓	✘	✓	✘	✘	✘	✘	✘	✘	✘	✘	✓
EDI[k]		✓	✓	✘	✓	✘	✘	✘	✘	✘	✘	✘	✘	✓
ERI	AlPO-17	✓	✓	✓	✓	✓	✓	✓	✘	✘	✓	✓	✓	✘
FAU	AlPO-37	✓	✓	✓	✓	✓	✓	✘	✘	✘	✓	✓	✓	✓
GIS	AlPO-43	✓	✘	✓	✓	✘	✘	✓	✓	✘	✓	✘	✘	✘
JRY	CoAPO-CJ40	✓	✘	✓	✘	✘	✘	✘	✘	✘	✘	✘	✘	✘
JSN	CoAPO-CJ69	✓	✘	✓	✘	✘	✘	✘	✘	✘	✘	✘	✘	✘
JSW	CoAPO-CJ62	✓	✘	✓	✘	✘	✘	✘	✘	✘	✘	✘	✘	✘
LAU[l]		✘	✓	✘	✓	✓	✘	✘	✓	✘	✘	✘	✘	✓
LEV	AlPO-35, AlPO-67	✓	✓	✓	✓	✓	✓	✓	✘	✘	✓	✓	✘	✓
LTA	AlPO-42	✓	✓	✘	✘	✓	✓	✘	✘	✘	✓	✓	✘	✓
LTL		✓	✘	✘	✘	✘	✘	✘	✘	✘	✘	✘	✘	✘
MEI	ECR-40	✓	✘	✘	✘	✘	✘	✘	✘	✘	✓	✘	✘	✘
MER		✓	✘	✓	✘	✘	✘	✘	✘	✘	✘	✘	✘	✘
PSI	PST-6	✓	✘	✘	✘	✘	✘	✘	✘	✘	✘	✘	✘	✘
RHO		✓	✘	✓	✘	✘	✘	✓	✓	✘	✓	✘	✘	✘
SAF	STA-15	✓	✘	✘	✘	✘	✘	✘	✘	✘	✘	✘	✘	✘

SAO	STA-1	✓	✘	✘	✘	✘	✘	✓	✘	✘	✘	✘	✘	✘
SAS	STA-6	✓	✘	✘	✓	✘	✘	✓	✓	✓	✓	✘	✘	✘
SAT	STA-2	✓	✘	✘	✘	✘	✘	✓	✘	✘	✓	✘	✘	✘
SAV	STA-7	✓	✘	✓	✘	✘	✘	✓	✘	✘	✓	✘	✘	✓
SOD[m]	AlPO-20	✓	✓	✓	✘	✓	✓	✓	✓	✓	✓	✓	✘	✘
THO[n]	ZCP-THO	✓	✘	✓	✘	✓	✘	✘	✘	✘	✘	✘	✘	✓
VFI	AlPO-54, VPI-5, MCM-9	✓	✘	✓	✓	✘	✘	✘	✘	✘	✓	✓	✘	✘
ZON	UIO-7	✓	✘	✓	✘	✓	✘	✘	✘	✘	✓	✘	✘	✓

The symbols ✓ and ✘ indicate whether a given element has been replaced within a AlPO-based framework. (a) Ca, Sn, Be, Cr, Cd, Mo, Zr. (b) Zr. (c) Cr. (d) Cd, Cr. (e) CoGaPO-5, ZnGaPO-5. (f) ZnGaPO6, CoGaPO-6. (g) Zr. (h) MnGaPO, ZnGaPO. (i) ZnBPO, MnGaPO, CoZnPO. (j) FeZnPO, ZnCoPO. (k) CoGaPO. (l) CoGaPO, FeGaPO, MnGaPO, ZnGaPO, ZnAlAsO. (m) CoGaPO, ZnGaPO. (n) GaCoPO.

References

[1] S.T. Wilson, B.M. Lok, C.A. Messina, T.R. Cannan, E.M. Flanigen, *J. Am. Chem. Soc.,* 1982, 104, 1146–1147.
[2] Ch. Baerlocher, L.B. McCusker, D.H. Olson, *Atlas of Zeolite Framework Types*, 6th revised edition, Elsevier, Amsterdam, 2007. http://www.iza-structure.org/databases.
[3] M. Afeworki, D. Dorset, G. Kennedy, K. Strohmaier, *Stud. Surf. Sci. Catal.*, 2004, 154, 1274–1281.
[4] J.K. Lee, A. Turrina, L. Zhu, S. Seo, D. Zhang, P.A. Cox, P.A. Wright, S. Qiu, S.B. Hong, *Angew. Chem. Int. Ed.*, 2014, 53(29), 7480–7483.
[5] E.M. Flanigen, B.M. Lok, R.L. Patton, S.T. Wilson, *Pure Appl. Chem.*, 1986, 58, 1351–1358.
[6] H.O. Pastore, S. Coluccia, L. Marchese, *Annu. Rev. Mater. Res.*, 2005, 35, 351–395.
[7] E.M. Flanigen, B.M.T. Lok, R.L. Patton, S.T. Wilson, R.T. Gajek, *US Patent 4,952,383*, 1990.
[8] E.M. Flanigen, B.M.T. Lok, R.L. Patton, S.T. Wilson, *US Patent 5,032,368*, 1991.
[9] B.M. Lok, C.A: Messina, R.L. Patton, R.T. Gajek, T.R: Cannan, E.M. Flanigen, *J. Am. Chem. Soc., 1984, 106*(20), 6092-6093.
[10] (a) M.S. Rigutto, H. Van Bekkum, *J. Mol. Catal.*, 1993, 81, 77–98. (b) R.J. Mahalingam, P. Selvam, *Chem. Lett.*, 1999, 455–456.
[11] M. Mertens, J. Martens, P. Grobet, P. Jacobs, *Guidelines for Mastering the Properties of Molecular Sieves: Relations Between the Physico-Chemical Properties of Zeolitic Systems and their Low Dimensionality*, Vol. 1, Springer, 1990, 1–52.
[12] S. Ashtekar, S.V.V. Chilukuri, D.K. Chakrabarty, *J. Phys. Chem.*, 1994, 98, 4878–4883.
[13] J.S. Chen, P.A. Wright, J.M. Thomas, S. Natarajan, L. Marchese, S.M. Bradley, G. Sankar, C.R.A. Catlow, P.L. Gai-Boyes, R.P. Townsend, C.M. Lok, *J. Phys. Chem.*, 1994, 98, 10216–10224.
[14] M. Hartmann, L. Kevan, *Transition-Metal Ions in Molecular Sieves Chemical Reviews*, Vol 99, 1999, 635–663.
[15] A.L. Picone, S.J. Warrender, A.M.Z. Slawin, D.M. Dawson, S.E. Ashbrook, P.A. Wright, S.P. Thompson, L. Gaberova, P.L. Llewellyn, B. Moulin, A. Vimont, M. Daturi, M.B. Park, S.K. Sung, I.-S Nam, S.B. Hong, *Microporous Mesoporous Mater.*, 2011, 146, 36–47.
[16] L. Ren, L. Zhu, C. Yang, Y. Chen, Q. Sun, H. Zhang, C. Li, F. Nawaz, F.-S. Xiao, *Chem. Commun.*, 2011, 47, 9789–9791.
[17] R. Martínez-Franco, M. Molinera, C. Franch, A. Kustov, A. Corma, *Appl. Catal., B*, 2012, 127, 273–280.
[18] U. Deka, I. Lezcano-Gonzalez, S.J. Warrender, A.L. Picone, P.A. Wright, B.M. Weckhuysen, A.M. Beale, *Microporous Mesoporous Mater.*, 2013, 166, 144–152.
[19] R. Martínez-Franco, M. Moliner, P. Concepcion, J.R. Thogersen, A. Corma, *J. Catal.*, 2014, 314, 73–82.
[20] R. Martínez-Franco, M. Moliner, A. Corma, *J. Catal.*, 2014, 319, 36–43.
[21] Y. Yang, J. Pinkas, M. Schäfer, H.W. Roesky, *Angewandte Chemie International Edition*, 1998, 37 (19), 2650–2653.
[22] P.A Wright, *Microporous Framework Solids*, RSC Publishing, Cambridge, UK, 2008.
[23] H.O. Pastore, S. Coluccia, L. Marchese, *Annu. Rev. Mater. Res.*, 2005, 35, 351–395.
[24] E.R. Cooper, C.D. Andrews, P.S. Wheatley, P.B. Webb, P. Wormald, R.E. Morris, *Nature*, 2004, 430, 1012–1016.

[25] D. Fan, P. Tian, S. Xu, Q. Xia, X. Su, L. Zhang, Y. Zhang, Y. He, Z. Liu, *J. Mater. Chem.*, 2012, 22, 6568–6574.
[26] R.E. Morris, S.J. Weigel, *Chem. Soc. Rev.*, 1997, 26, 309–317.
[27] C.S. Cundy, *Collect. Czech. Chem. Commun.* 1998, *63*, 1699–1723

7. Disassembly as a route to new materials

Pavla Eliášová[1], Russell E. Morris[2], Jiří Čejka[1]

[1]J. Heyrovský Institute of Physical Chemistry, Academy of Sciences of the Czech Republic, Prague, Czech Republic
[2] EaStCHEM, School of Chemistry, University of St. Andrews, United Kingdom

Introduction

Pushing and extending the synthetic limits of zeolites

Zeolites are traditionally perceived as regular three-dimensional (3D) frameworks built from silicon tetrahedra by sharing oxygen corners. However, in last two decades there has been an increasing interest in two-dimensional (2D) zeolites, a family of materials numbering now about 15-20 members [1-3]. Unlike 3D zeolites, layered materials may vary in the spatial arrangements of lamellas, which significantly affect their textural properties and consequently their catalytic performance [2]. Although most of them (if not all) are still only the subject of basic-science interest and not real industrial application, they have proved their importance by offering an alternative way to overcome diffusion limitations usually connected with bulk zeolites. Overall, zeolitic science seems to have the tendency to leave the chemistry of bulk rigid crystals and lean more towards zeolitic materials with decreased crystal proportions, *e.g.* with hierarchical, nano or layered nature. Such zeolites usually excel by facilitating mass transfer while keeping the advantages of zeolitic frameworks.

The solvothermal synthesis of zeolites is the most common synthetic approach applied for both 3D and 2D zeolites. This bottom-up method leads to energetically most favourable structures according to energy-density correlation, which causes some limitations to the diversity of synthesizable zeolites (more discussed later). There have been many efforts to modify the solvothermal conditions to expand these potential borders, *e.g.* using different mineralizing agents, ionic-liquids instead of water solvent, heating via microwaves, using new ammonium, phosphonium and phosphazene-based SDAs *etc.*

In 2011 top-down synthesis was developed as an alternative approach based on germanosilicates [4]. The novel synthesis protocol based on 3D-2D-3D transformation was called ADOR (Assembly-Disassembly-Organisation-Reassembly).

Step by step to novel structures

The ADOR abbreviation stands for four fundamental steps leading to new zeolites: Assembly, Diassembly, Organisation, Reassembly (see Scheme 1). The first means to synthesize the parent material (Assembly), a germanosilicate, by well-described bottom-up protocols. Germanosilicates are generally hydrolytically sensitive and it had been believed that their framework uncontrollably collapses in time when exposed to air moisture. Despite this fact, it was found that under specific conditions some germanosilicates can transform chemically selectively from 3D framework into 2D layered materials rather than totally and irreversibly collapse [4]. It proceeds by hydrolyzing and removing of specific secondary building units (*e.g.* double-four-rings, D4R, double-three-rings, D3Rs) located between the layers and preferentially occupied by sensitive dopant, here specifically germanium. This step is denoted as Disassembly. The third step, Organisation, can very closely follow the Disassembly or can be

performed as a separate treatment. The purpose is to organise the layers into an appropriate position towards each other to guarantee their full reconnection during the last Reassembly step (calcination at < 500˚C).

Although ADOR was already demonstrated on a couple of germanosilicates [5], zeolite UTL remains the most explored representative; therefore, here it will be used to demonstrate the ADOR potential. Germanosilicate UTL consists of almost purely siliceous layers with D4R units connecting them. D4R units are mostly composed of germanium atoms. The Assembly step of UTL is just a conventional synthesis published in many Refs. [6,7]. Disassembly was studied very carefully using various water solutions of 0-12M hydrochloric acid [8]. As germanium is a hydro-sensitive dopant in less than 5 minutes more than 90% of germanium is washed out of the UTL framework independently on the acid molarity. In the following Organisation step, we distinguish two types: I. *self-organisation*; and II. *organisation by intercalation of additive molecules*. The latter type is performed as a separate step and thus it will be discussed in the next section. Independently of the further modifications, the character/topology of the layer is identical with the parent zeolite UTL [4, 9].

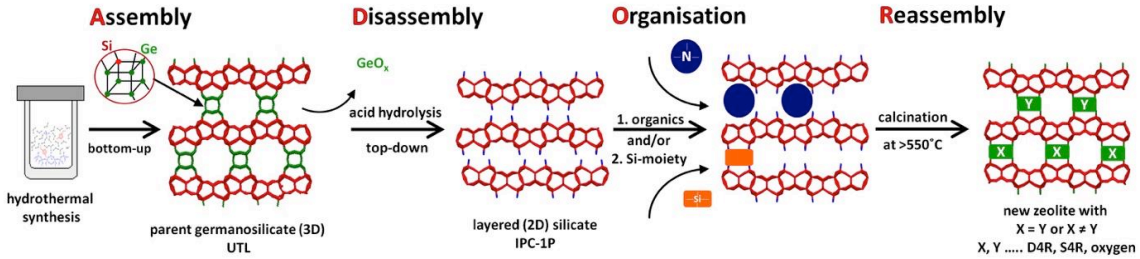

Scheme 1. The schematic view on the whole ADOR method showing the individual step.

Self-organisation directly follows the Disassembly step. Depending on the acid molarity two processes may occur presenting in fact two competing mechanisms - de-intercalation and re-organisation (Scheme 1). In pure water or diluted HCl solutions (< 0.1M) the de-intercalation prevails leading to removal of any hydrolysed D4Rs debris. The resulting layered material is called IPC-1P. During the Reassembly, surface silanol groups condense with the opposite counterparts forming Si-O-Si oxygen bridges. The final zeolite IPC-4 (IZA code PCR) has 10-8-ring channel system. On the other hand, the highly acidic solution like 12M HCl supports making-breaking of -Si-O-Si- bonds. It initiates a re-organisation of some framework atoms. Thereby some Si atoms, originally located intra-layers, may move to the layer surface and build precursors for novel layer connections. During the calcination it forms siliceous S4R units between the layers giving rise to 12-10-ring perpendicular channels of IPC-2 zeolite [8]. IPC-2 is topologically identical to zeolite COK-14 [10] (IZA code OKO), they have the same connectivity although different symmetry.

By careful control of the molarity one may balance between de-intercalation and re-organisation rates. With increasing [H^+] the re-organisation starts occurring and at certain point the equilibrium between de-intercalation and re-arrangement can be reached. In this case, specifically at 1.5M, about half of the layers are de-intercalated and half undergo rearrangement. Reassembled zeolite consists of ~ 50% layers connected with Si-O-Si bridges and 50% with S4R units and it was called IPC-6 [8]. At 5M it was found another staged material denoted IPC-7 containing ~ 50% of S4R connections and 50% of siliceous D4R connections [8]. Novel zeolites have two independent channel systems, 12-10- and 10-8-ring in IPC-6, and 14-12- and 12-10-ring system in IPC-7 (see Scheme 2).

Layer manipulation enabling structural diversity

The first product of the top-down synthesis, the layered IPC-1P, is by its properties similar to any other layered zeolites. Similarly to them, the interlayer space in IPC-1P can be variously modified pursuing two different objectives [1, 2]: 1) to increase the interlayer space and thus permanently separate the layers; or 2) to organise the layers in suitable positions in order to subsequently reconnect them into 3D frameworks. The first target is easily reached by well described swelling and pillaring treatments. Both inorganic (amorphous SiO_2) [9] and organic [11, 12] pillars may be built up between the layers. The incorporation of organic pillars like silsesquioxanes has a great potential for preparing a bifunctional acid-base catalyst.

In order to link the layers of any topology into 3D framework one should apprise the properties of the layer surface, particularly the surface silanol density, inter-silanol distances *etc.* [13-15]. It determines their possible mutual arrangement and consequently their new inter-layer linking. IPC-1P has the quadruplets of the silanols as a result of D4R hydrolysis. Based on the calculations performed with the periodic model consisting of two interacting IPC-1P layers at the density functional theory (DFT) level, the most stable arrangement was found for unshifted layers [13, 14]. This is exactly the inter-layer arrangement, which occurs during the self-organisation in the acid solutions (as described in the previous chapter). Nevertheless, there are at least three more possible inter-layer arrangements although they are energetically less favourable. To achieve the lateral shifts of adjacent layers one has to introduce an appropriate organising molecule.

Organic amines and ammonium cations showed a good ability and suitability to be intercalated between the layers [5]. For instance, octylamine nicely fits into the space between two unshifted layers [14]. The unshifted layers may be directly calcined forming zeolite IPC-4 with 10-8-ring channels. Alternatively, extra-silicon source like diethoxydimethylsilane (DEDMS) can be added. DEDMS molecules incorporate between the unshifted layers via bonds to the surface silanols. During the calcination they form new S4R units as interlayer links giving rise to 12-10-ring channels of zeolite IPC-2 [14]. On the other hand, choline molecules bind to the layers in other specific way (dependent as well on its amount), which forces the layers to shift with respect to each other. As a result, the direct reassembly of the laterally shifted layers leads to zeolite IPC-9 with unusual channel system 10-7-ring [16]. When DEDMS is incorporated before reassembly, another zeolite with S4R units can be formed. It is denoted IPC-10 and contains 12-9-ring channels [16] (Scheme 2).

The perspectives for ADOR

The main advantage of the ADOR method lies in the predictability of the final zeolite structure. It is not a matter of coincidence and luck as it has been with the bottom-up synthesis of most known zeolites. Here, the structure of the layers in parent and daughter zeolites is preserved and the nature of novel inter-layer connections can be easily controlled by choosing appropriate hydrolysis conditions or by intercalating suitable organic and silicon molecules. This greatly facilitates the structure solving, which may be very difficult and demanding for a completely unknown zeolitic structure.

More importantly, one can design the overall porosity of the system, *i.e.* the size and shape of the channels [8]. It is given by selecting the inter-layer links as discussed above. The control over the porosity is highly desired for any application, particularly in

catalysis where shape-selectivity is very appreciated as a mighty tool to inhibit undesired side reactions [17]. Thus, the ADOR shows that chemical weakness in the material (like low hydrothermal stability of germanosilicates) can be beneficial if you find the appropriate purpose or application [18].

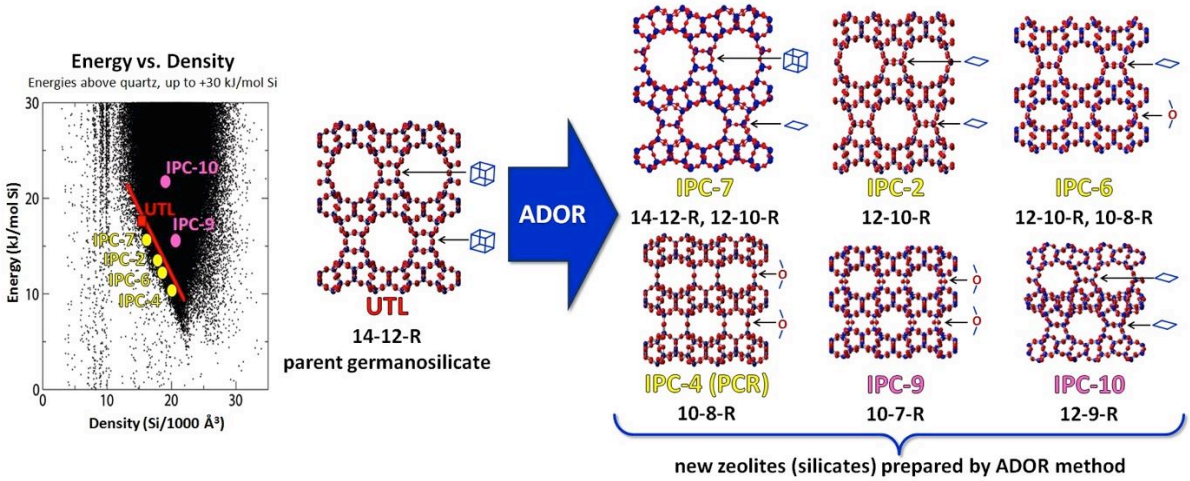

Scheme 2. The energy versus density plot (on the left) shows the distributions of thermodynamically accessible structures (black dots) and also linear fit of energy versus density for the known zeolite structures as solid red line (reprinted from Ref. [19]). The novel zeolites prepared by ADOR from parent UTL are marked on the plot as red dot for UTL, IPC-2, IPC-4, IPC-6 and IPC-7 as yellow dots and IPC-9 and IPC-10 as pink dots. Their structures with the connecting units are shown on the right.

Although ADOR was demonstrated on other germanosilicates, *e.g.*, ITH [5], still UTL remains the most fruitful example. This germanosilicate stands at the beginning of the synthesis until now 6 daughter zeolites varying in diversity of the size and shape of the individual channel system and a number of hybrid materials. The uniqueness of UTL probably lies in its two-dimensional channel system giving rise to compact solid layers after hydrolysis and the appropriate surface-silanol density allowing the layer manipulation. The limits and perspectives of the ADOR method are overviewed in a review paper Ref. [5].

One more and probably the most important advantage is connected with the ADOR. In 2009 Deem et. al constructed a database of computationally predicted zeolite-like materials where are over two millions of unique structures [19]. About 10% lie within the +30kJ/mol Si energetic band above α-quartz, which is considered as a reasonable area for zeolite frameworks. Nevertheless, all known zeolites are located on the low-density edge shown as a red line in Scheme 2. To evaluate the feasibility of hypothetical zeolite-like materials, so called feasibility factor was introduced [19]. It presents how far away from the low-density edge of the distribution is the hypothetical zeolite-like material. It is supposed that materials lying further away from the red line are less feasible. Thus, the question arises, why can we not prepare zeolites away from this line? As some scientists already suggested [19] the hitch might be in the synthetic protocol, the bottom-up crystallization, which usually proceeds from a low-density solution toward a high-density solid material. And here the ADOR offers an alternative route as the top-down method avoids other solution-assisted crystallization beside the initial one for the synthesis of the parent zeolite. Scheme 2 shows the location of the parent UTL zeolite very close to the red line (as it supposed to be) and all daughter IPC zeolites. It is clear

that zeolites IPC-9 and IPC-10 broke the rules of feasibility as they are high energy materials located on energy-vs.-density plot far from any other known zeolite. This is the most striking consequence of the ADOR, opening the pathway to novel zeolites 'unfeasible' via traditional bottom-up protocols.

References

[1] W. J. Roth, J. Čejka, Catal. Sci. Technol. 1 (2011) 43
[2] W. J. Roth, P. Nachtigall, R. E. Morris, J. Čejka, Chem. Rev. 114 (2014) 4807
[3] W. J. Roth, B. Gil, W. Makowski, B. Marszalek, P. Eliášová, Chem. Soc. Rev. in press, doi: 10.1039/C5CS00508F (2016)
[4] W. J. Roth, O. V. Shvets, M. Shamzhy, P. Chlubná, M. Kubů, P. Nachtigall, J. Čejka, J. Am. Chem. Soc. 133 (2011) 6130
[5] P. Eliášová, M. Opanasenko, P. S. Wheatley, M. Shamzhy, M. Mazur, P. Nachtigall, W. J. Roth, R. E. Morris, J. Čejka, Chem. Soc. Rev. 44 (2015) 7177
[6] O. V. Shvets, A. Zukal, N. Kasian, N. Žilková, J. Čejka, Chem. Eur. J. 14 (2008) 10134
[7] M. V. Shamzhy, O. V. Shvets, M. V. Opanasenko, P. S. Yaremov, L. G. Sarkisyan, P. Chlubná, A. Zukal, V. R. Marthala, M. Hartmann, J. Čejka, J. Mater. Chem. 22 (2012) 15793
[8] P. S. Wheatley, P. Chlubná-Eliášová, H. Greer, W. Zhou, V. R. Seymour, D. M. Dawson, S. E. Ashbrook, A. B. Pinar, L. B. McCusker, M. Opanasenko, J. Čejka, R. E. Morris, Angew. Chem. Int. Ed. 126 (2014) 13426
[9] P. Chlubná, W. J. Roth, H. F. Greer, W. Z. Zhou, O. Shvets, A. Zukal, J. Čejka, R. E. Morris, Chem. Mater. 25 (2013) 542
[10] E. Verheyen, L. Joos, K. Van Havenbergh, E. Breynaert, N. Kasian, E. Gobechiya, K. Houthoofd, C. Martineau, M. Hinterstein, F. Taulelle, V. Van Speybroeck, M. Waroquier, S. Bals, G. Van Tendeloo, C. E. A. Kirschhock, J. A. Martens, Nat. Mater. 11 (2012) 1059
[11] M. Opanasenko, W. O. N. Parker, M. Shamzhy, E. Montanari, M. Bellettato, M. Mazur, R. Millini, J. Čejka, J. Am. Chem. Soc. 136 (2014) 2511
[12] M. V. Opanasenko, E. Montanari, M. V. Shamzhy, ChemPlusChem 80 (2015) 599
[13] L. Grajciar, O. Bludský, W. J. Roth, P. Nachtigall, Catal. Today 204 (2013) 15
[14] W. J. Roth, P. Nachtigall, R. E. Morris, P. S. Wheatley, V. R. Seymour, S. E. Ashbrook, P. Chlubná, L. Grajciar, M. Položij, A. Zukal, O. Shvets, J. Čejka, Nat. Chem. 5 (2013) 628
[15] M. Trachta, O. Bludský, J. Čejka, R. E. Morris, P. Nachtigall, ChemPhysChem 15 (2014) 2972
[16] M. Mazur, P. S. Wheatley, M. Navarro, W. J. Roth, M. Položij, A. Mayoral, P. Eliášová, P. Nachtigall, J. Čejka, R. E. Morris, Nat. Chem. 8 (2016) 58
[17] N. Žilková, P. Eliášová, S. Al-Khattaf, R. E. Morris, M. Mazur, J. Čejka, Catal. Today in press, doi:10.1016/j.cattod.2015.09.033
[18] R. E. Morris, J. Čejka, Nat. Chem. 7 (2015) 381
[19] M. W. Deem, R. Pophale, P. A. Cheeseman, D. J. Earl, J. Phys. Chem. C 113 (2009) 21353

8. Synthesis of zeolites: seeding approach

Kenta Iyoki, Keiji Itabashi, Tatsuya Okubo

Department of Chemical System Engineering, The University of Tokyo, 7-3-1 Hongo, Bunkyo-ku, Tokyo 113-8656, Japan

Introduction

In the industrial crystallization including zeolite syntheses, the employment of seeding results in multiple advantages such as shorten induction period, higher product yield, controlled particle size distribution, and improved product quality. Seeding is also employed for special purposes, such as polymorphs control and production of single handedness in organic syntheses [1]. Furthermore, a unique use of seeding was reported for some zeolites. For the synthesis of CON-type zeolite (CIT-1), seeding of *BEA-type zeolite (beta) is considered to be essential although the detailed mechanism has not yet been clarified [2].

The zeolite synthesis process involves:

-Mixing of the initial sources in water to obtain a starting gel
- Aging at room temperature (if necessary)
-Heating
-Product recovery (after crystallization)
-Drying
-Calcination when an organic structure-directing agent (OSDA) is employed.

During the aging at ambient conditions as well as the heating, aluminosilicate mixtures are considered to convert into zeolite precursor. This is followed by the crystallization of zeolites, which consists of two steps: nucleation and crystal growth. The induction period before the nucleation is considered to be due to its high activation energies. The nucleation process can be altered by the use of seeds. They can act as nuclei and provide active surfaces for product growth. Once crystals start to grow, activation energies for the growth are considered to be lower, and crystal growth is faster than nucleation. Several mechanisms have been proposed in addition to a simple mechanism involving liquid-mediated supply of the dissolved (alumino)silicate species to the surface of the seed zeolite crystals. For example, secondary nucleation via the initial breeding mechanism caused by microcrystalline dust washed out from seed surfaces has been investigated. Polycrystalline breeding formed over seed crystals has been also reported as a potential pathway [3].

Although seeding methods have been well known and often used for the zeolite synthesis, the new aspects of seeding are recently developed focusing on the OSDA-free synthesis and on ultrafast synthesis of zeolites. These two trends will be described below in detail.

OSDA-free synthesis of zeolites by seeding

The OSDA is essential for the synthesis of some specific zeolites and especially the one with high silicon to aluminum ratio (SAR). However, the cost of OSDAs accounts for a large portion of the total cost of the starting materials. In addition, calcination and waste gas/water treatment are additional processes. Several recent publications revealed that OSDA-free synthesis of *BEA- [4–6], MTW- [7] and RTH-type zeolites [8]

were achieved by seeding approach in spite of using the classical synthesis in the presence of OSDAs. Moreover, it was shown that liquid-mediated crystal growth was dominant [9]. Secondary nucleation has not been observed so far. Using OSDA-free synthesis, more than 10 zeolites have been synthesized [10,11]. The OSDA-free synthesis of zeolites is summarized in Table 1. The data provide information about seed crystals and products obtained by the use of seeding approach. It is important to notice that without seeding, other zeolites, silicates, or amorphous matters are obtained.

The amount of seed crystals ranges from 0.5 to 33.3 wt.% relative to the silica sources used for the preparation of the initial mixtures. Seeds clearly direct the crystallization of targeted zeolites, and the products have the same framework types in the most cases. However, seeds and products have shown different structures in two cases: synthesis of MTW from *BEA [11] and NES from EUO [12]. Figure 1 schematically illustrates the difference between conventional and recently developed seeding methods.

Table 1. Summary of OSDA-free synthesis of zeolites.

Seeds				Products		References
Framework type code	Material name	SiO_2/Al_2O_3 ratio	Amount (wt% to silica)	Framework type code	SiO_2/Al_2O_3 ratio	
*BEA	Beta	No data	10	*BEA	No data	[4]
*BEA	Beta	52	0.5–2.5	*BEA	7.8–9.0	[5]
*BEA	Beta	14–24	1–10	*BEA	10.4–13.2	[6]
*BEA	Beta	20.4, 23.2	10.3	*BEA	Core:26.6, Shell:10.6	[11]
*BEA	Beta	50	9.1–33.3	*BEA	14.6–22	[11]
*BEA	Beta	No data	5	*BEA	9.8 SiO_2/Fe_2O_3 = 100	[11]
*BEA	CIT-6	∞ SiO_2/ZnO = 13	10	*BEA	10.9–21.4	[11]
*BEA	Beta	24	10	MTW	31.8–46.4	[11]
EUO	EU-1	15	10–15	NES	14.0–25.8	[12]
LEV	RUB-50	19.4	4.6	LEV	No data	[11]
LEV	Not specified	21.4	5–17	LEV	9.2–12	[11]
LEV	RUB-50	19.5	1.5–5	LEV	8.1	[11]
MAZ	Omega	5.6	10–20	MAZ	6.4–8.2	[13]
MAZ	Not specified	7.8	9.1–33.3	MAZ	9.6–12.8	[14]
MEL	ZSM-11	66.0	10	MEL	17.6	[11]
MSE	MCM-68	22	10	MSE	12–14	[15]
MTT	ZSM-23	No data	10	MTT	40	[16]
MTW	ZSM-12	101	10	MTW	No data	[11]
MTW	ZSM-12	94.6	1–10	MTW	23.4–32.4	[11]
PAU	ECR-18	No data	10	PAU	No data	[11]
RTH	RUB-13	∞ SiO_2/B_2O_3 = 46	2	RTH	82 ([Al]-TTZ-1), 216 ([Al, B]-TTZ-1.) SiO_2/B_2O_3 = 42–54 SiO_2/Ga_2O_3 = 504	[8]
SZR	SUZ-4	No data	1	SZR	No data	[11]
TON	ZSM-22	No data	1–10	TON	88	[17]
VET	VPI-8	SiO_2/ZnO = 13	10	VET	295–351, ∞ SiO_2/ZnO = 12.3–16.6	[18]

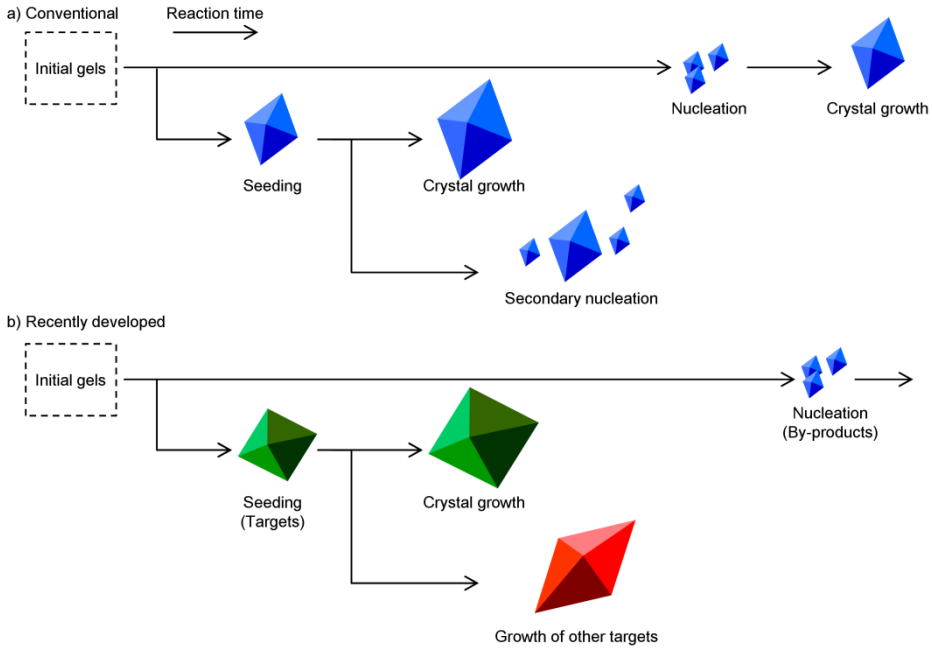

Figure 1. Schematic illustration of a) conventional and b) recently developed seeding methods.

The products obtained by this method have common characteristic features. Firstly, the products are well faceted, and the defects within the products are less than those synthesized with OSDAs. This is due to the fact that the crystallization process is focusing on the crystal growth, and that it is not necessary to calcine the product in order to remove the OSDAs, which often leads to dealumination and creation of defect sites. Moreover, the SARs of the products are lower than those synthesized with OSDAs. If necessary, a post-synthetic dealumination is applied to control the chemical composition of the final phase [15].

Ultrafast synthesis of zeolites by seeding

The synthesis of zeolites usually takes few hours up to few weeks during which the crystallization process is completed. Recently, seeding approach combined with fast heating in a preheated oil bath by employing a tubular reactor reveal that the crystallization of zeolite and related materials is completed within several minutes, i.e., one minute for AlPO-5 [19] and 10 minutes for SSZ-13 [20].

As shown in the introduction, the process of the zeolite synthesis consists of several steps in view of unit operation. In view of phenomena, it consists of precursor formation (conversion of starting mixture), nucleation and crystal growth of zeolite. In typical Teflon®-lined autoclaves with convection ovens, the heating rate of the gel is not high enough, and the heat transfer rate gives a significant influence on the crystallization time. Which is the rate-determining step?

Firstly, the heating problem was resolved by the use of a reactor made of stainless steel tube (1/4” OD) without Teflon®-lining instead of autoclave. In addition, preheated oil bath was employed in place of an air oven. The main advantage of a tubular reactor is continuous operation useful for mass production. Thanks to the fast heat transfer between the oil and the tube, through the tube wall and between the tube and the gel, the gel was heated to a targeted temperature within one minute although it took one hour for the conventional case. The solution of the heating problem resulted in reduction in

the crystallization time; however, further reduction was necessary to apply for the continuous operation. Moreover, skipping nucleation process was investigated when the seeding was employed. In OSDA-free synthesis, the problem of the dissolution of seeds during the heating was a common issue beyond the types of the zeolites. Thus, the most important point in seed-assisted synthesis is to match the timing between the conversion of the starting mixture to the precursor and the survival of seeds crystal during heating. In the fast heating system developed here, the damage of the seed could be reduced. In general, the conversion of the mixture to the precursor proceeds in aging (before heating) and heating steps. In the case of fast heating, the role of the aging step is more significant since the heating-up time is shortened. High temperature condition is advantageous in view of the crystal growth rate; however, OSDAs tend to be degraded more at higher temperature. It is the competition between the crystal growth and the degradation of OSDAs. If the heating time can be reduced by fast heating, the loss of the OSDAs before the onset of the crystal growth is effectively reduced. By tuning all the factors described above, ultrafast synthesis of zeolites was successfully achieved

The key aspect necessary for the successful, ultrafast synthesis of zeolites are summarized as follows:

-Preparation of suitable gel by tuning the composition with aging
-Removal of thermal time lag by fast heating
-Skipping nucleation stage by seeding
-Enhanced crystal growth at high temperature
-Limited degradation of OSDA by fast heating.

These results show that the crystal growth of zeolites itself is not as slow as they had been believed, compared with heating process of a conventional autoclave as well as the precursor formation and the nucleation processes.

Conclusions

From both scientific and engineering points of view, the OSDA-free synthesis and ultrafast synthesis have attracted considerable attention of researchers and engineers. These two cases show the importance of avoiding avoid high energy burrier of nucleation as well as the efficiency of seeding approach for zeolite syntheses. Although, so far these methods have been applied to limited structure types and compositions, it is expected that the applicable zeotypes will be broadened in near future. Moreover, there might be other advantages of seeding method beyond OSDA-free and ultrafast synthesis. There are still many unexploited routes for the synthesis of zeolites that left to be discovered.

References

[1] I. Weissbuch, M. Lahav, Chem. Rev. 111 (2011) 3236
[2] R.F. Lobo, M.E. Davis, J. Am. Chem. Soc. 17 (1995) 3766
[3] C.S Cundy, P.A. Cox, Micropor. Mesopor. Mater. 82 (2005) 1
[4] B. Xie, J. Song, L. Ren, Y. Ji, J. Li, F.-S. Xiao, Chem. Mater. 20 (2008) 4533
[5] G. Majano, L. Delmotte, V. Valtchev, S. Mintova, Chem. Mater. 21 (2009) 4184
[6] Y. Kamimura, W. Chaikittisilp, K. Itabashi, A. Shimojima, T. Okubo, Chem. Asian J. 5 (2010) 2182
[7] K. Iyoki, Y. Kamimura, K. Itabashi, A. Shimojima, T. Okubo, Chem. Lett. 39 (2010) 730
[8] T. Yokoi, M. Yoshioka, H. Imai, T. Tatsumi, Angew. Chem. Int. Ed. 48 (2009) 9884

[9] Y. Kamimura, S. Tanahashi, K. Itabashi, A. Sugawara, T. Wakihara, A. Shimojima, T. Okubo, J. Phys. Chem. C 115 (2011) 744
[10] K. Itabashi. Y. Kamimura, K. Iyoki, A. Shimojima, T. Okubo, J. Am. Chem. Soc. 134 (2012) 11542
[11] K. Iyoki, K. Itabashi, T. Okubo, Micropor. Mesopor. Mater. 189 (2014) 22.
[12] K. Iyoki, M. Takase, K. Itabashi, K. Muraoka, W. Chaikittisilp, T. Okubo, Micropor. Mesopor. Mater. 215 (2015) 191
[13] A. Ogawa, K. Iyoki, Y. Kamimura, S.P. Elangovan, K. Itabashi, T. Okubo, Micropor. Mesopor. Mater. 186 (2014) 21
[14] K. Honda, A. Yashiki, M. Sadakane, T. Sano, Micropor. Mesopor. Mater. 196 (2014) 254
[15] Y. Kubota, K. Itabashi, S. Inagaki, Y. Nishita, R. Komatsu, Y. Tsuboi, S. Shinoda, T. Okubo, Chem. Mater. 26 (2014) 1250
[16] Q. Wu, X. Wang, X. Meng, C. Yang, Y. Liu, Y. Jin, Q. Yang, F.-S. Xiao, Micropor. Mesopor. Mater. 186 (2014) 106
[17] Y. Wang, X. Wang, Q. Wu, X. Meng, Y. Jin, X. Zhou, F-S. Xiao, Catal. Today 226 (2014) 103
[18] K. Iyoki, K. Itabashi, W. Chaikittisilp, S.P. Elangovan, T. Wakihara, S. Kohara, T. Okubo, Chem. Mater. 26 (2014) 1957
[19] Z. Liu, T. Wakihara, D. Nishioka, K. Oshima, T. Takewaki, T. Okubo, Chem. Commun. 50 (2014) 2526
[20] Z. Liu, T. Wakihara, K. Oshima, D. Nishioka, Y. Hotta, S. P. Elangovan, Y. Yanaba, T. Yoshikawa, W. Chaikittisilp, T. Matsuo, T. Takewaki, T. Okubo, Angew. Chem. Int. Ed. 54 (2015) 5683

9. Post synthesis modification of zeolites

Robert Bedard and Suheil Abdo

UOP R&D, UOP a Honeywell Company, Honeywell UOP
25 E. Algonquin Rd. Des Plaines, IL 60016

Introduction

New nanoporous materials enable breakthrough improvements in catalytic and adsorptive processes in the refining, petrochemical, gas processing industries and in many other areas of technology. Although the discovery of new zeotype structures continues to be a fruitful materials research focus for these various applications, there are many cases where modification of zeolite and related materials after their synthesis can also lead to incremental and breakthrough improvements in applications. In fact, there are a greater number of research groups throughout the world that stress post-synthesis modification to generate new functional materials than focus on new zeolite structure discovery, perhaps because such modifications have led to many commercially significant materials.

For the purpose of this short review the various major post-synthetic modification chemistries are grouped according to the modification approach. Initial discovery of the impact of post synthesis modification on the properties and performance of zeolites dates back to 1950's starting with ion exchange to remove alkali metals from extra framework charge balancing positions. The major approaches outlined in this review include chemistries that are additive, subtractive, substitutive, and transformative. Additive chemistries start with as-synthesized or calcined zeolites and seek to modify the properties by adding to the bulk composition, usually at the surface of the zeolite material. Subtractive chemistries involve the removal of some of the mass, usually attempting selective removal in some way, to adjust acidity, diffusion behavior, or other properties. Substitutive methods sometimes are accomplished via an initial subtractive step, followed by insertion of components that lead to significant modification of acidic or perhaps framework charge properties. Ion exchange processes such as framework stabilization by rare-earth exchange can be viewed as substitutive as well and are often used in combination with other modification strategies. Transformative modifications have been accomplished in many forms, including using one zeolite as a reagent in the synthesis of another, exfoliation of layered materials to create high surface area "layered" zeolites, and reactions to connect layered zeolites through their interlammellar spaces, forming three-dimensional zeolite topologies.

Additive Methods

The general method of selectivation has been the subject of a great number of patents and a few of the early examples are referred to here.[1,2] Early pioneering work on zeolite surface passivation with phosphorus and boron compounds were carried by Kaeding et al.[3] The main processes that have been used in commercial applications have been selective in-situ or ex-situ coking of zeolite surfaces or ex-situ solution or perhaps gas phase silylation of the zeolite surface, mostly using MFI zeolite. The modification thus becomes either a carbon coke coating or silica coating of the zeolite

surface. These processes sometimes dramatically increase methyl benzene transformation selectivity to para-xylene by one or more mechanisms, which include passivation of the acid sites on the zeolite external surface and/or narrowing of the zeolite pores to increase shape selectivity. An interesting perspective on the chronology of development of para-selective zeolite catalysts at Mobil Oil Corporation has appeared. [4] Patents continue to issue in this area; modification procedures continue to increase in complexity and include more specific procedural steps. [5]

The mutual interaction of zeolite, binder and matrix components has been exploited in FCC and other catalysts for many years by industrial scientists. It is naïve to assume that binders are inert spectators in catalyst composites, necessary only for the purpose of minimizing pressure drop and loss of active catalytic phase from the reactor under operating conditions. This is because the chemistry involved in creating the binder and the subsequent calcination that produce the porous ceramic forms create new bonds between the binder/matrix and zeolitic and other catalyst components; and these bonds may generate new types of active sites in the finished catalyst.

Only recently have academic groups begun to focus on the chemistry of the binder/zeolite interaction. [6,7] This late focus on such important phenomena is likely due to the complexity of finished catalyst materials chemistry, structure, and the associated difficulty in thorough characterization aimed at eventual fundamental understanding of local structures and active sites. The dramatic improvements of many characterization techniques including solid state NMR, various forms of microscopy and imaging; powder diffraction and PDF analysis, tomographic methods, X-ray spectroscopy and new developments in operando and combined techniques, have finally begun to enable characterization of these complex composites. [8,9]

Subtractive Methods

The phenomenon of zeolitic aluminum expanding its coordination sphere and thereby becoming susceptible to removal from the framework is well established and long utilized in the preparation of industrial catalysts. Dealumination can be carried out using a number of liquid and gas phase chemical treatments using acids, steam, ion exchange and other chemical manipulations, in many cases a combination of one or more of these processes. Steam-stabilization was used to make the so-called 'Ultra Stable' Y family of Y zeolites, a commercially important family of materials that still is extensively used. Secondary synthesis methods based on steam stabilization caused significant porosity modification. The precise, geometrically defined, pores of zeolites measuring in the range of 5-13 Å were augmented by large 200-300 Å pores which are thought to enhance access of larger feed molecules to active sites and improve diffusivity.

A number of early patents outline the evolution of dealumination technology.[10] Dealuminated zeolites have numerous properties that increase commercial applicability including significant mesoporosity,[11] increased acidity,[12] and increased thermal and hydrothermal stability.[13] More recent work casts some doubt on the utility of mesoporosity derived from dealumination alone, however.[14] This realization has led to very active research targeting precise creation of 'mesoporosity' and 'macroporosity with the goal of overcoming the limitations of small, geometrically defined, pores.

These developments were critical in enabling the wide use of zeolites in key refining and petrochemical processes, including fluidized catalytic cracking and hydrocracking, and resulted in their major economic and societal impact. The mechanisms by which these modification methods led to framework stabilization and

enhanced catalytic performance were the subject of vigorous scientific debate in the zeolite catalysis literature. [15] Eventually it became clear that the enhanced stability, and improved performance, derived from these modification schemes were due to better control of indiscriminate framework de-alumination which otherwise led to framework collapse. The models eventually adopted by workers in the field suggest that steam stabilization, when carried out in a controlled manner, involved the hydrolysis of framework aluminum followed by 'healing' of the (more silicious) framework by insertion of silicon derived from other parts of the framework or from amorphous phases.

Desilication is a currently active area of zeolite modification. However, the dissolution of silica from zeolites using basic solutions was first studied long ago. [16] The example originally given was synthetic mordenite, although the inventors stated analogous results were obtained with other high silica zeolites. The inventors also indicated enhanced porosity and lowered Si/Al ratio in their treated materials, which are the major claimed advantages in the much more recent reports as well. A later patent combined acid treatment with subsequent base treatment in NaOH to enlarge pores in mordenite. [17] Several publications in the 1990s further outline the incongruent dissolution of aluminosilicate zeolite in basic solutions. [18]

Basic media used in desilication include alkali hydroxides and tetraalkylammonium hydroxides. A 1994 report indicated that mesoporosity can be generated by treatment of MFI zeolite with sodium carbonate solutions. [19] An extensive series of desilication studies have been carried out by the Perez-Ramirez group; representative references are listed. [20] In 2002, Goto et al reported and patented the desilication of zeolites in NaOH in the presence of surfactants. [21] Later Ying and Garcia-Ramirez reported similar materials. [22]

Substitutive Methods

A number of reports of realumination have appeared over the years, starting with one in 1977. [23] Subsequent independent studies by other groups both questioned [24] and supported [25] the original authors contention that aluminum could be reinserted by treatment of dealuminated zeolites with aqueous basic reagents after a dealumination process such as steaming or acid treatment. In light of recent studies of desilication of zeolites under similar conditions, however, it is possible that the original reports of realumination in basic solutions were at least in part unrecognized desilication reactions.

It has been claimed that acidic realumination also can take place, [26] however there are also studies that question acidic realumination as well. [27] One theory for realumination is that defects that are very similar to the original aluminum site, called hydroxyl nests, analogous to such defects found in hydrogarnets, [28] are easily "refilled" with aluminum cations by appropriate treatments. Recent studies have sought to disprove the existence of hydroxyl nests in zeolites, however. [29]

The early flurry of framework modification activities described above was followed by more elegant synthetic approaches employing chemical substitution methods. Silicon reinsertion has also been claimed by a number of authors. [30] The claimed mechanism for silicon insertion often invokes the filling of hydroxyl nests, similar to the proposed mechanism for re-alumination reactions. The reactions generally involved halo-silicate reagents such as SiF_6^-, or $SiCl_4$, or simple fluoride reagents such as NH_4HF_2. The driving force for the substitution reactions, which are dissociative in nature, is the reinsertion of Si after the extraction of aluminum and concomitant formation of soluble halo-aluminum species.

Transformative Methods

Transformative post-synthetic treatments of zeolites range from solid state phase transformations to complete dissolution/recrystallization reactions. Many of the solid state transformations are carried out on layered zeolite precursors or three-dimensional zeolites with periodic weak or reactive links within the structure. Dissolution/recrystallization reactions have been carried out widely on a number of zeolite compositions and structures.

Layered zeolite precursors have been known for some time.[31] Delamination and pillaring has been carried out on layered zeolites similar to manipulations of layered clays.[32] A number of studies have appeared over the last 15 years or so on the conversion of layered zeolites to three dimensional zeolite structures either by direct fusion of the layers,[29] by prior addition of pillaring agents followed by conversion to a three-dimensional material,[33] or by removal of some portion of a three-dimensional zeolite, for instance germanium oxide units, followed by re-conversion of the resulting two-dimensional material to a new three-dimensional zeolite.[34] The most broadly applicable method is the direct conversion of layered zeolites to three-dimensional zeolites, the latter two methods being less general and perhaps only feasible in a limited number of cases.

The use of zeolites as reagents in zeolite synthesis has been studied extensively for decades and could warrant a separate article on its own. The earliest reference, the original zeolite B patent from 1961, indicates that zeolite B forms via conversion of other known zeolites at long reaction times. [35] Recent examples of such transformations are the hydrothermal conversion of FAU-type zeolite to MSE and CHA types. [36,37]

Summary

A number of other post synthesis modifications have been carried out on zeolite materials, although some of the more commercially relevant methods have been mentioned in this essay. An extensive review has also recently appeared. [38]

Reference

1 US Patent 4,001,346 Jan. 4, 1977.

2 A) US Patent 4,002,697 Jan. 11, 1977; B) US Patent 4,090,981 May 23, 1978.

3 Kaeding, W.W.; Chu, C.; Young, L.B.; Weistein, B.; Butter, S.A., Selective Alkylation of Toluene with Methanol to Produce para-Xylene, *J. Catalysis* **67** (1981) 159-174.

4 Chen, Nai Y., Personal Perspective of the Development of Para Selective ZSM-5 Catalysts; *Ind. Eng. Chem. Res.* **40 (**2001) 4157-4161.

5 A) US Patent 5,990,366 Nov. 23, 1999; B) US 6,541,408 Apr. 1, 2003; C) US 7,094,941 Aug. 22, 2006

6 Hargreaves, J.S.J. and Munnoch, A.L., A survey of the influence of binders in zeolite catalysis, *Catal. Sci. Technol*., **3**, (2013), 1165-1171.

7 Michels N.L., Mitchell, S., and Pérez-Ramírez, J., Effects of Binders on the Performance of Shaped Hierarchical MFI Zeolites in Methanol-to-Hydrocarbons, *ACS Catal.*, **4**, (2014) 2409−2417.

8 Meirer, F.; Morris, D.T.; Kalirai,S.; Liu, Y.; Andrews, J.C.; and Weckhuysen, B.M., Mapping Metals Incorporation of a Whole Single Catalyst Particle Using Element Specific X-ray Nanotomography, J. Am. Chem. Soc. **137** (2015) 102−105.

9 Ristanovic´, Z.; Kerssens, M.M.; Kubarev, A.V.; Hendriks, F.C.; Dedecker, P.; Hofkens, J.; Roeffaers, M.B.J.; and Weckhuysen, B.M., High-Resolution Single-Molecule Fluorescence Imaging of Zeolite Aggregates within Real-Life Fluid Catalytic Cracking Particles, Angew. Chem. Int. Ed. **54** (2015) 1836-1840.
10 A) US Patent 3,257,310 Jun. 21, 1966; B) US Patent 3,293,192 Dec. 20, 1966; C) US Patent 3,374,057 Mar. 19, 1968; D) US Patent 3,383,169 May 14, 1968; E) US Patent 3,402,996 Sep. 24, 1968; F) US 3,449,070 Jun. 10, 1969; G) US Patent 3,929,672 Dec. 30, 1975; H) US Patent 5,013,699 May 7, 1991; I) US Patent 5,242,677 Sep. 7, 1993.
11 Lynch, J.; Raatz, F.; and Dufresne, P. Characterization of the textural properties of dealuminated HY forms, Zeolites, **7** (1987) 333-340.
12 Lunsford, J.H., Origin of Strong Acidity in Dealuminated Zeolite-Y, in Fluid Catalytic Cracking II (Ocelli, M. Ed.) ACS Symposium Series 1991.
13 Kerr, G.T., Chemistry of Crystalline Aluminosilicates. V. Preparation of Aluminum-Deficient Faujasite, J. Phys. Chem. **72** (1968) 2594-2596.
14 P. Kortunov, P.; Vasenkov, S.; Kärger, J.; Valiullin, R.; Gottschalk, P.; Fé Elía, M., Perez, M.; Stöcker, M.; Drescher, B.; McElhiney, G.; Berger, C.; Gläser, R.; and Weitkamp, J., J. Am. Chem. Soc. **127**(2005) 13055-13059.
15 Jacobs, P.; and Uytterhoeven, J.B.; Infrared Study of Deep-Bed Calcined NH4+ Zeolites, J. Catal. **22** (1971) 193-203.
16 US Patent 3,326,797 Jun. 20, 1967.
17 PL Patent 116845B2 1981.
18 Cizmek, A.; Komunjer, L.; Subotic, B.; Siroki, M.; and Roncevic, S., Kinetics of zeolite dissolution: Part 3. Dissolution of synthetic mordenite in hot sodium hydroxide solutions, Zeolites **12** (1992) 190-196.
19 Le Van Mao, R.; Xiao, S.; Ramsaran, A.; and Yaot, J., Selective removal of silicon from zeolite frameworks using sodium carbonate, J. Mater. Chem. **4** (1994) 605-610.
20 A) Groen, J.C.; Pérez-Ramírez, J.; and Peffer, L.A.A., Formation of Uniform Mesopores in ZSM-5 Zeolite upon Alkaline Post-treatment? Chem. Lett. (2002) 94-95; B) Groen, J.C.; Peffer, L.A.A.; Moulijn, J.A.; Pérez-Ramírez, J., Mesoporosity development in ZSM-5 zeolite upon optimized desilication conditions in alkaline medium, Coll. Surf. A **241** (2004) 53-58; C) Verboekend, D.; and Pérez-Ramírez, J., Design of hierarchical zeolite catalysts by desilication, Catal. Sci. Technol. **1** (2011) 879-890.
21 A) Goto, Y.; Fukushima, Y.; Ratu, P.; Imada, Y.; Kubota, Y.; Sugi, Y.; Ogura, M.; Matsukata, M., Mesoporous Material from Zeolite, J. Porous Mater. **9** (2002) 43-48.; B) Goto, Y.; Fukushima, Y.; Ratu, P.; Imada, Y.; Kubota, Y.; Sugi, Y.; Ogura, M.; JP2002128517 A2 May 9, 2002.
22 US Patent 7,589,041 Sep. 15, 2009.
23 A) Breck, D.W.; and Skeels, G.W.; in “Proceedings, 6th International Congress on Catalysis” (G. C. Bond, P. B. Wells, and F. C. Tompkins, Eds.) Chemical Society, London, 1977, 645; B) Breck, D.W.; and Skeels, G.W.; in “Proceedings, 5th International Conference on Zeolites” (L. V. C. Rees, Ed.), p. 335. Heyden, London, 1980.
24 Engelhardt, G.; Lohse, U., Reexamination of the Hypothesis of Breck and Skeels Concerning the Reinsertion of Aluminum in the Framework of Dealuminated Y Zeolites, J. Catal. **88** (1984) 513-515.
25 Liu, X.; Klinowski, J.; Thomas, J.M., Hydrothermal Isomorphous Insertion of Aluminum into the Framework of Zeolite Y: A Convenient Method of Modifying the Siting of Al and Si in Faujastic Catalysts, J.C.S. Chem. Commun. (1986) 582-584; A) Zhang, Z.; Liu, X.; Xu, Y.; and Xu, R., Realumination of dealuminated zeolites Y, Zeolites **11** (1991) 232-238; B) Calsavara, V.; Sousa-Aguiar, E.F.; and Machado, F., Reactivity of USY extraframework alumina in alkaline medium, Zeolites **17** (1996) 340-345.

26 Sano,T.; Tadenuma, R.; Wang, Z.; and Soga, K., Realumination of dealuminated HZSM-5 zeolites by acid treatment, Chem. Commun. (1997) 1945-1946.
27 Omegna, A.; Haouas, M.; Kogelbauer, A.; Prins, R., Realumination of dealuminated HZSM-5 zeolites by acid treatment: a reexamination, Micro. Mesopor. Mater. **46** (2001) 177-184.
28 Flint, E.P.; McMurdie, H.F.; and Wells, L.S., Hydrothermal and X-ray Studies of the Garnet-Hydrogarnet Series and the Relationship of the Series to Hydration Products of Portland Cement, J. Res. NBS **26** (1941) 14-33.
29 Halasz, I.; Senderov, E.; Olson, D.H.; and Liang, J., Further Search for Hydroxyl Nests in Acid Dealuminated Zeolite Y, J. Phys. Chem. C **119** (2015) 8619-8625.
30 A) Beyer, H.; Belenykaja, I., A New Method for the Dealumination of Faujasite-Type Zeolites in Catalysis by Zeolites, (B. Imelik et al Eds.) Elsevier 1980, 203-210; B) US Patent 4,503,023 Mar. 5, 1985; C) US Patent 5,100,644 Mar. 31, 1992; D) US Patent 5,262,141 Nov. 16, 1993.
31 A) Schreyeck, L.; Caullet, P.; Mougenel, J.;Gutha, J.; and Marler,B., A Layered Microporous Aluminosilicate Precursor of FER-type Zeolite, J. Chem. Soc. Chem. Commun. (1995) 2187-2188; B) Schreyeck, L.; Caullet, P.; Mougenel, J.C.; Guth, J.L.; Marler, B., PREFER: a new layered (alumino) silicate precursor of FER-type zeolite, Microporous Materials **6** (1996) 259-271; C) Corma, A.; Fornes, V.; Pergher, S.B.; Maesen, Th.L.M. & Buglass, J.G., Delaminated zeolite precursors as selective acidic catalysts, Nature **396** (1998) 353-356.
32 Roth, W.J.; and Čejka, J., Two-dimensional zeolites: dream or reality?, Catal. Sci. Tech. **1** (2011) 43-53.
33 Gies,H.; Müller, U.; Yilmaz, B.; Tatsumi, T.; Xie, B.; Xiao, F., Bao, X.; Zhang, W.; De Vos, D., Interlayer Expansion of the Layered Zeolite Precursor RUB-39: A Universal Method To Synthesize Functionalized Microporous Silicates, Chem. Mater. **23** (2011) 2545-2554;
34 A) Verheyen, E.; Joos, L.; Van Havenbergh, K.; Breynaert, E.; Kasian, N.; Gobechiya, E.; Houthoofd, K.; Martineau, C.; Hinterstein, M.; Taulelle, F.; Van Speybroeck, V.; Waroquier, M.; Bals, S.; Van Tendeloo, G.; Kirschhock, C.E.A.; & Martens, J.A., Design of zeolite by inverse sigma transformation, Nat. Mater. **11** (2012) 1059-1064. B) Roth, W.J.; Nachtigall, P.; Morris, R.E.; Wheatley, P.S.; Seymour, V.R.; Ashbrook, S.E.; Chlubná, P.; Grajciar, L.; Položij, M.; Zukal, A.; Shvets, O.; and Čejka, J., A family of zeolites with controlled pore size prepared using a top-down method, Nature Chem. **5** (2013) 628-633.
35 US Patent 3,008,803 Nov. 14, 1961
36 Inagaki,S.; Tsuboi, Y.; Nishita,Y.; Syahylah, T.; Wakihara, T.; and Kubota, T., Rapid Synthesis of an Aluminum-Rich MSE-Type Zeolite by the Hydrothermal Conversion of an FAU-Type Zeolite, Chem. Eur. J. **19** (2013) 7780 – 7786
37 Martín, N.; Moliner, M.; and Corma, A., High yield synthesis of high-silica chabazite by combining the role of zeolite precursors and
tetraethylammonium: SCR of NOx, Chem. Commun. **51** (2015) 9965-9968.
38 Valtchev, V.; Majano, G.; Mintova, S. and Pérez-Ramírez, J., Tailored crystalline microporous materials by post-synthesis modification, Chem. Soc. Rev. **42** (2013) 263-290.

10. Diffraction methods for zeolite structural characterization

Lynne B. McCusker [a,b] and Xiaodong Zou [b]

[a]*Department of Materials, ETH Zurich, CH-8624 Zurich, Switzerland*
[b]*Department of Materials and Environmental Chemistry, Stockholm University, SE-106 91 Stockholm, Sweden*

Introduction

In the context of zeolite syntheses, diffraction methods are indispensable in the initial structural characterization of a product. Is the phase crystalline? Is it the desired phase? Is it a known phase? Is it pure? Is it novel? These questions can usually be answered by applying simple X-ray powder diffraction (XPD), electron diffraction (ED) and/or electron microscopy (EM) techniques. Each method has its strengths and weaknesses, but they are highly complementary, so with a judicious choice of techniques, the desired information can be obtained. For example, an XPD pattern can be used as a fingerprint for identification purposes, and scanning electron microscopy (SEM) will reveal the size and morphology of the crystallites and whether or not impurities are present. However, more information can be derived, if needed (Table 1). Therefore, it is important to know where the information can be found and how to extract it. For example, high resolution transmission electron microscopy (HRTEM) can also show the pores/channels and TO_4 tetrahedra in a zeolite, but the technique requires a certain level of expertise. Here we describe a few practical considerations for collecting and interpreting simple XPD, ED and EM data.

Table 1. Information that can be derived by applying different XPD and ED/EM techniques.[a]

Information	XPD	ED	EM
Crystallite morphology			SEM
Crystallite size	profile fitting		SEM
Crystalline impurity	unindexed peaks	different patterns	SEM
Amorphous impurity	high background	No diffraction	SEM
Stacking faults	broad peaks	streaking	HRTEM
Unit cell dimensions	reflection positions (1D but accurate)	reflection positions (3D but approximate)	HRTEM
Symmetry	systematic absences (obscured by overlap)	systematic absences (no overlap)	HRTEM
Crystal structure	reflection intensities	reflection intensities	HRTEM

	(obscured by overlap) (kinematical)	(no overlap) (dynamical)	(phase information)

[a] The recommended technique for obtaining each kind of information is shown in bold.

X-ray powder diffraction

Data Collection

It is not possible to go into detail in the space available here, but the basic considerations for XPD data collection and a few common sources of error will be discussed. For more information, the reader is referred to the volume entitled "Modern Powder Diffraction" edited by Bish and Post [1] or to the article entitled "Practical Aspects of Powder Diffraction Data Analysis" by Baerlocher and McCusker [2].

Peak positions

If an XPD pattern is to be indexed (*hkl* assigned to each of the peaks and thereby the unit cell dimensions derived), it is essential that the peak positions be determined accurately. In this case, the 2θ scale of the diffractometer needs to be calibrated using a standard material (e.g. NIST Silicon standard 640d). The sharper a peak, the better its 2θ value can be determined, so the diffractometer should also be adjusted to optimize the sharpness of the peaks. As a guide, almost any laboratory instrument can be adjusted to give a full width at half maximum (FWHM) for the Si 111 reflection (28.44°2θ with CuKα_1 radiation) of 0.08°2θ or less. The measured 2θ values for the peaks in the pattern of the standard material should agree with the literature values to within 0.01°2θ.

If the sample is off-center, this will affect the 2θ zeropoint correction, so ideally, the sample should be mixed with a small amount of the standard (that is, measured with an internal standard), so that the 2θ calibration can be done simultaneously. However, if care is taken in positioning the sample, a 2θ calibration using an external standard is usually sufficient. In reflection mode, thin samples are preferred for peak position determination, so effects of sample transparency can be eliminated, but care should be taken to ensure that the crystallites are randomly oriented or not all reflections will be recorded.

Peak intensities

For indexing purposes, the intensities of the reflections are irrelevant, but for identification or for structure analysis, accurate relative intensities are essential. There are three commonly ignored factors that can have a significant effect on the relative intensities measured: (1) sample thickness, (2) preferred orientation, and (3) divergence slits.

Bragg-Brentano (reflection) geometries require an "infinitely thick" sample. That is, it is assumed that the sample is thick enough that all impinging X-rays interact with the sample (by absorption or diffraction) before they reach the sample holder. In this way, the volume of sample effectively irradiated remains constant as 2θ changes. If this is not the case, the intensities must be adjusted for the transparency of the sample. In general, the intensities of the low angle reflections will be too large if the "infinite thickness" criterion is not met. For transmission geometries, on the other hand, the sample must be thin enough that the X-rays are not too strongly attenuated by absorption.

Most powder diffraction data analyses assume that the sample consists of millions of randomly oriented crystallites. If this is not the case, relative intensities will be

distorted. For example, if the crystallites have a plate-like morphology, they are likely to lie flat. Assuming that the c-axis is parallel to the short dimension, crystallites aligned in the 00*1* diffraction condition will be overrepresented, and those in the *hk*0 diffracting condition underrepresented. This will then lead to a bias in the relative intensities recorded. Various sample preparation techniques have been used to reduce preferred orientation (such as back or side loading of flatplate sample holders, mixing amorphous glass beads with the sample, or spray drying), but none is foolproof. Measurements in transmission mode with the sample loosely packed in a rotating capillary are less susceptible (but not immune - needles will tend to align themselves with the capillary) to this problem.

A related problem is that of a "rock in the sand". That is, if a larger crystal is present, its diffraction pattern will distort the measured intensities, becaue its orientation will be overrepresented, so the assumption of random orientation will not be met. This non-random distribution cannot be corrected for in the subsequent analysis, so care should be taken to assure that the crystallites are of similar sizes and/or that they are free to tumble.

In Bragg-Brentano geometry, the X-ray beam is spread over a larger surface of the specimen at low angles than it is at high angles. To ensure that the X-rays interact only with the sample (and not the edges of the specimen holder) a divergence slit is inserted between the X-ray source and the sample to confine the beam to the sample. As the 2θ angle increases, this slit can be opened wider to allow more X-rays through and thereby increase the counting rate, but then the resulting data must be corrected for the increased volume of sample irradiated. The slit size can be varied during the measurement either continuously (using an automatic divergence slit) or manually (using a series of calibrated slits). For data comparison purposes, the data should then be transformed to constant sample volume (single constant slit) data. In many laboratories, data are recorded using a relatively wide single slit that is appropriate for higher angle data, but not for the lower 2θ values. In such a measurement, the intensities of the low angle peaks will appear to be too low, because only part of the X-ray beam interacts with the sample.

Phase identification

In a zeolite laboratory, powder diffraction data are most commonly used to identify a newly synthesized material or to monitor the effects of a post-synthesis treatment. In both cases, the measured pattern is compared with an existing one, whether it is a pattern in the Collection of Simulated XRD Powder Patterns for Zeolites [3], the Powder Diffraction File (PDF) of the ICDD [4] or an inhouse data file. Such comparisons are not easy for zeolites, especially if the data collection or sample preparation conditions differ. A few practical considerations are presented briefly below.

(1) Intensities are important for identification, so the data should be collected accordingly.

(2) Data should be in the form of a constant volume measurement if the Collection, the PDF or any of the common databases is to be used in a search/match procedure.

(3) Peak position information is often given in terms of *d*-values rather than 2θ values, because *d*-values are independent of the X-ray wavelength (λ) used. ($d=\lambda/(2\sin\theta)$)

(4) The low angle reflections are the ones most strongly affected by non-framework species [2]. These reflections are usually more intense in the calcined material than in the as synthesized form, and similar materials containing different cations or different organic species may have quite different relative intensities at low angles. However, the intensities of the higher angle reflections can be compared quite well.

(5) Different synthesis conditions or different post-syntheses treatments can cause subtle distortions in a zeolite framework structure that can complicate identification. The symmetry may be reduced, although the basic framework connectivity remains unchanged. In this case, indexing the pattern can facilitate identification.

Electron Diffraction

Electron diffraction (ED) is complementary to XPD, and can also be used for phase identification and structure determination. Each crystallite in a powder sample behaves like a single crystal in ED, and there is no peak overlap. While an XPD pattern provides information on the entire bulk sample, each ED pattern gives information on individual crystallites in the sample. Thus ED has a unique advantage for studying multiphasic samples. Here the basic considerations for ED data collection and applications will be discussed. More information can be found in the book by Zou et al. [5] or in the review articles [6-7].

Sample preparation and data collection

Samples for TEM investigations are prepared by dispersing the powder in absolute ethanol, and transferring a droplet of the suspension onto a copper grid coated with a holey carbon film. An ED pattern is obtained by selecting one crystallite, aligning it along a crystallgraphic axis (zone axis), and recording the pattern of the selected crystallite. Recently new 3D ED methods were developed, i.e. automated diffraction tomography (ADT) [8] and rotation electron diffraction (RED) [9], for collecting a series of ED patterns from an arbitarily-oriented crystal. Almost complete 3D ED data can be collected by ADT and RED. For phase identification, it is important to calibrate the camera length and ensure that the crystal is at the eucentric height so that the *d*-values are determined accurately. For structure determination, it is important to collect the ED data from very thin crystals (< 100 nm) in order to minimize dynamical effects and thereby obtain more kinematical ED intensities.

Phase identification from zone axis ED patterns

An ED pattern is a 2D section of the 3D reciprocal lattice that can be used as a fingerprint for phase identification. The two shortest reciprocal lattice vectors (in $Å^{-1}$) and the angle between them can be determined from the ED pattern. They are compared with those calculated for a given zeolite. If these three values fit, it is likely that the ED pattern is from that zeolite. However, in some cases, more than one zeolite might give a good fit to an ED pattern, especially if the ED pattern is taken along a zone axis with high indices or if the zeolite structures have some identical projections. In order to resolve the ambiguity, more than one ED pattern should be taken from the same crystal and all ED patterns and the tilt angles between them be used to search for the best fit [5]. The program PhIDO was developed for this purpose [10].

Phase identification and structure determination from 3D RED data

Phase identification is more easily done using 3D ED data. The 3D peak positions and peak intensities can be extracted from the ADT/RED data and combined into a 3D reciprocal lattice. The unit cell parameters can be determined directly from this reconstructed reciprocal lattice [8-9]. Possible space groups can be deduced from the systematically absent reflections. The unit cell and space group are used to identify the zeolite. If no zeolite is found to have similar unit cell parameters and space group, the structure of the crystal is likely to be new. In such a case, the ED intensities extracted

from the 3D ED data can be used together with the unit cell and space group to determine the structure of the new zeolite. The procedure is similar to that used for determining a structure from single-crystal X-ray diffraction data. Indeed, the same software can be used for both X-ray and ED data [6-7,9].

The values of reciprocal lattice vectors (in $Å^{-1}$) and angles from ED often have larger errors than those from XPD. It is sometimes difficult to distinguish between zeolites that only have small differences in their unit cell parameters. In such cases, intensities and systematic absences from ED and chemical composition from energy dispersive spectroscopy (EDS) might provide further information to facilitate the phase identification. One drawback of ED is that the unit cell parameters and symmetry can change in the TEM as a result of the vacuum or interaction of the sample with the electron beam.

Complementary electron microscopy (EM) techniques

SEM is very useful for finding the size and morphology of the crystallites. The morphology often reflects the symmetry (point group) of the crystals. If more than one morphology is apparent in the SEM images, the sample may contain impurities. While crystals usually have well-defined shapes, an amorphous impurity has an ill-defined one. HRTEM images can also be used for phase identification and structure determination, but this technique is more demanding [6]. The crystallographic phase information that can be obtained from HRTEM images can also facilite both space group and structure determination. HRTEM has unique advantages for studying disordered zeolite materials, because the local atomic arrangement can be see directly. Finally, chemical compositions can be obtained by EDS on both SEM and TEM.

Conclusion

By applying the appropriate combination of simple XPD, ED and EM techniques to a zeolite material, much can be learned about its structural characteristics. The morphology of the crystallites can be ascertained (SEM), the unit cell dimensions can be determined (ED, XPD), the purity of a sample verified (XPD, SEM), a known phase can be identified (XPD, ED), and disorder can be visualized (HRTEM). The techniques are highly complementary and the combination needed depends upon the information required. More sophisticated data analysis can also lead to the determination of the structure of a novel zeolite material.

References

[1] D. L. Bish, J. E. Post (eds), Reviews in Mineralogy 20 (1989)
[2] Ch. Baerlocher, L. B. McCusker in Stud. Surf. Sci. Catalysis 85, J. C. Jansen, M. Stöcker, H. G. Karge, J. Weitkamp (eds), Amsterdam, 1991, pp. 391-428
[3] M. M. J. Treacy and J. B. Higgins, Collection of Simulated XRD Powder Patterns for Zeolites, 5th revised ed., Elsevier, Amsterdam, 2007; Ch. Baerlocher and L. B. McCusker, Database of Zeolite Structures: http://www.iza-structure.org/databases
[4] The Powder Diffraction File, ICDD, Newton Square, PA: http://www.icdd.com/products /powderdiffractionfile.htm
[5] X. Zou, S. Hovmöller, P. Oleynikov, Electron crystallography - Electron microscopy and electron diffraction, IUCr texts on crystallography 16, Oxford University Press, 2011
[6] T. Willhammar, Y.F. Yun, X. Zou, Adv. Funct. Mater. 24 (2014) 182

[7] Y. Yun, X. Zou, S. Hovmöller, W. Wan, IUCrJ 2 (2015) 267
[8] U. Kolb, T. Gorelik, C. Kübel, M. T. Otten, D. Hubert, Ultramicroscopy, 107 (2007) 507
[9] W. Wan, J. L. Sun, J. Su, S. Hovmöller, X. Zou, J. App. Crystallogr**. 46 (2013)** 1863
[10] Calidris, PhIDO – a program for phase identification and indexing ED patterns. www.calidris-em.com (2001).

11. Advanced methods applied on zeolites

Gareth T. Whiting and Bert M. Weckhuysen

Inorganic Chemistry and Catalysis group, Debye Institute for Nanomaterials Science, Utrecht University, Universiteitsweg 99, 3584 CG, Utrecht, The Netherlands.

Introduction

Recent advances in the development of *in situ* techniques that are able to obtain both spatial and chemical information simultaneously, are paving the way to obtaining an increased understanding of catalytic solids, in particular zeolites. These *in situ* micro-spectroscopic techniques offer a toolbox, in which a technique (or a combination there of) can be selected based on the scientific question at hand. In this article, we highlight some recent examples from our group of innovative lab-based and synchrotron-based methods, applied on zeolite-based systems. Not only do we focus on zeolite powders and model single crystals, but also on industrial-scale catalysts, namely Fluid Catalytic Cracking (FCC) particles (50-150 □m) and zeolite-based extrudates (mm-sized), showing the full range of possibilities of these systems.

Lab-based micro-spectroscopy

The coupling of a microscope with a spectrometer offers several advantages for studying zeolites, mainly in linking structural and chemical information in a spatiotemporal manner, such as zeolite pore structure and molecular species present therein. Depending on the type of molecules and whether they are produced within the zeolite over time (*i.e*, during a reaction), or introduced (*i.e*, as guest molecules to study absorption properties), determines the technique(s) required, whether it is electronic (UV-Vis, fluorescence) or vibrational (IR, Raman) micro-spectroscopy.

The combination of *UV-Vis and confocal fluorescence microscopy*, make an interesting proposition to study several catalytic properties of zeolites. Taking a staining probe reaction such as styrene oligomerization, which forms light absorbing species, UV-Vis microscopy can spatially resolve the types of species formed during the reaction. [1] A unique feature of this system is that the same *in situ* cell used for the UV-Vis microscopy experiments can be transferred to a confocal fluorescence microscope in order to obtain a 2-D/3-D chemical map of the molecular species formed on Brønsted acid sites inside the ZSM-5 crystals. This involves the use of multiple laser line wavelengths to selectively excite individual groups of molecules within or at the surface of the zeolite material.

Recently, a combination of UV-Vis and confocal fluorescence micro-spectroscopy was employed to study binder effects and Brønsted acidity in partially and fully proton-exchanged Na-ZSM-5-based SiO_2-bound extrudates. [2,3] Using acid-catalyzed thiophene oligomerization as a probe reaction, the activity and selectivity of the materials were monitored using time-resolved UV-Vis microscopy. An understanding of the type and relative quantity of oligomers produced inside the 2-6 □m Na(H)-ZSM-5 crystals were determined. It was found that fully proton-exchanged samples containing a higher Brønsted acid site density favored the formation of ring-opened species (thiol-like compounds). This was in contrast to the further oligomerization route taken by partially proton-exchanged samples, due to the lower Brønsted acid site density present. Confocal fluorescence microscopy experiments on the same samples showed that the

partially proton-exchanged samples obtained a non-homogeneous distribution of acid sites, which is in contrast to the homogeneous distribution in the fully proton exchanged samples.

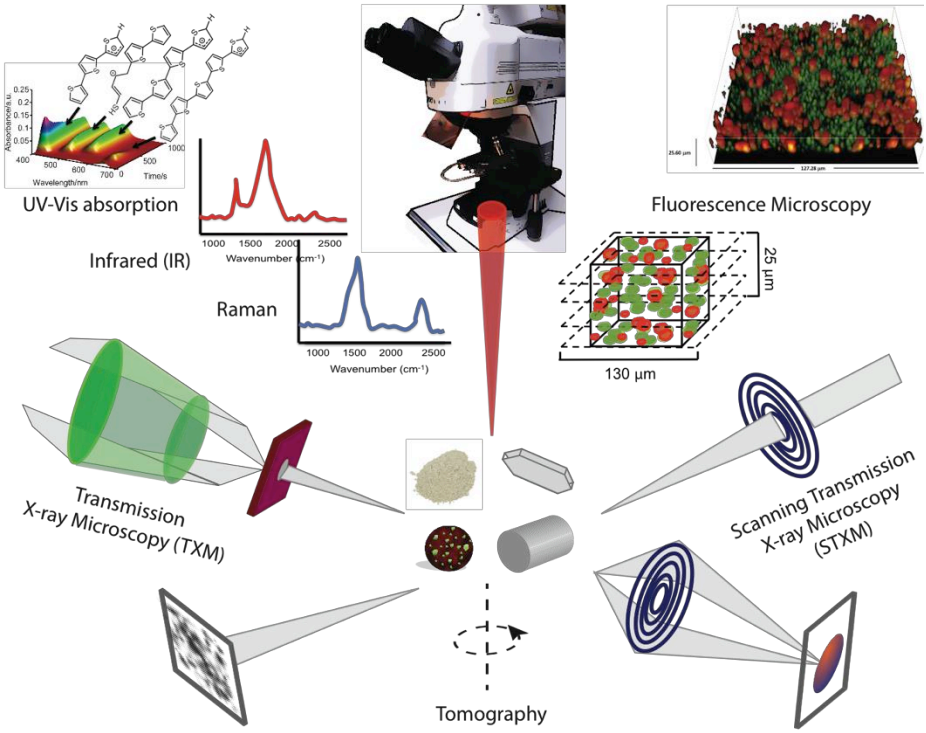

Figure 1. Schematic depicting advanced lab- and synchrotron-based micro-spectroscopic techniques applied on zeolite-based materials. From zeolite powder, model zeolite crystals to industrial-scale zeolite-containing catalyst bodies, these techniques are an arsenal to probe zeolite properties in significant detail.

Given the unique nature of the various zeolite pore architectures and their shape-selective properties, fluorescence microscopy has been shown to provide an exemplary means to study such features using polarization and staining probe molecules. The acid-catalyzed oligomerization of 4-fluorostyrene is one such example, which Sprung *et al.* applied on industrial FCC particles and large ZSM-5 crystals (100 x 20 x 20 □m) in order to develop structure-activity relationships, by linking the distribution of active phase and pore structure therein with oligomer selectivity.[4,5] Focusing on the model catalysts, the six sub-units of a large coffin-shaped ZSM-5 crystal each contain either straight or sinusoidal channel pores, which are perpendicular to each other along the long axis of the crystal. Taking either parent, steamed at 500 °C or 700 °C ZSM-5 crystals, multiple laser line wavelengths in combination with a confocal fluorescence microscope showed that by analyzing the polarization plane of the emitting fluorescence, the orientation of the restricted oligomer molecules can be distinguished, and hence the pores they occupy. The confocal ability of the fluorescence microscope allows a 3-D chemical map to be formed, clearly depicting the shape-selective nature of zeolite crystals.

Using the same batch of parent and steamed large ZSM-5 crystals, Ristanović *et al.* have taken fluorescence microscopy to its ultimate sensitivity limit, performing quantitative 3-D imaging of single catalytic turnovers during the oligomerization of furfuryl alcohol.[6] *Single molecule fluorescence microscopy* is widely used in the life sciences, but in this case it was uniquely used to show that depending on the surface porosity and degree of dealumination, ZSM-5 crystals operate at significantly different single turnover

kinetics (at varying spatial regions) with nanometer resolution. It was observed that mild steaming (i.e., at 500 °C) obtained a higher surface reactivity than parent crystals, with up to 4 times higher local turnover rates. This was confirmed by *Time-Of-Flight-Secondary-Ion-Mass-Spectrometry* (TOF-SIMS) to be attributed to the 3-D distribution of Al, influencing surface diffusion barriers. Severe steaming (i.e., at 700 °C) obtains a drastically reduced turnover rate (2 orders of magnitude lower), due to the substantial dealumination of the material (hence lower Brønsted acid site number). This advanced technique is not limited to model systems, as it was previously applied to larger-scale systems with smaller zeolite domains, in the form of FCC particles. [7]

These advanced lab-based micro-spectroscopic techniques are paving the way to efficiently obtain significant detail into zeolite catalytic properties, without excessive pre-treatment of the sample prior to analysis and allows realistic operation conditions.

Synchrotron-based micro-spectroscopy

The recent developments of 3rd and 4th generation synchrotron sources offer a means to study zeolitic materials with improved spectral brightness, detector sensitivity, as well more advanced focusing optics. [8] This allows imaging of materials with a significantly increased photon flux (compared to conventional methods) with high spatiotemporal resolution from IR to X-ray regions.

Vibrational spectroscopy techniques allow the identification of the molecular structures, composition and interactions present within a sample. The use of *synchrotron IR* micro-spectroscopy coupled with multiplex *Coherent Anti-Stokes Raman Scattering* (CARS), offers a novel tool to analyze catalytic properties of zeolites, by achieving a 2-4 fold improvement in the spatiotemporal resolution over conventional IR and Raman micro-spectroscopy. Kox *et al*. utilized this unique technique to follow *in situ* the oligomerization of 2-chlorothiophene in large H-ZSM-5 crystals, in order to reveal the interaction of reactant (CARS) and formed molecular species (IR) within the zeolite pores. [9] CARS allows the added benefit of performing 2-D/3-D chemical mapping, with intrinsic lateral resolution (*x*, *y*) of ~400 nm and a depth-resolution (*z*) of 1 mm. By analyzing the distribution of the =C-H stretching vibration (3115 cm^{-1}) at varying *x, y*, *z* positions within the ZSM-5 crystal impregnated with 2-cholorothiophene, gradients of reactant concentration were found. An increase in concentration towards the middle of the crystal was noted (2.5 times more than the outer regions), most likely due to capillary forces induced by the micropore structure, or evaporation of reactant from the surface of the crystal by local laser heating. In an additional experiment, IR-microscopy was employed to study the formation of intermediate/product species upon heat treatment. Firstly, polarization dependency experiments showed that bands attributed to ring stretching vibrations of aromatic reaction products (1401, 1506, 1550 cm^{-1}) were highly influenced by the polarization angle. This backs up earlier studies by Sprung *et al.* that elongated molecules are entrapped/aligned within the straight channels of the ZSM-5 crystal. Mapping of the reactant (1412 cm^{-1}) and elongated product (1401 cm^{-1}) species at different reaction times depicts the decreasing intensity of the reactant as the reaction proceeds. Furthermore, the edge region contains significantly less reactant and product. This corroborates well with CARS experiments, showing the synergy of both techniques.

X-ray-based micro-spectroscopic techniques also offer a valuable method to analyze zeolites, due to their highly penetrating nature, as well their energy tunability to study features such as oxidation/coordination states, chemical compositions, and crystallinity, among others. Aramburo *et al.* provide a good example of applying soft X-rays to study a single zeolite particle. [10] *Scanning Transmission X-ray Microscopy*

(STXM) utilizes chemical sensitivity using a Fresnel zone plate, to focus the X-ray beam onto a nm-size area of the sample, raster-scanning in a specific focal plane and recording the transmitted X-ray intensity. This technique was used on both calcined and steamed (i.e., at 700 °C) H-ZSM-5 particles to chemically map at the aluminum *k*-edge, in order to determine the distribution and coordination environments of aluminum in 2-D/3-D. At a spatial resolution of 30 nm and a field of view of 3 x 3 □m, STXM images were recorded at three different energies to allow measurements of 4-fold and 6-fold aluminum. In the case of the calcined particle, 89 % 4-fold aluminum was homogeneously distributed and 11 % 6-fold aluminum was present at random isolated regions, confirming no aluminum zoning. In contrast, the steamed ZSM-5 particle depicts not only the presence of two different types of 4-fold and 5-fold aluminum, but also a higher overall coordination number (no aluminum zoning).

In situ STXM and tomography, coupled with ^{27}Al and ^{31}P magic angle spinning nuclear magnetic resonance (MAS NMR) spectroscopy, were applied by van der Bij *et al*. to determine if three industrial type zeolites, MOR, FAU and FER were able to form an aluminum-phosphate binder after hydrothermal treatment and reaction with phosphoric acid. [11] Unlike the FER framework topology, MOR and FAU both formed an AlO(OH) extra-framework (EF) aluminum phase after dealumination. This was due to the EF Al being trapped within the pores of the FER framework. Upon reaction with phosphoric acid, the AlO(OH) readily reacts to form an $AlPO_4$ phase. Whether $AlPO_4$ is present outside or inside the channels of the zeolite, determines whether it forms $AlPO_4$ islands, or remains amorphous, respectively. Therefore, in order to form an $AlPO_4$ phase within a zeolite structure, the following parameters should be taken into account: Si/Al ratio, pore dimensions and accessibility, as well as stability of the aluminum atoms in the framework.

Meirer *et al.* have recently applied the use of hard *X-ray nano-tomography* using *Transmission X-ray microscopy (TXM)* for the first time to correlate differences in pore structure/connectivity with metal deposition in Fluid Catalytic Cracking (FCC) particles at varying stages of life cycles.[12] TXM allows us to study sub-30 nm with 2-D resolution, but by stitching together multiple fields of view (i.e. 30 x 30 □m^2) at varying angles, a 3-D reconstruction can be made.[13] FCC particles are 40-70 □m spheres that contain a mixture of zeolite active phase, matrix and filler. As these particles crack long-chain feedstock molecules (of crude oil) into smaller, valuable molecules, metals accumulate and influence the activity and selectivity of the catalyst particles. The 3-D distribution of Ni and Fe in a fresh particle and those with varying degrees of deactivation showed that they are mainly present at the near-surface layer of the particle (most concentrated in the early stages of life cycle). This effectively impedes entry of reactant molecules to the macropores of the matrix surrounding the zeolite crystals, hence reducing catalytic activity overtime.

Conclusions

The advanced lab- and synchrotron-based methods discussed in this article have provided new insights into the catalytic properties of zeolites that have previously been lacking with conventional ‘standard’ bulk characterization techniques. Not only are we now able to couple structural and chemical properties of a fresh zeolite material in a spatially resolved manner, but we are also able to monitor, in a time-resolved manner, their reactivity and deactivation during a catalytic process. Resolving spatiotemporal physicochemical information on a variety of length scales, offers a plethora of

opportunities in understanding and developing zeolites further, which will eventually enhance process efficiency.

References

[1] I.L.C. Buurmans, B.M. Weckhuysen, Nat. Chem. 4 (2012) 873.
[2] G.T. Whiting, F. Meirer, D. Valencia, M.M. Mertens, A-J. Bons, B.M. Weiss, P.A. Stevens, E. de Smit, B.M. Weckhuysen, Phys. Chem. Chem. Phys. 16 (2014) 21531.
[3] G.T. Whiting, F. Meirer, M.M. Mertens, A-J. Bons, B.M. Weiss, P.A. Stevens, E. de Smit, B.M. Weckhuysen, ChemCatChem 7 (2015) 1312.
[4] C. Sprung, B.M. Weckhuysen, Chem. Eur. J. 20 (2014) 3667.
[5] C. Sprung, B.M. Weckhuysen, J. Am. Chem. Soc. 137 (2015) 1916.
[6] Z. Ristanović, J.P. Hofmann, G. de Cremer, A.V. Kubarev, M. Rohnke, F. Meirer, J. Hofkens, M.B.J. Roeffaers, B.M. Weckhuysen, J. Am. Chem. Soc. (2015) doi: 10.1021/jacs.5b01698.
[7] Z. Ristanović, M.M. Kerssens, A.V. Kubarev, F.C. Hendricks, P. Dedecker, J. Hofkens, M.B.J. Roeffaers, B.M. Weckhuysen, Angew. Chem. Int. Ed. 54 (2015) 1836.
[8] A.M. Beale, S.D.M. Jacques, B.M. Weckhuysen, Chem. Soc. Rev. 39 (2010) 4656.
[9] M.H.F. Kox, K.F. Domke, J.P.R. Day, G. Rago, E. Stavitski, M. Bonn, B.M. Weckhuysen, Angew. Chem. Int. Ed. 48 (2009) 8990.
[10] L.R. Aramburo, Y. Liu, T. Tyliszczak, F.M.F. de Groot, J.C. Andrews, B.M. Weckhuysen, ChemPhysChem 14 (2013) 496.
[11] H.E. van der Bij, D. Cicmil, J. Wang, F. Meirer, F.M.F. de Groot, B.M. Weckhuysen, J. Am. Chem. Soc. 136 (2014) 17774.
[12] F. Meirer, S. Kalirai, D. Morris, S. Soparawalla, Y. Liu, G. Mesu, J.C. Andrews, B.M. Weckhuysen Sci. Adv. 1 (2015) e1400199.
[13] F. Meirer, D.T. Morris, S. Kalirai, Y. Liu, J.C. Andrews, B.M. Weckhuysen, J. Am. Chem. Soc. 137 (2015) 10

12. Modeling of zeolites: from the unit cell to the crystal

François-Xavier Coudert and Alain H. Fuchs

Chimie ParisTech, PSL Research University, CNRS,
Institut de Recherche de Chimie Paris, 75005 Paris, France

Introduction

Molecular simulation offers a new dimension, complementary to experimental techniques and pen-and-paper theoretical models, to the study of numerous physical and chemical phenomena in gas, liquid, and solid phases. Since its emergence in the 1950s, and its popularization in the next decades, it has seen ever-growing use in the research community in physics, chemistry, materials science and biology. The uninterrupted development and publication of novel methods, combined with the exponential increase in available computational power (thanks to Moore's law), have widely expanded the range of problems that can be addressed through modeling.

Various computational techniques have reached the status of being relatively "routine" computations, at least for well-known systems, and are now considered an integral part of the researcher's toolbox just as, e.g., X-ray diffraction and NMR spectroscopy. Among those, we can cite Density Functional Theory calculations and Grand Canonical Monte Carlo simulations. It is possible to become a *user* of these tools with relatively little training, relying either on commercial or academic software with user-friendly interfaces. However, as with any technique, one should always take great care in checking the validity of the tools for the system at hand, as well as in interpreting the results obtained.

Here, we give an overview of some of the computational chemistry methods commonly used in the field of nanoporous materials in general, and zeolites in particular. It is by no means a systematic review (though some can be found in the existing literature), but rather an introduction to the topic of molecular simulation in zeolite science.

Adsorption

As in all nanoporous materials, adsorption of molecular fluids and fluid mixtures is both one of the most common tools for the characterization of zeolites and one of their most sought-after properties for industrial applications. As such, a very large body of theoretical work has focused on the molecular modeling of gas and liquid adsorption in zeolitic materials, in order to shed light into the microscopic root of the behaviors observed experimentally (i.e., decrypting the adsorption mechanism behind a measured isotherm) and also to predict co-adsorption and separation properties in fluid mixtures.

The standard (and well-established) technique for molecular simulation of adsorption thermodynamics in rigid nanoporous materials is the Monte Carlo simulation method in the Grand Canonical ensemble, also known as Grand Canonical Monte Carlo (GCMC). [1,2,3] This approach, schematized in Figure 1, models the adsorption of molecular fluids or mixtures inside a rigid zeolite (system of fixed volume V), for given values of the temperature (T) and chemical potential of the bulk fluid (μ) or fluid mixtures components (μ_1, μ_2, …). These simulation conditions are close to the thermodynamic conditions during experimental adsorption measurements, where the temperature and pressure P_{fluid} of the external fluid typically are controlled. Notably, the experimental

pressure of the bulk fluid (P_{fluid}) can be related to its chemical potential (μ), used in the GCMC simulations, through an equation of state.

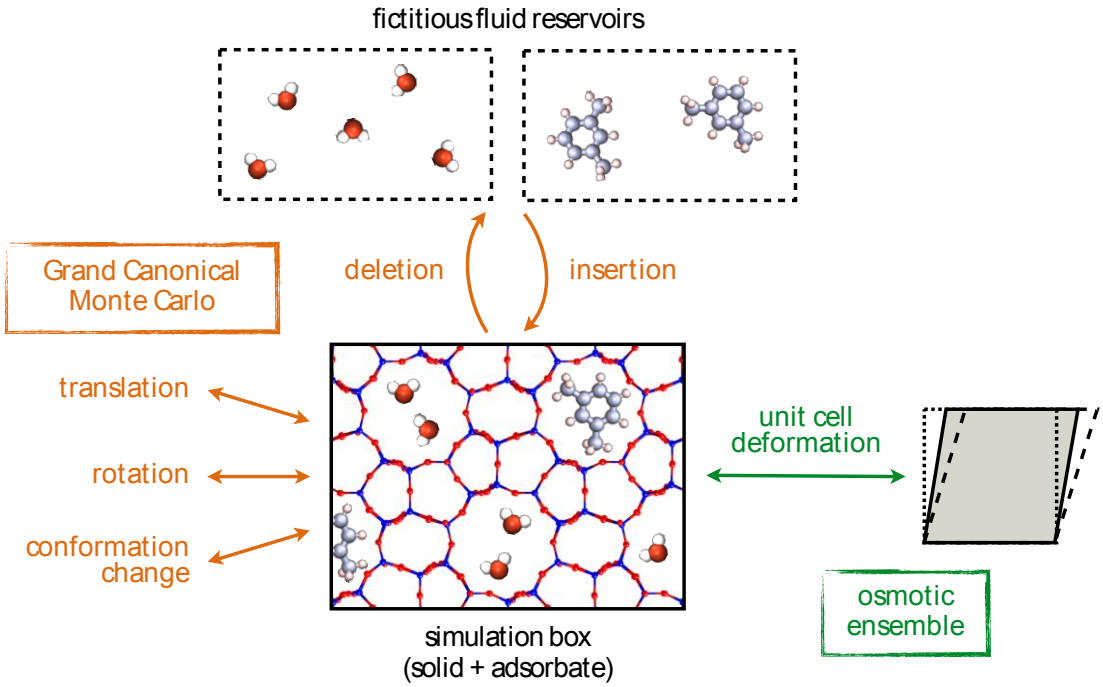

Figure 1. Schematic diagram of the Monte Carlo simulation of adsorption in a porous host, in the Grand Canonical thermodynamic ensemble (in orange) and in the osmotic ensemble (allowing deformation of the material, in green). Reproduced with permission from Ref. [4], Copyright 2016, with permission from Elsevier.

Grand Canonical Monte Carlo simulations allow the calculation of equilibrium thermodynamic quantities, such as the average number of adsorbed molecules, or absolute adsorption uptake $\langle N \rangle$, the isosteric heat of adsorption q_{st}, and the Henry's constant K. Such macroscopic observables can be compared to experimental data, and used directly in the comparison of different materials or as input to the numerical simulation of industrial processes, e.g. fixed-bed adsorption columns. In addition, GCMC simulations provide detailed structural information, including density distributions of adsorbed molecules, yielding valuable insight into the adsorption mechanism and driving forces at the atomistic scale. Moreover, as hinted above, GCMC simulations can directly probe coadsorption, i.e. the adsorption of fluid mixtures, as well as that of pure components. This is of particular interest, in particular in the computational prediction of fluid separation properties, which can be difficult and time-consuming experimentally, in particular due to the large number of control parameters (temperature, pressure, mixture composition).

A key factor in the realization of high-quality GCMC simulations is the description of the interactions between fluid molecules and the zeolite (framework and cations). These interactions are typically described by so-called *force fields* or *classical interaction potentials*, and break down the host–guest and guest–guest interactions into physically relevant terms with simple analytical expressions, including Coulombic interactions, long-range dispersion, short-range interatomic repulsion, polarizability, etc. These force fields need to be optimized for each specific system and property studied, by comparison either to experimental data or reference quantum chemistry calculations. It should be stressed that the choice of force field, as input to the molecular simulation method, controls the quality of the results obtained and needs to be carefully considered. A large

number of force fields for various zeolites have been made proposed and validated in the literature in the last 25 years.

Finally, it should be noted that Monte Carlo simulations in the Grand Canonical ensemble, although considered the golden standard in the simulation of adsorption in zeolites, assume that the zeolitic framework is rigid. This approximation is very reasonable when it comes to the thermodynamics of adsorption in most zeolites, where framework flexibility is limited. It is not universally valid, however, as some zeolites show adsorption-induced structural transitions (as do some more flexible nanoporous materials, such as metal–organic frameworks). Extension of the GCMC technique to flexible materials, taking into account the material's deformation in the osmotic ensemble (see Figure 1), has been recently implemented in some Monte Carlo simulation codes. [5,6]

Dynamics of adsorbate and transport properties

Monte Carlo simulations provide both thermodynamic characterization on the adsorption process, and structural information on the adsorbed phase (such as location of adsorbed species). However, by its very nature it does not provide any results on the dynamics of the adsorbed phase. Yet, dynamic properties of adsorbates play a key role in separation processes and reactions, as even the zeolite with the largest thermodynamic separation properties is useless if diffusion of guest molecules is too slow. There is thus a need of being able to model the dynamics of adsorbates and their transport properties. The "gold standard" technique for this is Molecular Dynamics (MD), [2,7,8] which is a direct simulation of the physical movements of the atoms in a given system over time. It can thus be used to study both structural and dynamical properties of nanoporous materials.

Observables quantities that can be calculated from molecular dynamics simulations include many dynamical properties. At the smallest time and length scale, one can characterize framework and guest deformation (if flexible molecular models are used), as well as the orientational dynamics of the guest species. From dynamics at larger time and length scales, one can characterize the translational dynamics, i.e. the diffusion of guest molecules in the pores of the material. The determination of diffusivities in zeolites, either from experiments or calculations, is key to understanding the transport within their pore systems. In particular, it can be linked to the permeability coefficient of zeolite membranes, a crucial quantity for many membrane-based applications. Moreover, molecular dynamics simulations can provide valuable microscopic insight into the observed diffusivities of confined fluids and mixtures, by detailed analysis of the trajectories of individual molecules over time.

Molecular dynamics, like Monte Carlo simulations, typically require *force fields* model for the interatomic interactions in the system. However, contrary to the thermodynamic properties of adsorption, the influence of the zeolitic framework flexibility is actually very important in the dynamics of adsorbates. This is particularly the case in zeolites with small cages, or large cages connected by small windows. In such cases, where the dimensions of the zeolite pore spaces are close to the molecular diameter of the adsorbed fluid, the detailed atomic motion of the framework vibrations influences significantly the diffusion and transport of guest molecules. As such, studies of diffusion and transport in small-pore zeolites are typically done with flexible frameworks, using intramolecular zeolite force fields.

Finally, we note that it is also possible to perform molecular dynamics simulations based on quantum chemistry evaluation of the interatomic forces (in the Density

Functional Theory approach), rather than relying on *ad hoc* optimized classical force fields. While much less used in the literature than force field-based MD, the continuous increase in computational power available has lead to more frequent use of this computationally demanding technique, often called *ab initio* MD or first principles MD. This is particularly useful to study detailed atomic motions at short time scales, such as vibrational and orientational properties.

Catalysis

Catalysis is one of the most important applications of zeolitic materials, and thus catalytic processes in zeolites have been extensively studied from a theoretical point of view. This analysis of reactivity requires the modeling of the breaking and formation of chemical bonds, electron transfers as well as change in the electronic environment and oxidation states of atom. Therefore, it needs to be modeled at the quantum mechanical level, which can be performed at different levels of theory: the most popular methods with the necessary accuracy to predict chemical reactivity are post-Hartree–Fock methods and calculations based on Density Functional Theory (DFT).

Another choice to be made for the quantum chemical modeling of reactivity in zeolites is that of the size of the system studied. For zeolites with small enough unit cells, it is possible to use a “solid state” approach, where the full unit cell of the crystalline solid is represented, with periodic boundary conditions. However, for larger systems, the computational cost of a periodic calculation can be avoided by performing calculations on a subsystem, i.e. a carefully chosen cluster cut out from the zeolite structure around the region where the reaction occurs.

Quantum chemistry calculations, once set up, allow for both the structure and energetic characterization of catalytic cycles and reaction pathways. See refs. [9 and 10] for reviews on this topic, and refs. [11 and 12] for research papers (out of the large body of literature on this topic) exemplifying the quantum chemical modeling of zeolite catalysis. First, for each possible structure, conformation or state of interest (reactant, products, and intermediaries), one needs to build an input structure: this can be hand-built from chemical intuition, extracted from earlier work or obtained from classical (MD or MC) simulations. Then, these initial structures will be *relaxed* in a process of energy minimization, until local energy minima are found. Both the resulting structures themselves, as well as their energies, are of interest. Finally, a full mapping of the reaction pathways can be performed by searching for transition states between these structures. This allows for the determination of activation energies, and thus kinetic parameters such as reaction rate constants.

It should be noted that, while quantum chemical calculations only allow to calculate the relative energies of molecular and crystalline structures, it can also be used to estimate their relative entropies. For relatively rigid structures (with no soft vibration modes), the vibrational entropy of all structures is approximated in the (quasi-)harmonic approximation. It can thus be calculated from vibration frequencies (or phonon frequencies, for a solid), themselves computed in quantum chemistry calculations through the second derivatives of the energy with respect to the atomic coordinates. This allows for a rough estimation of relative entropies, and thus relative free energies of the states of interest (reactants, products, intermediaries and transition states) at a given temperature.

Structure prediction and feasibility

While more than 200 zeolite frameworks have been observed in natural or synthesized zeolitic materials, and more are discovered every year, this is only a very small number compared to the infinite number of mathematically generated edge-sharing tetrahedra networks. Moreover, most framework types can only be obtained for specific ranges of chemical composition; for example, less than a quarter of that number (46 out of 206, at time of writing) can be experimentally obtained as pure silica compounds. It is thus not surprising that the question of computationally predicting zeolite structures has been the focus of a lot of effort from the research community, as has the issue of evaluating the experimental "feasibility" of predicted structures (whether they can be obtained in given experimental conditions). The ultimate goal here would be for theoreticians to be able to guide the design and synthesis of novel zeolites with targeted properties: being able to suggest synthesis conditions (solvent, templates, temperature, etc.) for materials with specific pore sizes or catalytic activity. This remains today,

The first step in predicting zeolite structures and feasibility is the enumeration of a large number of four-connected net topologies, and their scoring - i.e., the assignment of rough "figures of merit" to each structure, associated to their relevance as zeolitic framework. Such figures of merit are typically based either on geometric criteria (bond angles, ring sizes, etc.) or relative energies (obtained using classical force fields). Using this approach, Deem et al. generated 2.6 million unique hypothetical zeolite frameworks, including ~500 000 with reasonably low energy. [13] This is still much larger than the total number of known zeolitic frameworks, calling for better feasibility criteria to discriminate between these hypothetical structures. As can be expected, the energetics of the zeolitic frameworks has been one of the key factors investigated, and in particular the link between framework topology, geometric properties (e.g. strained rings), chemical composition and relative stability. [14,15,16] Some studies have focused on the matching between the zeolite framework and templating agents. [17] Other feasibility criteria have also been proposed, such as the framework flexibility [18] or mechanical properties. [19] However, the question of feasibility of zeolitic frameworks remains, for the most part, an entirely open question to date. [20]

More than the unit cell…

Most of the discussion in this introduction to modeling of zeolites relies on the representation of the solid either as an infinite periodic crystal, for adsorption and diffusion studies, or as a cluster of atoms representative of the active site in a catalytic process. It should however be noted that the understanding the behavior of zeolites at interfaces, such as grain boundaries or external crystal surfaces, is still largely an unsolved challenge. It involves the determination of the nature of external surface structures, [21] as a function of the synthesis protocol and thermodynamic conditions. It also typically requires the modeling of several crystal facets, who can have markedly different structure and properties. Finally, the particularly reactive nature of the external surface sites makes it in most cases necessary for those to be treated at the quantum chemical level, making the modeling of zeolite surfaces a very computationally expensive issue.

Referenc

[1] A. H. Fuchs, A. K. Cheetham, J. Phys. Chem. B 105 (2001) 7375
[2] B. Smit, T. L. M. Maesen, Chem. Rev. 108 (2008) 4125
[3] P. Ungerer, B. Tavitian, A. Boutin, Applications of Molecular Simulation in the Oil and Gas Industry, Editions Technip (2005).
[4] F.-X. Coudert, A. H. Fuchs, Coord. Chem. Rev. 307 (2016) 211
[5] F.-X. Coudert, A. Boutin, M. Jeffroy, C. Mellot-Draznieks, A. H. Fuchs, ChemPhysChem 12 (2011) 247
[6] D. Dubbeldam, S. Calero, D. E. Ellis, R. Q. Snurr, Molecular Simulation 42 (2016) 81
[7] J. Kärger, S. Vasenkov, S. M. Auerbach, “Diffusion in Zeolites”, in Handbook of Zeolite Science and Technology, CRC Press, 2003.
[8] F. Leroy, B. Rousseau, A.H. Fuchs, Phys. Chem. Chem. Phys. 6 (2004) 775
[9] X. Rozanska, R. A. van Santen, “Reaction mechanisms in protonic zeolites”, in Computer Modelling of Microporous Materials, Elsevier Ltd, 2004.
[10] V. Van Speybroeck, K. De Wispelaere, J. Van der Mynsbrugge, M. Vandichel, K. Hemelsoet, M. Waroquier, Chem. Soc. Rev. 43 (2014) 7326
[11] S. Svelle, C. Tuma, X. Rozanska, T. Kerber, J. Sauer, J. Am. Chem. Soc. 131 (2009) 816
[12] M. Boronat, P. M. Viruela, A. Corma, J. Am. Chem. Soc. 126 (2004) 3300
[13] R. Pophale, P. A. Cheeseman, M. W. Deem, Phys. Chem. Chem. Phys. 13 (2011) 12407
[14] C. Mellot-Draznieks, S. Girard, G. Férey, J. Am. Chem. Soc. 124 (2002) 15326
[15] M. A. Zwijnenburg, F. Corà, R. G. Bell, J. Am. Chem. Soc. 129 (2007) 12588
[16] G. Sastre, A. Corma, J. Phys. Chem. C 114 (2010) 1667
[17] R. Pophale, F. Daeyaert, M. W. Deem, J. Mater. Chem. A 1 (2013) 6750
[18] C. J. Dawson, V. Kapko, M. F. Thorpe, M. D. Foster, M. M. J. Treacy, J. Phys. Chem. C 116 (2012) 16175
[19] F.-X. Coudert, Phys. Chem. Chem. Phys. 15 (2013) 16012
[20] Y. Li, J. Yu, Chem. Rev. 114 (2014) 7268
[21] B. Slater, J. D. Gale, C. R. A. Catlow, T. Ohsuna, O. Terasaki, Stud. Surf. Sci. Catal. 154 (2004) 1197

13. Nanoporous materials in adsorptive separation science & technology

Philip Llewellyn

Aix-Marseille University, MADIREL (UMR CNRS 7246) Centre Scientifique de St. Jérôme 13013 Marseille / France

Introduction

The separation step in any process is vital as it helps to define product yield and purity. Separation process can account for up to 40% of capital expenditure (capex) and 60% of operational expenditure (opex). For gases and liquids, various separation technologies are used and these include processes using distillation, absorption and adsorption. For adsorption-based separation, nanoporous solids are used including active carbons, silica, alumina and zeolites. These approaches have potential benefits in terms of energy saving. [1]

As there is a need to reduce both the cost the environmental footprint of processes, there is still much room to optimize the separation step. Indeed, one example is that of CO_2 capture using amine solutions, which, whilst very selectively capturing this greenhouse gas, can suffer from problems including corrosion and toxicity. A further problem with this process is associated with the large cost of regeneration, which is carried out by heating the amine solution to above 100°C, with the inefficiencies of heating a significant amount of water which does not take part in the capture process. A second example is that of propylene or ethylene recovery from propane or ethane respectively. These are probably the most energy intensive commercial separation processes using distillation with up to 200 stages and often at sub-ambient temperatures. Separation processes using adsorption could provide elegant solutions to these and other problems.

Adsorption

We know the phenomenon of adsorption as the increase in concentration of a fluid close to surfaces. [2] As we increase the pressure (or partial pressure …) of a gas we can encounter adsorption at active sites (cations, hydroxyls …), monolayer and multilayer formation, filling of micropores, as well as capillary condensation. In the laboratory, an understanding of the adsorption phenomena is most often used for the characterization of powders and porous solids. Indeed, the adsorption of nitrogen or argon at cryogenic temperatures is used to gain information about the accessible surface area of the solid as well as information about any pore volume, size and in some cases, pore shape. [3]

Separation

In adsorption based separation processes, we may exploit the fact that some molecules may adsorb at a surface more strongly than others and we can estimate the extent of these interactions by measuring or calculating the enthalpies of adsorption. We can also exploit the possibility for stearic hindrance and even size exclusion, and in these cases adsorption kinetics are of great interest to measure. Furthermore, in some cases, we can use the fact that molecules may have a ‘good fit’ inside the porosity leading to entropy effects.

Pressure Swing Adsorption (PSA)

Of the various separation processes, Pressure Swing Adsorption (PSA) has the advantage of ease of applicability under various conditions of temperature. One generally considers PSA of interest when the concentration of the fluid to be recovered is above a few percent. [4] In this process, the gas mixture is adsorbed in an adsorbent column at pressures above atmospheric. The adsorbent regeneration then occurs by rinsing at a lower working pressure, which can be as low as 1 bar. Several beds can be used with each working at different stages of the process (e.g. pressurization, adsorption, rinse, blowdown, purge …) in order to allow for continuous gas production. The first, and most well known cycle, using several beds, was patented by Charles Skarstrom for oxygen enrichment. [5] A various to PSA is Vacuum Swing Adsorption (VSA) where the lower working pressure is below atmospheric. Hybrid vacuum-pressure swing adsorption systems also exist.

Temperature Swing Adsorption (TSA)

Temperature Swing Adsorption (TSA), as its name implies, employs a variation in temperature where adsorption/separation occurs at the lower working temperature and adsorbent regeneration occurs at higher temperatures. This upper working temperature of often achieved using a hot purge gas or stream. TSA is a relatively slow process compared to PSA. Whilst adsorption steps of a few seconds can be achieved using PSA, several hours may be required for TSA. However, gas pressurization in PSA may be less cost effective than using intelligent heat management to obtain the hot purging gas in TSA. On the other hand, the short cycles that can be used in PSA processes mean that adsorbents do not necessarily need to have very high capacities. The long adsorption times used in TSA mean that this process is adapted to mixtures in which the component to recover is low in concentration.

Towards faster regeneration methods

One of the problems of temperature swing adsorption is that the regeneration step is relatively slow. This is leading to research into methods to increase the rate of regeneration. One method is known as Electric Swing Adsorption (ESA) [6] where the regeneration step is performed by increasing the temperature of the adsorbent using the Joule effect of passing electricity through a conductor. One can equally use microwave heating for the regeneration, which again is seen to increase the time needed for adsorbent regeneration. [7]

Materials

Adsorption based separation processes traditionally use active carbons, silica, alumina and zeolites. Whilst much research is being devoted to the use functionalized mesoporous silica or metal-organic frameworks, to the best of the author's knowledge, only a few pilot scale schemes have been studied.

Zeolites in separation

The main zeolite structures used in separations are the same as those used in many catalytic processes. The LTA structure (NaA, CaA, KA) can be used in drying, CO_2 recovery from natural gas, O_2 recovery from air, as well a linear /paraffin hydrocarbon separation. The FAU structure, especially BaX, is extensively used in xylene

separations. NaX can use for hydrogen purification and CaX is used for mercaptan removal from natural gas. Silicalite (MFI) is used for the removal or organics from water whereas ZSM-5 can again be found in xylene separations.

Shaping

In all adsorption-based process, shaping is critical. In PSA or TSA, materials can be found in the shape of spherical beads beads or cylindrical extrudates. The shaping allows the micron sized zeolite crystals to be agglomerated into millimeter-sized pellets, which are more practical for the separation process. For this agglomeration typically clays, alumina, silica or a mixture of these inorganic binders are used in the range of 10-20 weight %. Critical points are the mechanical strength of the pellet along with the possibility to gain optimal mass transfer properties. The binder should ideally not influence the adsorption properties of the adsorbent. This shaping process is an art in itself and it is not simple to gain insight into some of the 'secrets' involved.

Depending of the final application, the active materials can be immobilized on the surface of other types of support. These can include paper like filters, on metal heat exchangers or in honeycomb type monoliths. In these cases, the aggregation of the zeolite to the surface is critical.

Equally critical for shaping is the crystal size and shape with often the wish for small crystals. However, as the crystal size odes decrease, adsorption on the external surface can be of importance, especially when this external surface contains defect sites.

Zeolites in membranes

A further separation process in which zeolites can used involves membranes in which the feed is flowed across one side, potentially under pressure ad a sweep gas flows on the other side of the membrane. Zeolites are also used in pervapouration studies in which liquid mixtures can be separated. [8] This operation differs from PSA or TSA in that it is a continuous process and does not involve transient steps. Membrane operation is potentially cheaper and easier to operate than PSA or TSA as no moving parts are required. From a materials standpoint, the operational performance of a membrane is dependent on the selectivity and permeability. These factors can be compared with the factors such as capacity, selectivity and kinetics in PSA or TSA. Industrial scale gas separations using membranes are not common although interesting results have been obtained with small pore zeolites (SOD, CHA, DDR) and the zeotype SAPO-34 for CO_2 recovery from CH_4. [9] Large scale commercial pervapouration used for organic molecule dehydration is made with LTA. For this application, these zeolite membranes have higher selectivities and permeabilities than polymeric membranes.

In general, zeolite membranes are generally attractive in terms of separation performance and stability (chemical, thermal). However, this is offset by significant fabrication costs and in some cases, production reproducibility. In a recent review on the subject [10] the authors argue that advances in this area will be a hand in hand improvement in membrane support and active layer along with better adhesion between these elements. The tendency to decrease active layer thickness is clear with, in some cases, the use of further coating to aid the healing of defects.

Membranes can be supported on other porous materials such as macroporous alumina and again this porous support should not influence the membrane properties. Freestanding membranes also exist. Recent research is focusing on mixed matrix membranes in which the active materials (zeolite) is embedded in a resin or polymer. The advantage of the mixed matrix membrane idea lies in the combination of the ease of polymer film processing with the high selectivity and permeability of the zeolite.

Laboratory scale evaluation of nanoporous materials for separations

Turning back to laboratory scale evaluation of novel zeolites and other nanoporous materials for adsorptive separations there is a problem of scale. Whilst process engineers require often kilogram quantities of material, synthesis chemists are often preparing milligram quantities of new sample. It is impossible to relate measurements of pore volume or surface area, obtained during many synthesis studies, to process scale parameters. However, it is relatively simple to carry out single gas adsorption experiments at temperatures and in the pressure range used in processes using commercially available equipment. From these isotherms, it is possible to predict properties relevant to the separation process. Parameters such as working capacity and selectivity can be obtained from this data. Isotherms obtained at several temperatures can be used to estimate adsorption enthalpies or alternatively direct measurement of these quantities can be obtained by microcalorimetry. Adsorption/desorption kinetics are more difficult to accurately estimate. Quasi-elastic neutron scattering or Pulsed-Field Gradient NMR gain insight into diffusion with the pores, however for the process, diffusion between the in the bed and between pellets can equally be of importance. Thus for a laboratory scale comparison between materials, various comparisons have been suggested. These include simple ratios of Henry constants [11] or selectivities to the more elaborate PSA selection parameter, [12] Adsorbent Performance Indicator [13] or Adiabatic Separation Factor. For membranes, parameters such as selectivity and permeability/permeance can be obtained at the laboratory scale with a relatively small amount of material.

Concluding remarks

Understanding adsorption phenomena in zeolites and zeotypes can require a multi-disciplinary approach often coupling the adsorption with complementary approaches such as calorimetry to gain the adsorption heats, and diffraction to follow the structure of the solid and/or adsorbed phase. Spectroscopy can be used to gain information about local interactions and variable temperature IR can be equally used to gain information about the adsorption enthalpies. All of these experimental methods can be accompanied by theoretical approaches using computer modeling structures and molecular simulation of the adsorption and diffusion processes. These approaches can be a very good inputs to for the development of structure property relationships, which are starting to be developed for applications in gas storage.

In summary, there are still a large number of strategic areas where separations using adsorption with zeolites, zeotypes or other nanoporous materials could lead to significant progress or breakthroughs. However, the young synthesis chemist making novel materials, often on quite a small scale, needs to keep in the back of their mind that a number of significant hurdles lie ahead prior to testing by process engineers. However, initial laboratory scale evaluations and comparisons are possible and these can give very clear ideas concerning future directions for materials design.

References

[1] A. Mersmann, B. Fill, R. Hartmann, S. Maurer, Chem. Eng. Technol., 23 (2000) 937

[2] J. Rouquerol, F. Rouquerol, P. Llewellyn, G. Maurin, K.S.W. Sing, “Adsorption by Powders and Porous Solids, Principles, Methodology and Applications”, 2nd Ed., (2014) Academic Press, Oxford (G.B.)
[3] M. Thommes, K. Kaneko, A. V. Neimark, J. P. Olivier, F. Rodriguez-Reinoso, J. Rouquerol, K. S.W. Sing, Pure and Applied Chemistry, 87 (2015) 1051
[4] C. A. Grande, ISRN Chemical Engineering, 2012 (2012) 982934
[5] C. W. Skarstrom, U.S. Patent 2944627 (1960)
[6] R. R. Judkins, T. D. Burchell, US Patent 5912424A (1997)
[7] J. Reuß, D. Bathen, H. Schmidt-Traub, Chem. Eng. Technol., 25 (2002), 381
[8] T. C. Bowen, R. D. Noble, J. L. Falconer, J. Membrane Science, 245 (2004) 1
[9] J. Caro, M. Noack, Micro. Meso. Mater., 115 (2008) 215
[10] N. Kosinov, J. Gascon, F. Kapteijn, E. J. M. Hensen, J. Memb. Sci., 499 (2016) 65
[11] K. S. Knaebel, Chem. Eng., 102 (1995) 92
[12] S. U. Rege, R. T. Yang, Sep. Sci. Technol., 36 (2001) 3355
[13] A. D. Wiersum, J.-S. Chang, C. Serre, P. L. Llewellyn, Langmuir, 29 (2013) 3301

14. New zeolite-based catalytic processes

Jean-Pierre Gilson[a,b]*, Svetlana Mintova[a], Valentin Valtchev[a]

[a]ENSICAEN, Université de Normandie, CNRS, Laboratoire Catalyse & Spectrochimie, 6 boulevard Maréchal Juin, 14050 Caen, France
[b]Dalian National Laboratory, Dalian Institute of Chemical Physics, 457 Zhongshan Road, 116023, China

Introduction

The already significant contributions of zeolites in many segments of the chemical industry are documented in numerous reviews and books. [1-3] Zeolites are used as heterogeneous catalysts and adsorbents, the latter often combined with catalytic processes. Their impact is felt by two types of innovations:

Breakthroughs: FCC (Fluid Catalytic Cracking) is the best example where a zeolite-based (Y type of the FAU family) catalyst swiftly displaced, around 1964, the previous generations (amorphous silica-alumina). The new catalysts yielding far more gasoline, the effect was spectacular as the US FCC capacity did not need to increase while serving a growing market. [1]

Incremental improvements: Again in FCC, many improvements of zeolite Y (crystal quality, efficiency of the synthesis, post-synthesis treatments…) led to today's catalysts, far superior to the original brought to market over 50 years ago.

The case of FCC is very illustrative since the combination of a breakthrough innovation followed by a sustained stream of incremental improvements met all the challenges of this difficult but key process. Over the years, FAU-based FCC catalysts proved always better than any other zeolite catalyst; and the story is not over yet…

This short introduction cannot be another review of zeolite-based processes since space is very limited, but also because identifying new zeolite-based processes is in fact very challenging. While new processes are advertised and some of their characteristics are openly available, the core of these processes, *i.e.* the zeolite used and its detailed properties are often well-kept secrets. Even a careful survey of the patent literature helps little in identifying the precise nature of the specific zeolite (framework type, chemical composition, particle size and shape…) in use. Moreover, improved catalysts are often loaded in existing units, as drop-in solutions, further increasing the difficulty of noticing that a new catalyst generation is commercialized.

Two types of complementary activities take place in the preparation of zeolitic materials:

Synthesis of new structures: this avenue has over the years been very successful; more than 230 framework types are so far recognized by the IZA' Structure Commission and more are in the pipeline as the potential is immense. [4]

Zeolite crystal engineering: many existing zeolites can be produced with very tight specifications on their properties such as particle size and shape, chemical composition (framework and extra-framework), additional mesoporosity, *in-situ* growth on a support….

About a dozen zeolite framework types (AEL, BEA, CHA, EUO, FAU, FER, LTA, LTL, MFI, MOR, MTT, MTW, MWW, TON…) out of 230 are thought to be in commercial use; it is only 5% of the currently available structures. It should not be wrongly concluded that the search for new structures is vain; some are inherently unstable and will find no use in industry, but emerging needs may require one of the currently "exotic" structures.

The creativity of some chemists to produce new structures (BEA, MFI…) combined with the ability of others to design catalysts with the right properties explains that a few structures can be tailored to meet the requirements of quite different processes (*eg.* FAU in FCC, Hydrocracking and separation processes…).

We will briefly review some recent/emerging applications of 3 framework types (CHA, MOR, MWW) and highlight the reasons for their successful commercial deployment.

Emerging applications of zeolites

CHA (SSZ-13 & SAPO-34)

The CHA structure is commercially used both as an aluminosilicate (SSZ-13) and a silicoaluminophosphate (SAPO-34) for different reasons.

Cu loaded SSZ-13 is currently the best ammonia selective catalytic reduction (NH_3-SCR) catalyst for NO_x. [5] Cu-SSZ-13 displays a very high NO_x conversion and N_2 selectivity together with exceptionally high hydrothermal stability at high temperatures. Moreover, it provides the best environment for the Cu active sites (location either in 6 or 8 member rings), Figure 1. Their exact nature and location under reaction conditions is still debated (complex interplay between redox and acidic sites) and the detailed mechanism is not yet fully understood.

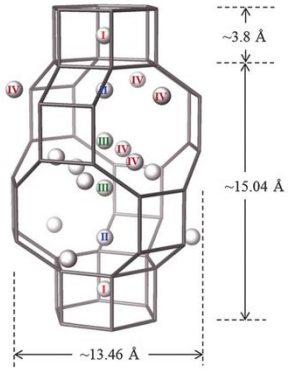

Figure 1. CHA cage with the various cation positions (Reproduced from ref. 5 with permission of the RSC).

Another success story of CHA is the use of SAPO-34 in the Methanol to Olefins reaction (MTO). MTO is currently deployed commercially in China on a grand scale since 2010. Two processes, one developed by the Dalian Institute of Chemical Physics (DICP) [6] and the other by UOP LLC [7] contribute to meet the need of light olefins in China. The CHA cage made of Si, Al and P tetrahedral framework cations is unique in building an inorganic-organic hybrid catalytic site during an induction period and releasing selectively lower olefins (ethylene and propylene mostly) in a steady-state from an “hydrocarbon-pool” before deactivation and rejuvenation in a fluid bed reactor, Figure 2. [8]

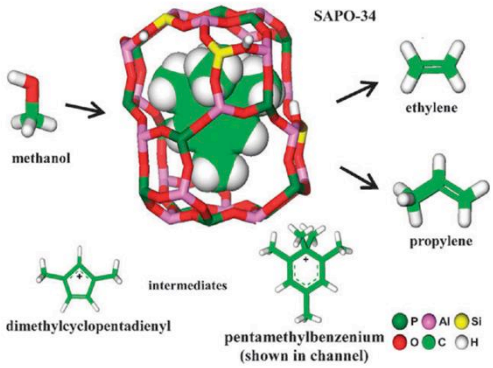

Figure 2. MTO reaction on SAPO-34 (Reproduced from ref. 8 with permission of the RSC)

Such a reaction is a stunning example of the building of an active site during the early stages of the reaction, often referred to as “catalysis by coke deposits” and already encountered with zeolitic [9] and non-zeolitic [10] catalysts.

MOR (H-Mordenite and UZM-14)

Some of the early applications of MOR were as bifunctional catalysts, Pt/H-MOR, for light naphtha (pentane and hexane) and C_8 aromatics (xylenes and ethylbenzene) hydroisomerization. In light naphtha hydroisomerization, MOR is dealuminated in such a way to promote enhanced acidity and add mesoporosity to lower diffusion limitations. [11] In xylene and ethylbenzene isomerization, the number and location of acid sites is adjusted by a selective neutralization of the side pocket acidity by Na^+ exchange, leaving acid sites only in the main channels. Such a treatment blocks most bimolecular reactions and increases dramatically p-xylene yields. [12, 13]

More recently, refinements of the MOR properties allowed dramatic improvement in the: *i*) transalkylation of toluene with $C_{9\text{-}10}$ alkyl aromatics to produce xylenes (UOP’s Tatoray process), *ii*) carbonylation of methanol and dimethyl ether to produce acetic acid and methyl acetate. Using the so-called “Charge Density Mismatch” methodology, UOP produced high quality nanosized MOR crystals with increased accessibility along the pore openings and displaying superior performances (activity and stability) in the transalkylation of toluene with $C_{9\text{-}10}$ alkyl benzenes (lower value aromatics) to xylene (high value aromatics). [14] This is a typical example of an incremental improvement of a catalyst that can swiftly replace a less performing one, a so-called drop-in solution.

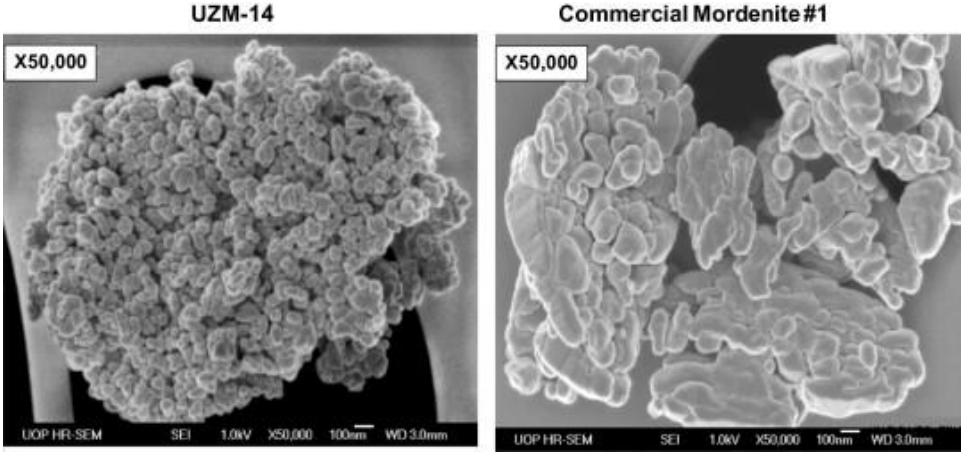

Figure 3. UZM-14 size and morphology compared to a commercially available Mordenite (Reproduced from ref. 14 with permission of Elsevier).

In the carbonylation of methanol and dimethyl ether, the replacement of corrosive homogeneous catalysts (Rh or Ir organometallic complexes combined with halide promotors) by a MOR-based catalyst greatly reduces the investment in the reactor (no need for exotic metals such Zr) and downstream processing (distillation of non-corrosive mixtures). A process named SaaBre is currently developed by BP and a 1 million metric tons per year unit is considered for a petrochemical investment in Oman. [15] Here, elegant and fundamental studies (spectroscopy, kinetic studies and molecular modelling) indicate that the MOR catalytic sites are tailored at the nanometer level. The groups of Iglesia [16], and Corma [17], working with BP, unraveled the design rules of such a catalyst, namely that the active sites are located in the side-pockets (8 MR) of MOR and that secondary reactions leading to deactivation take place in the main channels (12 MR). So, a reverse strategy than in the design of C_8 aromatics isomerization, *vide supra*. The Brønsted sites in the side pockets are promptly methoxylated by methanol or dimethyl ether. The orientation of these methoxy groups (T3–O33 position), deep inside the side-pockets allows the perfect fitting of a linear transition state after their attack by a CO and further stabilized by framework oxygens. Bulkier nucleophiles are prevented from attacking any molecules inside the side pockets. On the contrary, at the rim of the side pockets/main channels (T4–O44 position), hydrocarbons can be produced due to lesser steric constrains and these lead to deactivation; here the hydrocarbon pool mechanism, so useful in MTO, leads to a fast deactivation by rapidly blocking the one-dimensional porosity of MOR main channels.

In order to avoid such excessive side reactions, a shortening of the diffusion pathlength for the product molecules could be beneficial; moving to nanosized MOR crystals indeed improves further the catalytic performances. [18]

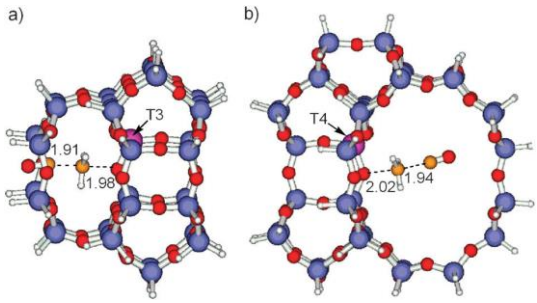

Figure 4. Methoxy groups a) inside the MOR side pockets, b) at the interface between main channels and side pockets (Reproduced from ref. 17 with permission of the RSC).

MWW (MCM-22)

Cumene is an important molecule in petrochemistry and was first produced by the alkylation of benzene with propylene on very corrosive $AlCl_3$ or H_3PO_4 supported on SiO_2. High silica zeolites displaced these catalysts due to their superior yields, better selectivities and longer cycle times. [1,19,20] Although many zeolite structures (BEA, MOR, MWW, USY…) are used as catalysts in this reaction, one deserves a particular attention, MWW. This zeolite displays the usual microporosity found in many zeolites but its external surface is dotted with pockets (diameter: 0.71 nm) promoting benzene alkylation with propylene in an open catalytic nest providing an easy escape route for the product, cumene, therefore avoiding undesired multiple alkylations and other side reactions.

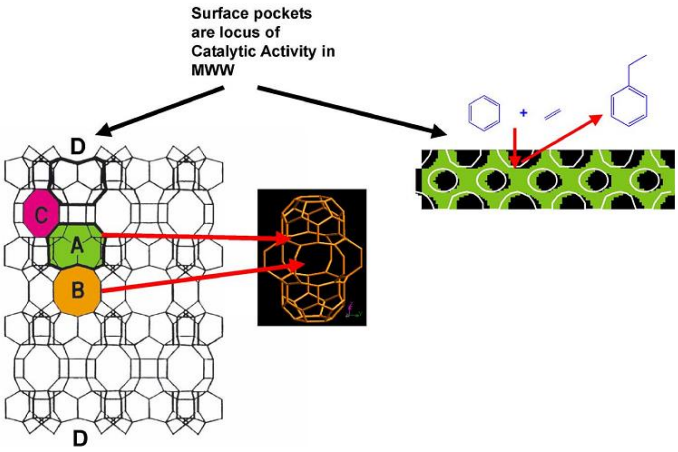

Figure 5. Structural features of MWW: i) 12-ring cavity (A) accessible through a 10-ring aperture (B), ii) 10-ring channel system (C), iii) 12-ring surface pockets (D) (Reproduced from ref. 20 with permission of Elsevier).

The reaction also takes place in the liquid phase easing the cleaning of the surface resulting in an extended stability of the catalysts. In fact, all the desirable reactions take place on the outer surface of the MWW crystals and the microporosity is not participating in the desired reaction. Corma *et al*. showed that delaminating such a zeolite, leads to ITQ-2, a material with an even higher external surface and a superior catalyst in the dealkylation of 1,3,5-triisopropylbenzene. [21]

Conclusions and perspectives

This short overview points to an ever greater need to master the properties of zeolites at ever finer levels: particle size, shape, chemical composition, hierarchization (during

synthesis and postsynthesis treatments) up to the precise location of framework Al, *i.e.* active sites. The amazing flexibility of zeolite chemistry and the remarkable creativity of researchers led to multiple uses of a small fraction of the structures available. Again, it does not imply that searching for new structures is useless; on the contrary, the discovery of many new synthetic structures over the years (MFI, BEA, TON, MTT, MWW…) also met industrial needs for cleaner processes. These two approaches are not mutually exclusive but very complementary.

References

[1] W. Vermeiren, J.-P. Gilson, Top. Catal., 52 (2009) 1131
[2] C. Martínez, A. Corma, Coord. Chem. Rev., 225 (2011) 1558
[3] S. Kulprathipanja, *Zeolites in Industrial Separation and Catalysis*, Wiley-VCH, Weinheim, 2010
[4] M.M.J. Treacy, M.D Foster, I. Rivin, in: K.D.M. Harris, P. P. Edwards (Eds.), *Turning Points in Solid-State, Materials and Surface Science*, RSC Publishing, Cambridge, 2007, p. 208
[5] A.M. Beale, F. Gao, I. Lezcano-Gonzalez, C.H.F. Peden, J. Szanyi, Chem. Soc. Rev., 44 (2015) 7371
[6] P. Tian, Y. Wei, M. Ye, Z. Liu, ACS Catal., 5 (2015) 1922
[7] B.V. Vora, T.L. Marker, P.T. Barger, H.R. Nilsen, S. Kvisle, T. Fuglerud, Stud. Surf. Sci. Catal., 107 (1997) 87
[8] J.M. Thomas, J.C. Hernandez-Garrido, R. Raja, R.G. Bell, Phys. Chem. Chem. Phys., 11 (2009) 2799
[9] M. Guisnet, J. Mol. Catal. A: Chem., 182–183 (2002) 367
[10] I. Ivanova, V.L. Sushkevich, Y.G. Kolyagin, and V.V. Ordomsky, Angew. Chem. Int. Ed., 52 (2013) 12961
[11] S. van Donk, A. Broersma, O.L.J Gijzeman, J.A van Bokhoven, J.H Bitter, K.P de Jong, J. Catal., 204 (2001) 272
[12] T. Terlouw, J.-P. Gilson, EP 458,378 B1 (1994), assigned to Shell Int. Res. Mij. B.V.
[13] M.A. Makarova, A.E. Wilson, B.J. van Liemt, C.M.A.M. Mesters, A.W. deWinter, C. Williams, J. Catal., 172 (1997) 170
[14] R.W. Broach, E.P. Boldingh, D.-Y. Jan, G.J. Lewis, J.G. Moscoso, J.C. Bricker, J. Catal., 308 (2013) 143
[15] A. Tullo, Chem. Eng. News (2013) November 25, 20
[16] A. Bhan, A.D. Allian, G.J. Sunley, D.J. Law, E. Iglesia, J. Am. Chem. Soc., 129 (2007) 4919
[17] M. Boronat, C. Martínez, A. Corma, Phys. Chem. Chem. Phys., 13 (2011) 2603
[18] H. Xue, X. Huang, E. Ditzel, E. Zhan, M. Ma, W. Shen, Ind. Eng. Chem. Res., 52 (2013) 11510
[19] R. Millini, G. Perego, J.W.O. Parker, G. Bellussi, L. Carluccio, Micropor. Mater., 4 (1995) 221
[20] T.F. Degnan, J. Catal., 216 (2003) 32
[21] A. Corma, U. Diaz, V. Fornés, J.M. Guil, J. Martínez-Triguero, E.J. Creyghton, J. Catal., 191 (2000) 2